This is to certify that the

dissertation entitled

Fundamental Studies of Capillary Columns

in Liquid Chromatography

presented by

Christine Esther Evans

has been accepted towards fulfillment
of the requirements for

Doctoral degree in Chemistry

Victoria McGuffin
Major professor

Date January 3, 1991

FUNI

FUNDAMENTAL STUDIES OF CAPILLARY COLUMNS IN LIQUID CHROMATOGRAPHY

By

Christine Esther Evans

A Dissertation

Submitted to

Michigan State University

in partial fullfillment of the requirements

for the degree of

DOCTOR OF PHILOSOPHY

Department of Chemistry

1990

ABSTRACT

FUNDAMENTAL STUDIES OF CAPILLARY COLUMNS IN LIQUID CHROMATOGRAPHY

By

Christine Esther Evans

The correlation between theory and experiment is of fundamental importance in modern separation science. Such correlations are frequently hindered by the inability to measure solute zone profiles directly and accurately during the separation process. With the advent of optically transparent columns and laser-based detection methods, direct examination of high-efficiency chromatographic columns is now feasible.

In this dissertation, an on-column detection scheme is developed which makes possible the accurate measurement of solute retention and dispersion directly on the column. This detection scheme employs two or more identical, laser-induced fluorescence detectors to monitor the solute zone profile as it traverses the chromatographic column. By measuring the difference in the zone characteristics between detectors, local retention and dispersion processes can be examined. Solute retention or capacity factor is determined directly from the difference in the first statistical moment (retention time), which is measured as the solute zone passes sequentially through each detector block. Likewise, the solute dispersion or plate height between detectors is calculated from the difference in the second statistical moment (variance). In this design, the mobile detectors allow any specific region to be isolated from the remainder of the column as well as from any extra-column effects.

After initial fabrication and verification of system performance, this detection scheme is applied to the direct examination of separation processes in reversed-phase liquid chromatography. Initial measurements performed under nearly ideal chromatographic conditions indicate a gradient in both retention and dispersion with distance along the column. Further studies accomplished under varying inlet pressure conditions, while maintaining a constant pressure gradient, establish a clear dependence of retention on the local pressure which is consistent with solubility parameter theory. Finally, zone dispersion is systematically evaluated in the inlet and exit regions of the chromatographic column. Although often assumed to be unimportant, substantial changes in zone dispersion arise from the abrupt transition in retention encountered by the solute zone. Thus, the detection scheme described herein offers the unique opportunity to probe hydrodynamic and physicochemical interactions directly on the chromatographic column. Although investigations in this dissertation are limited to liquid chromatography, this experimental approach should also be compatible with gas and supercritical fluid chromatography, as well as high-voltage capillary electrophoresis.

Dedicated to the memory of Jimmie Anders,
for challenging everything and for believing in me.

ACKNOWLEDGEMENTS

It is not often when the opportunity presents itself to acknowledge publicly those people who have been instrumental in your learning. People who, in a variety of capacities, have made possible the impossible, allowing you to see farther than you ever dreamed. People who create a sense of the wonder which becomes part of you. People who will share with you the moments which arise after much hard work when "ah ha" is the only word to describe the feeling of discovery. People who do not consider giving up on you, even when the going gets quite rough. Everyone has their own group of people who have offered them nothing short of the best, and I would like to take this opportunity to thank my people and introduce them to you.

I would like to begin with my mother and father, who instilled me the fundamental understanding that I could do anything and, just as important, the desire to give it the very best I've got. I wish to thank the rest of my family for their support as well, especially Carol and Lark, who continually amaze me with their understanding and capacity for life.

I would also like to introduce you to my extended family, who are as various and wonderful as anyone could dream of: Adrianne Allen, who routinely checks up on me and my reality; Marie deAngelis, with whom I can be crazy and sane at the same time; Lindy Smith, who's irrepressible self keeps me honest; and Jarl Nischan, who joins me for coffee and wades through life's many confusions. I also wish to express my heartfelt appreciation to Pat Hughes. Without her clear sight and patience, I would still be travelling in circles. Finally, my very special thanks to Clint Jones, who's encouragement and support throughout the years are more important than I can express.

In addition to my personal friends, my gratitude is also extended to my professional colleagues. I would like to thank the McGuffin group for their continued support, especially the original members, John Judge and Jon Wahl. My special thanks to Jong Shin Yoo for his technical expertise in designing and constructing the temperature controller (Chapter 8), and to Shu Hui Chen for her assistance in the successful completion of the pressure studies (Chapter 6). Many thanks to Dr. George Yefchak for his support and many enlightening discussions, to Dr. Kevin Hart for his sanity maintenance skills, and to Kate Noon for her careful reading of this dissertation. I also wish to acknowledge the MSU machine shop (Russ Geyer, Deak Waters, and Dick Menke) for their excellent workmanship in fabricating the on-column detection system.

In addition, the importance of review and discussion in scientific research cannot be overemphasized. For this reason, I would like to thank the members of my committee for their advice and guidance. A special thanks to Dr. Stanley Crouch for his clear and honest discussions. My gratitude is also extended to those members of the scientific community at large for their excellent research manuscripts, many of which are cited herein. Finally, I cannot begin to express my appreciation to Dr. Vicki McGuffin for her support throughout my stay at Michigan State. The insistence on clarity of thought, and the high standards of quality which are inherent in her approach, have improved my research and communication abilities immeasureably.

Last, but not in any way least, I would like to take this opportunity to dedicate this dissertation to the memory of Jimmie Anders. Mr. Anders was an extraordinary junior high school teacher, as honest and straightforward as anyone I've ever met. He made possible a level of learning which was always your best, and would not allow you to trick yourself into any less. I will treasure his gift and carry it with me always.

List of

List o

List o

Cha

A

C

TABLE OF CONTENTS

LIST OF TABLES

7.2

8.1

8.2

8.3

8.4

LIST OF FIGURES

A mu

B_0 sp
B_M lo
B_S lo

C_{OFF} s
C_{ON} s
C_M r
p
C_S r
p

d_i s
D_M
d_p
D_S

E_{11d}
E_{11i}
E_{11o}

F

H_{COL}
H_{MEAS}

I

K_{NJ}
K_{MP}
K

L
L_{FC}
L_{TOT}

LIST OF SYMBOLS

multiple path contribution to dispersion

specific permeability
longitudinal diffusion contribution to dispersion in the mobile phase
longitudinal diffusion contribution to dispersion in the stationary phase

solute concentration detected off-column
solute concentration detected on-column
resistance to mass transfer contribution to dispersion in the mobile phase
resistance to mass transfer contribution to dispersion in the stationary phase

stationary phase film thickness
diffusion coefficient in the mobile phase
particle diameter
diffusion coefficient in the stationary phase

interaction energy arising from dispersion or London forces
interaction energy arising from induction forces
interaction energy arising from orientation forces

volumetric flowrate

on-column height equivalent to a theoretical plate
measured height equivalent to a theoretical plate

ionization energy

solute capacity factor in the injection solvent
solute capacity factor in the mobile phase
distribution coefficient

distance along the chromatographic column
viewed length of the flowcell
total column length

zeroth statistical moment; area of zone profile
first statistical moment; retention time
second statistical moment; zone variance
third statistical moment; zone asymmetry

number of theoretical plates

pressure at the column inlet
pressure at the column outlet
pressure as a function of distance along the column

radial position in cylindrical open tube
mean distance between molecules 1 and 2
gas constant (1.987 cal/K mol)
column radius
connecting tube radius
flowcell radius

skewness of zone profile

retention time of nonretained solute
retention time of retained solute
temperature

off-column linear velocity of mobile phase
on-column linear velocity of mobile phase
linear velocity of mobile phase as a function of distance
spatial average linear velocity of the mobile phase
linear velocity of solute zone

detection volume
injection volume
molar volume of solute i
volume occupied by the mobile phase
total volume of unpacked column
volume between packed particles

polarizability of molecule 1
chromatographic selectivity between molecules i and j

phase ratio of the column

Hildebrand solubility parameter of solute i
Hildebrand solubility parameter of the mobile phase
Hildebrand solubility parameter of the stationary phase

intra-particle porosity
total porosity
inter-particle porosity
permitivity of free space

tortuosity factor in the mobile phase
tortuosity factor in the stationary phase

packing structure constant

dipole moment of molecule 1

density at critical temperature and pressure
density at the column inlet
density at the column outlet
reduced density ($= \rho/\rho_C$)
density as a function of distance along the column
spatial average of density

zone variance in length units
zone variance in time units
zone variance in volume units
variance arising from detector
variance arising from injector
variance arising from detector time constant
total variance of zone profile

detector time constant

viscosity

flow resistance parameter
volume fraction of solvent n

fractional increase in the column variance from extra-column sources

CHAPTER 1

HISTORICAL BACKGROUND: THEORETICAL AND EXPERIMENTAL EVALUATION OF CHROMATOGRAPHIC SEPARATIONS

1.1 Introduction

The separation of complex mixtures is an essential process in a wide range of research and industrial applications. By taking advantage of the different extent to which solute molecules interact with a stationary medium, Martin and Synge (1) discovered the powerful separation technique known as chromatography. In this technique, a flowing mobile phase is continuously introduced onto a chromatographic column, and selective interaction of solutes with the stationary phase causes their differing migration rates through the column. The resulting solute zones are then monitored sequentially as they pass a detector. This method allows samples of environmental and biochemical significance to be analyzed in a remarkably short period of time. Since this discovery in 1941, researchers in fields as diverse as oceanography and medicine have benefited from the ability of this technique to separate the constituents present in very complex sample matrices.

The effectiveness of a separation in chromatography is determined by the differential migration rate of solutes as well as by the broadening or variance of the solute zones. In the analysis of complex mixtures where the sample components are distributed statistically (2), altering the migration rate merely transposes the order of solute elution while not improving the separation to any significant extent. However, minimizing the spreading of solute zones on the chromatographic column allows a greater number of species to be separated simultaneously. Thus, understanding the influence of the various separation parameters on solute zone dispersion is central to the advancement of the field of separation science. For this reason, the primary emphasis in this chapter will be on the theoretical prediction and experimental measurement of zone dispersion, with solute retention discussed in less detail.

1.2 Column Characteristics

It may be helpful to begin by describing the types of chromatographic columns presently utilized in high-performance liquid chromatography (HPLC). Column design has advanced considerably in the past ten years, and several types of HPLC columns are commercially available or under active development. The most common of these and their characteristics are shown in Table 1.1 (3). The predominant trend in developing new columns has been to decrease inner diameters (i.d.) and increase column lengths (4,5, and references cited therein). Although most theories predict chromatographic efficiency of packed columns to be independent of column diameter (Section 1.4), clear advantages are realized in miniaturization. As shown in Table 1.1, the low flowrates required with decreased diameter allows an increase column length, leading to an increase in

Table 1.1: Typical characteristics of liquid chromatographic columns.

COLUMN TYPE	I.D.	LENGTH	FLOWRATE	N	ϕ'
conventional	4.6 mm	25 cm	1 mL/min	10,000	500-1000
packed capillary	50-500 μm	1-10 m	0.5-2 μL/min	100,000	500-1000
open-tubular capillary	1-10 μm	1-10 m	<1 μL/min	1,000,000	32

the chromatographic performance. Diminished flowrates also yield the practical advantage of decreased solvent consumption and related disposal problems. In addition, a variety of new detection options are possible with these smaller columns (5), including mass spectrometric detection (6). Because many of the smallest columns are fabricated from fused-silica capillaries, detection directly on the chromatographic column is also feasible (7). In the research presented here, this technological advancement is used to advantage by probing the hydrodynamic and kinetic behavior of packed-capillary columns directly.

1.3 Solute Retention

The selective interaction of solutes with the stationary and mobile phases forms the basis for separations in liquid chromatography. Differences in interaction energies, often less than 100 cal/mol between similar solute molecules, cause differential migration rates along the chromatographic column. Although the subject of considerable investigation, the exact nature of this phenomenon is not yet fully understood.

In the reversed-phase separations of interest in this study, the stationary phase is composed of a porous silica substrate which has been chemically modified with straight-chain alkyl moieties. The mobile phase is a polar organic solvent (i.e., methanol, acetonitrile, tetrahydrofuran), and is often utilized in aqueous mixtures. A variety of mechanisms have been proposed to describe the retention of solutes under these conditions (8-17), although conclusive proof favoring any specific mechanism is presently lacking (17).

A number of factors contribute to the difficulty in assessing the precise mechanism(s) involved in a separation. First, the chemical and physical nature

of the stationary phase is quite complex. The environment at the surface of these modified particles is not accurately modeled by bulk solution chemistry, as individual alkyl chains are anchored to the silica substrate (18). It is also unclear how to model the presence of surface-adsorbed mobile phase, which may act as a chemically distinct stationary phase. Furthermore, the composition of the mobile phase is known to alter the stationary phase environment and structure (18-20). Finally, derivatization of the silica substrate inevitably leads to incomplete surface coverage, often leaving an unknown number of silanol and siloxane sites available on the surface for adsorption interactions with the solutes. If this were not enough, the chemical composition of the mobile phase is also quite complex. The organic solvents commonly utilized in reversed-phase separations are quite polar, exhibiting an appreciable extent of self interaction and hydrogen bonding. Moreover, aqueous mixtures of these organic solvents, frequently utilized to optimize separation conditions, often behave anomalously (21-24), displaying minima and maxima in physical properties (e.g., density, viscosity, surface tension, etc.) as a function of composition.

Theoretical Prediction. The prediction of solute retention is central to the control and optimization of separations, and, thus, has been studied extensively (8-17). Among these theories, the solvophobic theory of Horvath (9,10) and the solubility parameter approach (11-13) are the most commonly employed. However, recent advances in the development of a unified theoretical approach to separations by Martire (15,16) shows much promise. In this statistical thermodynamic approach, a lattice model is utilized to describe both the absorption (partition) phenomenon of interest here (15,16) and the adsorption mechanisms (25) as well. In addition, numerous empirical correlations are routinely employed (26), including the recent use of solvatochromic indicators as

a measur

environme

To

the gener

Dispersio

are the n

interactio

$E_{IM} = -$

where a

the mea

may be

$E_{IM} = -$

where

are in

based

indep

expec

that

None

betw

sepa

dipo

inte

a measure of the polarity of the mobile (27,28) and stationary (29) phase environments.

To begin the discussion of solute retention, it is important to understand the general types of chemical interactions which are possible between molecules. Dispersion or London forces arising from induced dipole-induced dipole forces are the most common and are present to some extent in all interactions. The interaction energy (E_{11d}) between two identical molecules may be described by

$$E_{11d} = - \frac{3 \alpha_1^2 I_1}{4 r_{11}^6} \qquad [1.1]$$

where α_1 is the polarizability of molecule 1, I_1 is the ionization energy, and r_{11} is the mean distance between molecules. Interactions between different molecules may be described in an analogous manner,

$$E_{11d} = - \frac{3 \alpha_1 \alpha_2 \ I_1 I_2}{2 r_{12}^6 \ (I_1 + I_2)} \qquad [1.2]$$

where the polarizability for each molecule and the reduced ionization potential are incorporated. Dispersion forces between molecules are often estimated based on group polarizabilities. If group interactions are considered independent, dispersion forces in molecules of a homologous series are expected to increase directly with carbon number. It is clear from Equation [1.2] that these forces are quite weak and decrease rapidly with distance. Nonetheless, these nonspecific interactions are the primary forces acting between solute molecules and the nonpolar stationary phase in reversed-phase separations.

In addition, a permanent dipole in one molecule may induce a temporary dipole in a second molecule. The energy of dipole-induced dipole or induction interactions (E_{12i}) is given by

$$E_{12i} = -\frac{1}{4\pi\varepsilon_0}\frac{2\mu_1^2\alpha_2}{r_{12}^6} \qquad [1.3]$$

where ε_0 is the permitivity of free space and μ_1 is the dipole moment of the molecule. Alternatively, if both molecules contain permanent dipole moments, orientation or electrostatic interactions are possible. The energy of orientation interactions (E_{12o}) can be expressed as

$$E_{11o} = -\frac{1}{4\pi\varepsilon_0}\frac{2\mu_1^2\mu_2^2\cos\theta}{3\ k\ T\ r_{12}^6} \qquad [1.4]$$

where k is the Boltzmann constant, T is the absolute temperature, and θ is the angle formed by the vectors of the two dipoles. Based on Equation [1.4], the interaction energy is the greatest when the two molecules are aligned. In addition to these weak forces, molecules may also form hydrogen bonds. This specific interaction is slightly more energetic and is often described as a combination of donor-acceptor and electrostatic interactions. Interactions between ions and molecules, not considered here, may also be important in separation schemes other than reversed phase. Although solute molecules may encounter any or all of these interactions, because of the alkyl-based stationary phase, dispersion forces are by far the most prevalent in reversed-phase separations.

On traversing the chromatographic column, solute molecules will interact with the mobile and stationary phases, residing for varying amounts of time in each phase. This retention of solutes is given by the capacity factor (k)

$$k = \frac{t_R - t_0}{t_0} \qquad [1.5]$$

where t_R is the time required for the solute to traverse the column and t_0 is the column void time. In the simplest case, the distribution of the solute between these phases can be described by the equilibrium constant, K. For an isothermal process, the distribution constant is given by

$$k = \beta K = \beta \exp(-\Delta G^0/RT) = \beta \exp[(-E_{TOT}/RT) + (\Delta S/R)] \quad [1.6]$$

where β is the volume ratio of the mobile to stationary phase, and ΔG^0 is the change in Gibbs' free energy associated with the transfer between the mobile and stationary phases resulting from a change in interaction energy of E_{TOT}.

Theoretical approaches to the retention process often diverge at this point. The solubility parameter approach is chosen for discussion here because the fundamental basis provides a reasonably good physical understanding of the separation process. Based on regular solution theory (30), the interaction energies between molecules are directly additive and assumed to be independent. In addition, this model assumes that the molecular volume is fixed and molecules are randomly distributed, with no preferred orientation. Although these assumptions seem to exclude most conditions present in chromatographic separations, the model is quite good in describing the dispersion interactions which predominate in reversed-phase separations (12-14).

In the solubility parameter approach, the sum of the interaction energies (E), which were described above, per molar volume (V) are incorporated in a cohesive energy density or solubility parameter ($\delta = -E/V$). This quantity, often a direct indication of the solvent polarity, can be related to the capacity factor of solute i (k_i) via Equation [1.7] (14).

$$\ln k_i = \frac{V_i}{RT}[(\delta_i - \delta_M)^2 - (\delta_i - \delta_S)^2] + \ln(1/\beta) \quad [1.7]$$

In this expression, the retention of solutes is described by the difference between the solute (δ_i) and mobile phase (δ_M) parameters and the solute (δ_i) and stationary phase (δ_S) parameters. For reversed-phase separations, the mobile phase is always more polar than the stationary phase ($\delta_M > \delta_S$), with the solute parameter usually at some intermediate value. If the solute parameter (δ_i) is exactly centered between the mobile- and stationary-phase parameters, the solute will spend half of the time in each phase (k = 1). Selectivity between solutes i and j (α_{ij}) may, likewise, be written in terms of solubility parameters (14),

$$\ln \alpha_{ij} = \frac{\ln k_j}{\ln k_i} = \frac{2V_i}{RT} (\delta_i - \delta_j)(\delta_M - \delta_S) \qquad [1.8]$$

assuming equal molar volumes (V_i). Based on this expression, the separation of similar compounds is dependent not only on the difference in their solubility parameters ($\delta_i - \delta_j$), but that of the mobile and stationary phases ($\delta_M - \delta_S$) as well. Thus, the successful separation of solutes which are quite similar ($\delta_i \sim \delta_j$) is facilitated by a large difference in the mobile and stationary phase environments ($\delta_M >> \delta_S$).

Solubility parameters have been applied to liquid chromatographic separations under a wide variety of conditions, including variations in temperature (31), mobile-phase composition (32), and pressure (33). Although the assumptions necessary to derive these solubility parameter expressions are quite limiting, the use of this approach in predicting trends in retention has been surprisingly successful. Solubility parameters are presently tabulated for a number of compounds of interest in reversed-phase liquid chromatographic separations (34), including recent evaluations of a variety of commercially available stationary phases (19,20).

Experime
measurin
nonretain
determina
evaluatin
this dete
propositi
(35,36).
marker,
materia
conditio
for exa

1.4 Se

act to
dispe
Thes
caus
capa
sepa
the
sepa
bec
a c

Experimental Evaluation. Solute retention is determined experimentally by measuring the time required for a solute to elute from the column (t_R) relative to a nonretained species (t_0). Although the peak maximum is often utilized for this determination, the first statistical moment is the most accurate means of evaluating the true solute retention time (*vide infra*). Based on Equation [1.5], this determination of the solute capacity factor (k) appears to be a simple proposition. However, the selection of a truly nonretained solute is quite difficult (35,36). It has been proposed that each solute requires a different nonretained marker, as the accessibility of solutes to the pore structure of the packing material may differ (36). In addition, the precise control of experimental conditions (temperature, flowrate, mobile-phase composition, etc.) is necessary for exact measurements of solute retention (37-39).

1.4 Solute Dispersion

In addition to interactions which act to separate solutes, a variety of forces act to increase the entropy of the system, often resulting in broadening or dispersion of the solute zone as it traverses the chromatographic column (40). These dispersion processes are detrimental to the separation performance, causing the overlap of neighboring solute zones. Thus, the column peak capacity is reduced and the maximum number of solutes that can be successfully separated is decreased (2,41,42). Although the subject of considerable study, the fundamental processes contributing to the total dispersion in chromatographic separations are not yet fully understood. Nonetheless, as the samples of interest become more complex, the need for truly optimal separation conditions requires a clearer knowledge of dispersion processes. In this section, the present status

of theoretical predictions and experimental measurements of solute zone dispersion is addressed. The assumption of additivity of variance, implicit in most theoretical and experimental approaches, is discussed in Appendix 1.

Theoretical Predictions. In the isolation of individual components from a mixed sample, both separative and dissipative forces act on the solute zone. Separative forces, by the various interactions discussed above, selectively displace solutes to different spatial/temporal locations. Simultaneously, however, dissipative forces are acting to increase disorder, diluting and remixing solute zones. Thus, the success of any separation is based on the ability to design a system which favors separative forces (40). The understanding of solute zone dispersion is central to this success, especially in the separation of mixtures containing a large number of components.

In this section, an overview of the prevalent theories regarding the chromatographic dispersion of solute zones will be presented. The discussion will begin with open-tubular columns, which are well characterized and well understood, and continue with the more complex, packed columns.

Open-tubular Columns. The dispersion arising in straight, smooth open tubes is well understood for the laminar flow regimes of interest in chromatographic separations. The pressure-driven flow of fluid in this simple system can be modeled as sheaths or layers. Momentum is transfered between adjacent layers resulting in a radial velocity profile, u_r, across a tube of radius R, which may be expressed in the following parabolic form (43),

$$u_r = 2u\,[1 - (r/R)^2] \qquad [1.9]$$

where u represents the average linear velocity of the fluid. Under these laminar flow conditions, the maximum linear velocity (2u) occurs at the tube center (r = 0).

The dispersion arising under these flow conditions was first derived by Taylor and Aris (44,45) for open-tubular columns with no stationary phase. In this equation, the dispersion of a solute zone is expressed as the plate height (H) or length variance (σ_L^2) per unit length (L) along the column.

$$H = \frac{\sigma_L^2}{L} = \frac{2 D_M}{u} + \frac{R^2 u}{24 D_M} \qquad [1.10]$$

This equation has been shown to predict accurately the dispersion arising when a solute with diffusion coefficient D_M is injected into a fluid with an average linear velocity u (46). However, Equation [1.10] is only valid if the time spent on the column is long compared with R^2/D_M (47-49). Although not directly applicable to chromatographic columns, the Taylor-Aris equation is valid for predicting dispersion in most connecting tubes utilized in chromatographic systems.

The dispersion arising from open-tubular columns which contain a thin coating of stationary phase was first derived in the classic manuscript by Golay (50). In this well-known equation, the dispersion of a solute zone of capacity factor k is expressed as the plate height (H) for a stationary phase thickness d_f and solute diffusion coefficient in the stationary phase D_S.

$$H = \frac{\sigma_L^2}{L} = \frac{2 D_M}{u} + \frac{(1 + 6k + 11k^2)\ R^2 u}{24\ (1 + k)^2\ \ D_M} + \frac{2\ \ k\ \ d_f^2 u}{3\ (1 + k)^2\ D_S} \qquad [1.11]$$

$$= B_M/u \quad + \quad C_M u \quad + \quad C_S u$$

In Golay's original development, three factors contribute to the dispersion of solute zones in open-tubular columns: longitudinal diffusion in the mobile phase

(B_M), and resistance to mass transfer in the mobile (C_M) and stationary (C_S) phases. All of these factors are presumed to be independent in this theoretical development and, therefore, the length variances are considered to be additive (Appendix 1). Longitudinal diffusion in the stationary phase (B_S) was considered negligible in Golay's original development, but will be included here for completeness.

A physical description of each of these individual processes is illustrated in Figure 1-1. The B term in the Golay equation represents longitudinal diffusion resulting from the Brownian motion of molecules. The resulting flux, given by the second law of thermodynamics, arises from entropic driving forces. This diffusional process is given by Fick's laws (51), where the first law describes the solute flux (J) or mass flow per unit area.

$$J = - D \, \partial C/\partial x \qquad [1.12]$$

Assuming an initial concentration C at time t = 0, this broadening process is driven by the solute concentration gradient ($\partial C/\partial x$) along the column axis (x). The resulting change in concentration with time ($\partial C/\partial t$) is given by Fick's second law,

$$\partial C/\partial t = D \, \partial C^2/\partial x^2 \qquad [1.13]$$

where the diffusion coefficient (D) is considered constant. For a narrow injection profile, the concentration as a function of time calculated from Equation [1.13] yields a Gaussian form.

$$C(t) = \frac{1}{2(\pi \, Dt)^{1/2}} \exp(-x^2/4Dt) \qquad [1.14]$$

Figure 1-1: Schematic illustration of longitudinal diffusion (B) and resistance to mass transfer (C) processes on zone length variance.

Figure 1-1

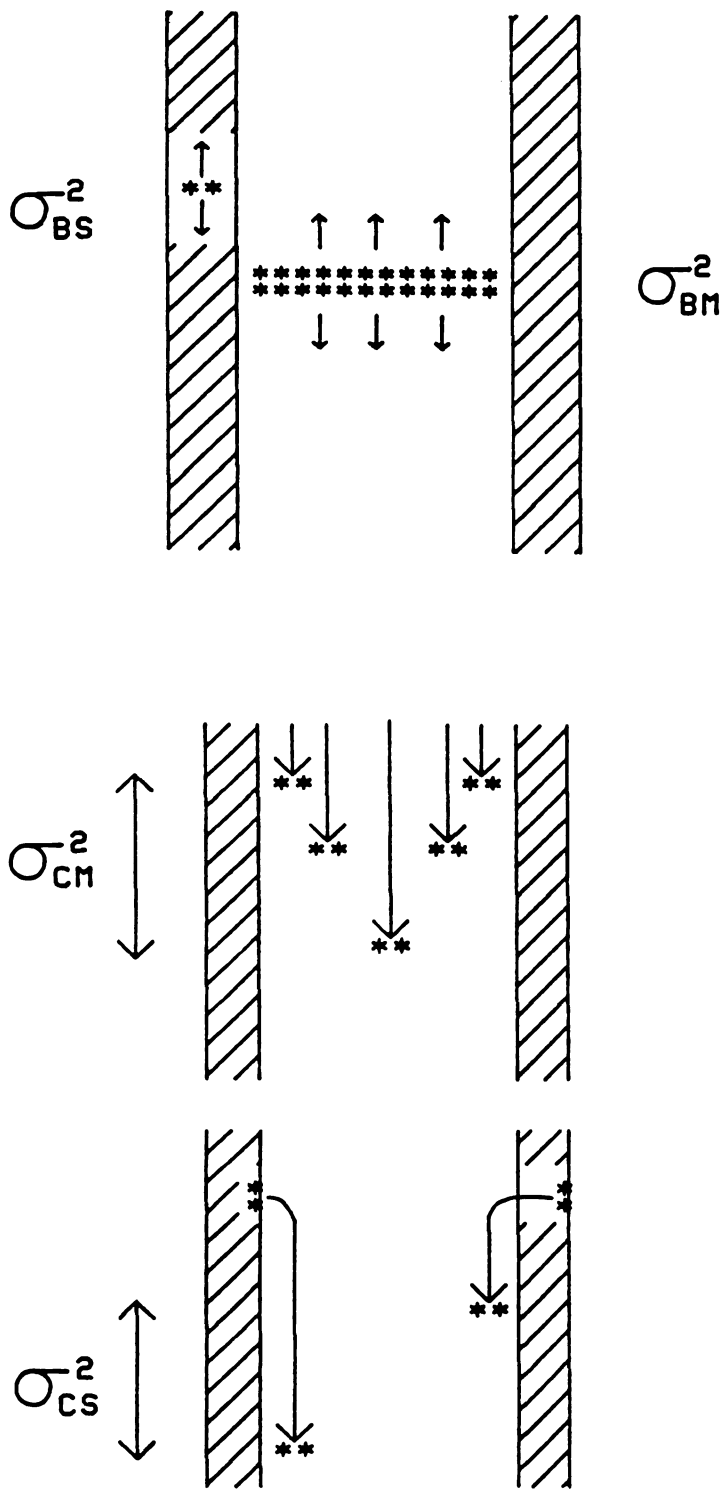

Comparison with the normalized Gaussian distribution results in the length variance for one-dimensional mass transport derived by Einstein (52).

$$\sigma_L^2 = 2\,Dt \qquad [1.15]$$

This mathematical description of the variance, equivalent to the B term variance in Equation [1.11], yields the diffusional contribution to the zone dispersion. Although this contribution is shown in Equation [1.11] to be present only in the mobile phase (B_M), longitudinal diffusion may occur in the stationary phase (B_S) as well. Because the Golay equation was originally derived for gas chromatographic applications, stationary phase effects are considered negligible as mobile-phase diffusion coefficients (D_M) are typically a factor of 10^4 greater than those in the stationary phase (D_S). The stationary phase contribution cannot be neglected in liquid chromatographic applications, however, where diffusion coefficients in the mobile and stationary phases are approximately 10^{-5} and 10^{-6} cm^2/s, respectively. In this case, the stationary-phase longitudinal diffusion is given by

$$B_S = \frac{2\,D_S\,k}{u} \qquad [1.16]$$

and must be included in Equation [1.11].

The resistance to mass transfer contribution to the zone dispersion is also illustrated in Figure 1-1, for both the mobile (C_M) and stationary (C_S) phases. These sources of dispersion result from the finite time required for solute molecules to transfer through the mobile or stationary phase. In the mobile phase, the limited solute movement between flow streams results in different rates of movement across the chromatographic column. Thus, solute molecules within the same zone are displaced to differing extents along the column by the parabolic flow profile. In the stationary phase, the resistance to mass transfer

contribution arises because solute molecules reside in the stationary phase for varying amounts of time. This distribution of interaction times within the same zone yields a range of spatial displacement along the column. In contrast to the longitudinal diffusion term, however, the plate height contribution from C_M and C_S actually decreases with diffusion coefficient. In this case, diffusion increases mass transfer of solutes, providing more rapid movement of molecules between the mobile and stationary phases. As seen in Equation [1.11], the plate height dependence on capacity factor is quite complex. If mass transfer in the mobile phase is predominant, plate height is predicted to increase with retention, whereas a decreasing trend is expected for stationary-phase processes. The rigorous mathematical derivation of these terms is not presented here, and the reader is referred to the excellent development in the original manuscript (50).

Although dispersion in open-tubular columns has been quite well characterized (50), recent theoretical developments provide an "exact proof" of the Golay equation (53). The few terms that must be assumed to be negligible in the original derivation are unnecessary with this new approach. In addition, this recent derivation incorporates the finite equilibration time between the mobile and stationary phases. Thus, an additional term is included in the Golay equation for the contribution of equilibration rate to the zone dispersion.

Packed Columns. Similar to open-tubular columns, the dispersion in packed columns arises from a combination of diffusion and hydrodynamic considerations. Unfortunately, fluid flow within a packed bed is much more complex and, as a result, much more difficult to derive from fundamental principles. Although the effect of each force within the system may be rigorously evaluated utilizing the Navier-Stokes equation (54), application of this expression to the complex

geometry in packed beds is intractable. Thus, the empirical approach proposed by Darcy (55) and based on resistance to flow is most often utilized.

$$u = -\frac{B_0}{\varepsilon_T \eta}\frac{P_o - P_i}{L} \qquad [1.17]$$

This description of fluid flow is directly analogous to the flow of electrical current given by Ohm's law, where the average linear velocity ($u \equiv$ current) results from an applied pressure drop ($P_o - P_i \equiv$ voltage) per unit length (L) along the column. The resistance to fluid flow is, therefore, given by the fluid viscosity (η) and specific permeability (K^o) of the packed bed. Derivation of the specific permeability, accomplished by Kozeny (56) and Carman (57), is given below.

$$B_0 = \frac{d_P^2\, \varepsilon_u^3}{180\, \psi^2\, (1-\varepsilon_u)^2} = \frac{d_P^2}{\phi'} \qquad [1.18]$$

The column permeability is dependent on the particle diameter (d_P) as well as the total porosity of the packed bed (ε_T), and may be described in terms of the flow resistance parameter (ϕ'). In this expression, the total porosity is the fraction of the column volume which is accessible to the solute and comprises both interparticle (ε_u) and intraparticle (ε_i) contributions (58).

$$\varepsilon_T = \varepsilon_u + \varepsilon_i \qquad [1.19]$$

The effect of the packing structure is given by the empirical constant ψ^2, which is 1.0 for spherical nonporous beads and 1.7 for irregular porous particles.

Although the dispersion arising under these flow conditions is difficult to model, appreciable theoretical advances have been made in describing the chromatographic technique. The first theory to describe zone dispersion is the well-known plate theory proposed in the original work of Martin and Synge (1). In this approach, the chromatographic column is divided into small vessels or

plates. Within each plate, complete mixing and equilibrium are assumed to occur. Although effectively applied to distillation processes (59), the plate theory is inadequate in describing zone dispersion in chromatographic separations (60). The shortcomings in this theoretical approach arise from the discrete nature of the model and the assumption of equilibrium within each discrete section or plate. These assumptions are in direct conflict with the fact that chromatographic separations are dynamic and continuous in nature, comprising many processes that are driven by nonequilibrium. Although these limitations are cited in the original manuscript by Martin and Synge, this theory has been applied without regard for these assumptions for many years. Although the numerous failures of this theory have been detailed elsewhere (60), a few are included here for completeness. The stipulation of discrete, individual plates results in the inability of the plate model to account for the effect of longitudinal diffusion on zone dispersion. Moreover, this model does not yield any information regarding the effect of many primary variables present in any separation (e.g., particle size, diffusion coefficient, temperature, etc.). Thus, although the height equivalent to a theoretical plate (H) remains in common usage, as seen earlier in this section, the meaning is quite different from the original term cited by Martin and Synge.

Since the plate model, many other approaches to the theoretical description of dispersion have been proposed. These are quite varied in approach and detail, and include the random walk model (62,63), the mass balance method (63-67), general nonequilibrium theory (68,69), and the rate theory (70). A clear discussion and comparison of these theories has been presented by Weber and Carr (71). The most widely utilized of these theories, is the rate approach proposed by van Deemter, Zuiderweg, and Klinkenberg (70). In this theory, rate constants for the various dispersion processes are evaluated individually and the total zone dispersion is calculated as the sum of the length variance contributions.

$$H = A + B_M/u + B_S/u + C_M u + C_S u$$
$$= \{(\sigma_L^2)_A + (\sigma_L^2)_{BM} + (\sigma_L^2)_{BS} + (\sigma_L^2)_{CM} + (\sigma_L^2)_{CS}\}/L \qquad [1.20]$$

In this familiar expression, the A term represents the dispersion arising from the multiple paths possible through the packed bed. This contribution does not affect dispersion in open tubes which contain only one path, and, thus, the A term is absent from Equation [1.11]. As illustrated in Figure 1-2, it may be necessary for solute molecules within the same zone to travel different distances to traverse the column length. The dispersion in length variance resulting from this process ($(\sigma_L^2)_A$) may be expressed as

$$(\sigma_L^2)_A = 2 \lambda d_P L \qquad [1.21]$$

where λ is a constant dependent on the homogeneity of the packed bed, typically 0.1 to 0.5 (72). In this model, the A term is assumed to be independent of the mobile-phase velocity. This presumption, later disputed by Giddings (73,74), does not account for the possibility of molecules changing flow streams. This movement, whether by diffusion or by turbulence, would allow different possible paths through the packed bed and result in the coupling of the A and C terms. In this case, the processes are not independent and, therefore, the variances are not strictly additive. Instead, the resulting coupled length variance ($(\sigma_L^2)_{AC}$) has the following form:

$$(\sigma_L^2)_{AC} = \frac{1}{1/A + 1/Cu} \qquad [1.22]$$

At high linear velocities, this relationship predicts a lower plate height than expected from the van Deemter form.

Figure 1-2: Schematic illustration of multiple pathways through a packed bed (A) on zone length variance.

Figure 1-2

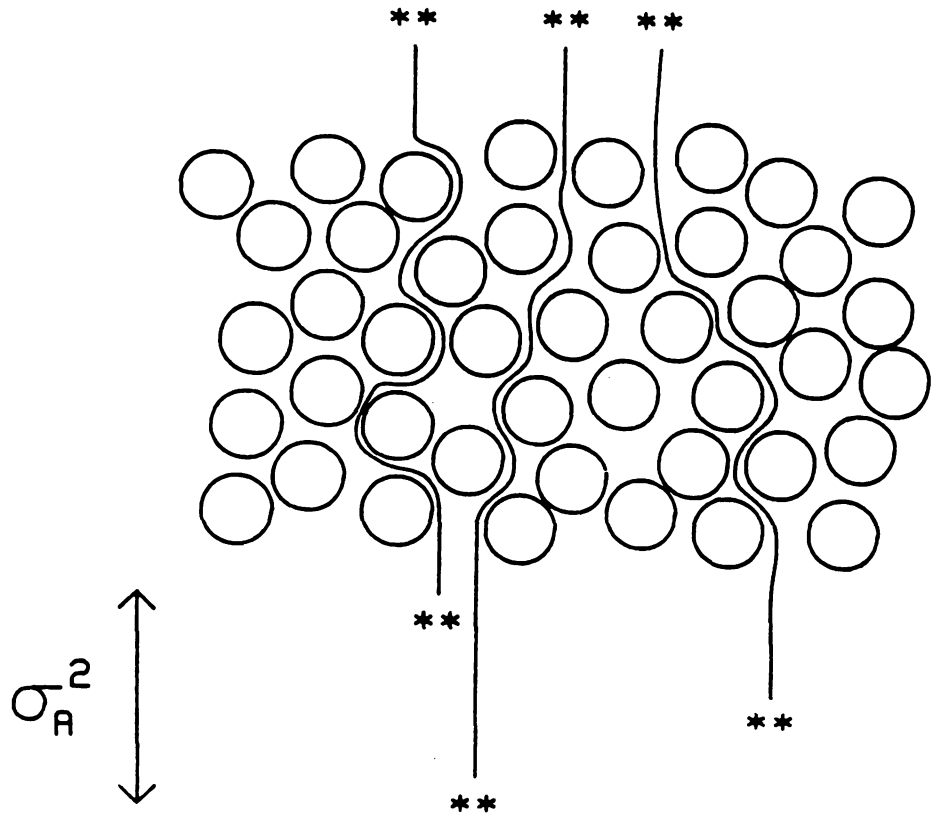

Th

column

directly

to the tir

$(\sigma_L^2)_{SM}$

$(\sigma_L^2)_{BS}$

Unlike

longitu

particl

tortuo

station

for no

desc

earli

betw

disp

$(\sigma_L^2$

Thi

sq

inv

de

st

de

The B terms in Equation [1.20] result from molecular diffusion along the column length, as described earlier. These longitudinal diffusion terms are directly proportional to the solute diffusion coefficient and inversely proportional to the time spent in the phase of interest.

$$(\sigma_L^2)_{BM} = 2\,\gamma_M\,D_M\,t = 2\,\gamma_M\,D_M\,L/u \qquad [1.23]$$

$$(\sigma_L^2)_{BS} = 2\,\gamma_S\,D_S\,k\,t = 2\,\gamma_S\,D_S\,k\,L/u \qquad [1.24]$$

Unlike the analogous expressions for open tubes (Equations [1.11] and [1.16]), longitudinal diffusion in packed beds may be hindered by the presence of particles or by the uniformity of the stationary phase film. The obstruction or tortuosity factors represent the regularity of packing (γ_M) and the continuity of the stationary phase film (γ_S). Typical values of γ_M for packed bed systems are 0.73 for nonporous, spherical particles and 0.63 for porous, irregular particles (75,76).

Finally, the C terms in the van Deemter expression (Equation [1.20]) describe the resistance to mass transfer of solute molecules. As discussed earlier, inertial forces resist the movement of molecules between flow streams or between the mobile and stationary phases and, thus, cause an increase in zone dispersion. The mobile-phase contribution is given by

$$(\sigma_L^2)_{CM} = \frac{k^2\,d_p^2\,u\,L}{100\,(1+k)^2\quad D_M} \qquad [1.25]$$

This relationship is analogous to that in an open tube (Equation [1.11]) with a squared dependence on particle diameter (instead of column diameter) and an inverse dependence on diffusion coefficient. However, the capacity factor dependence is quite different from that derived for an open tube. The packing structure may act to force mass transfer of the solute, thus decreasing the k dependence in a packed bed system. In contrast, the dispersion arising from

resistance to mass transfer in the stationary phase in packed columns is directly analogous to that in open tubes, as shown below.

$$(\sigma_L^2)_{cs} = \frac{c \quad k \quad d_f^2 \quad u \quad L}{(1 + k)^2 \quad D_S} \qquad [1.26]$$

The form of the expressions vary only in the value of the constant c, which is equal to 2/3 for an open tube and $8/\pi^2$ for a packed tube with uniform stationary phase film. Derivations by Giddings (77) indicate that the magnitude of c is dependent on the variation in film thickness, as well as the shape and distribution of the stationary phase in the column. In addition, the shape and depth of the pore structure is predicted to have a significant effect. Thus, determination of the expected value for this constant is difficult, if not impossible, under practical conditions.

Although the van Deemter equation provides a good qualitative description of zone dispersion, the limited number of processes and the assumption of independent contributions is quite simplistic. However, the number of unknown parameters is less than for other more sophisticated theories. This overall problem has been circumvented in a number of investigations by utilizing an empirical approach (78-80). Although often helpful for diagnostic purposes (81), these curve fitting methods are not appropriate for the evaluation of fundamental dispersion processes. Thus, although many theoretical advances have been made, the accurate prediction of zone dispersion from known experimental parameters remains elusive.

Experimental Evaluation. The advancement of the theoretical basis for zone dispersion has been limited, in part, by the lack of accurate, systematically

acquired experimental measurements of zone variance. Verification and development of the theoretical models discussed above require the accurate and precise determination of dispersion arising solely from separation processes. A variety of factors contribute to difficulties in this experimental measurement, including calculational methods and extra-column effects.

Calculational Methods. Although often presumed unimportant in dispersion determinations, the accuracy and precision of the measured variance are directly affected by the method of calculation. The variety of calculational methods employed for the evaluation of variance from a recorded profile have been critically reviewed and compared in several excellent manuscripts (82-85). In the simplest case, the measured profile is modeled as Gaussian distribution (86).

$$C(t) = \frac{1}{\sigma_T (2\pi)^{1/2}} \exp\left[- \frac{(t - t_R)^2}{2 \sigma_T^2} \right] \qquad [1.27]$$

As illustrated in Figure 1-3, the variance of the zone is commonly calculated from the inflection points at 60.7% of the peak height (2σ), from the curve at 50.0% peak height (2.35σ), or from the tangent lines (4σ). The plate height may then be determined by substitution of the measured time variance (σ_T^2) into the following expression,

$$H = L (\sigma_T^2/t_R^2) \qquad [1.28]$$

where the retention time (t_R) is determined at the peak maximum for a column of length, L. Although these methods are commonly utilized because of the ease of calculation, the assumption of a Gaussian profile is not always valid for actual experimental measurements. In fact, many measured profiles are asymmetric and, therefore, arise from sources which are not entirely Gaussian in nature.

Figure 1-3: Example variance measurements on a Gaussian zone profile.

Figure 1-3

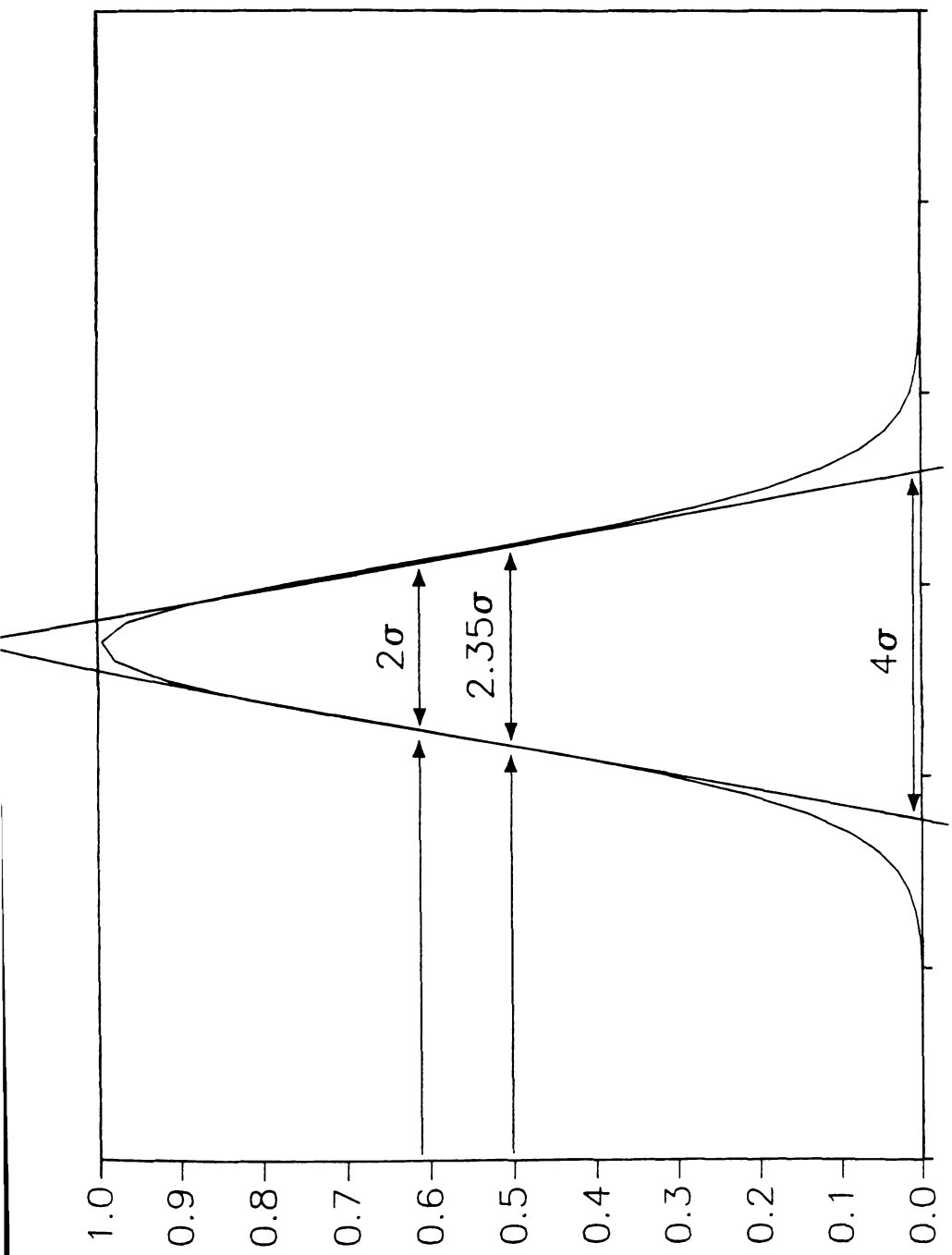

Other models have been proposed for the determination of the zone variance as well, among which the exponentially modified Gaussian (EMG) is the most common (87-94). In this model, the chromatographic zone is assumed to result from the convolution of Gaussian (with variance, σ_G^2) and exponential (with variance, τ^2) contributions yielding the final measured variance (σ^2).

$$\sigma^2 = \sigma_G^2 + \tau^2 \qquad [1.29]$$

The EMG profile is modeled based on the following expression for the concentration as a function of time, C(t).

$$C(t) = \frac{1}{2\tau} \exp\left(\frac{\sigma^2}{2\tau^2} + \frac{(t - t_R)}{\tau} \right)\left[\operatorname{erf}\left(\frac{t_R}{2^{1/2}\sigma} + \frac{\sigma}{2^{1/2}\tau} \right) + \operatorname{erf}\left(\frac{(t - t_R)}{2^{1/2}\sigma} - \frac{\sigma}{2^{1/2}\tau} \right) \right] \qquad [1.30]$$

The literature includes many errors in the presentation of this model which have been reviewed and corrected by Hanggi and Carr (94). Using this model, the Gaussian and exponential components (σ_G and τ, respectively) may be determined iteratively. Because this determination is calculationally intensive, several approaches have been proposed to simplify parameter evaluation. Barber and Carr (90,94) have proposed a series of calibration curves for the determination of σ_G and τ graphically. This technique yields an accuracy of ± 2.4% with a corresponding precision of ± 5.0% in the determination of plate height on a synthetically generated peak. This corresponds to an accuracy of ± 1.5% and a precision of ± 3.1% in the evaluation of the second moment. An alternate approach based on least squares fitting has been examined by Foley and Dorsey (91). This method yields the following expression:

$$H = \frac{L\,(A/B + 1.25)}{41.7\,(t_R/W_{0.1})} \qquad [1.31]$$

where A/B is the commonly measured asymmetry and $W_{0.1}$ is the peak width at 0.1 of peak height, as shown in Figure 1-4. This technique offers the advantage of improved accuracy (± 1.5%) and precision (± 2.5%) in the determination of plate height (with an accuracy and precision in the second moment of ± 1.5% and ± 2.4%, respectively), and also utilizes easily measureable parameters. However, as with any fitting method, the EMG model restricts the determination of fundamental parameters to those implicit in the chosen model. Thus, although widely accepted, use of the EMG approach assumes the zone profile includes only one symmetric and one asymmetric parameter. Moreover, it may not be reasonable to presume that both these parameters arise exclusively from column processes.

Many other fitting approaches have been investigated as well (95-99). The most common of these are the Chesler-Cram equation (97,98) and the Edgeworth-Cramer series (99). Although relatively successful at fitting chromatographic profiles, both techniques require a number of adjustable parameters and provide little physical insight into the separation process.

The final, commonly utilized calculational method is that of statistical moments. Unlike the preceding techniques, the evaluation of statistical moments requires no *a priori* assumptions regarding the shape of the chromatographic peak (92,100-105). Mathematically, statistical moments are defined as:

$M_0 = \int I(t)\, dt$	zeroth moment	
$M_1 = \int t\, I(t)\, dt / M_0$	first moment	[1.32]
$M_2 = \int (t - M_1)^2\, I(t)\, dt / M_0$	second moment	
$M_n = \int (t - M_1)^n\, I(t)\, dt / M_0$ $n = 3,4,5...$	higher moments	

Figure 1-4: Example variance measurements on an exponentially modified Gaussian zone profile.

Figure 1-4

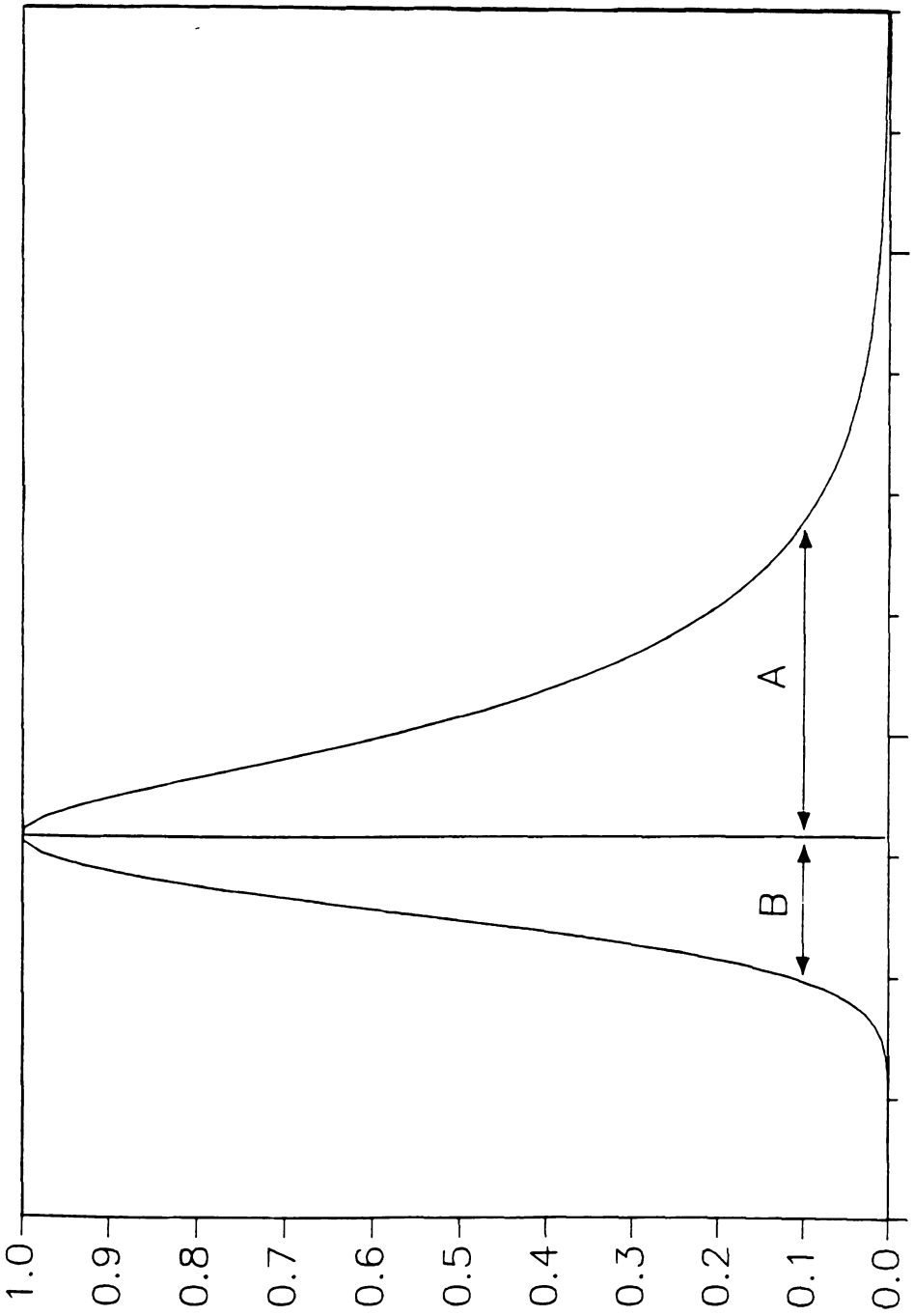

where the zone profile is described as a distribution of the detector response, I(t), as a function of time, t. Although deceptively simple, this method allows mathematical treatment which gives a complete and exact characterization of the profile.

Statistical moments are related to the physical and chemical behavior of the zone profile (Figure 1-5). The zeroth moment expresses the area under the chromatographic peak. The retention time or centroid of the peak can be obtained directly from the first moment. The second moment is the variance or dispersion of the zone profile. Information about the peak asymmetry is derived from the third moment, where the skewness (S) is defined as

$$S = M_3/M_2^{3/2} \qquad [1.33]$$

It is interesting to note that the even statistical moments describe symmetric aspects of the profile, whereas the odd moments characterize asymmetric aspects. The integration variable need not be restricted to time (t) as shown in Equation [1.32], but might alternately represent a distance or volumetric displacement.

Although the method of statistical moments is rigorously correct, calculations are not without difficulties (84,92,103-105). In practice, mathematical calculation is most often performed by finite summation of the detector response across the peak profile. The primary errors in this evaluation arise from the determination of the beginning/ending of the peak and the A/D conversion rate (92,103,104). In addition, as seen from the statistical moments expression (Equation [1.32]), intensity measurements that are farther from the mean are weighted to a greater extent. This increases the imprecision in statistical moment determinations by increasing the influence of data with an inherently lower signal-to-noise ratio. Nonetheless, statistical moments are the

Figure 1-5: Schematic diagram of statistical moments on a zone profile.

Figure 1-5

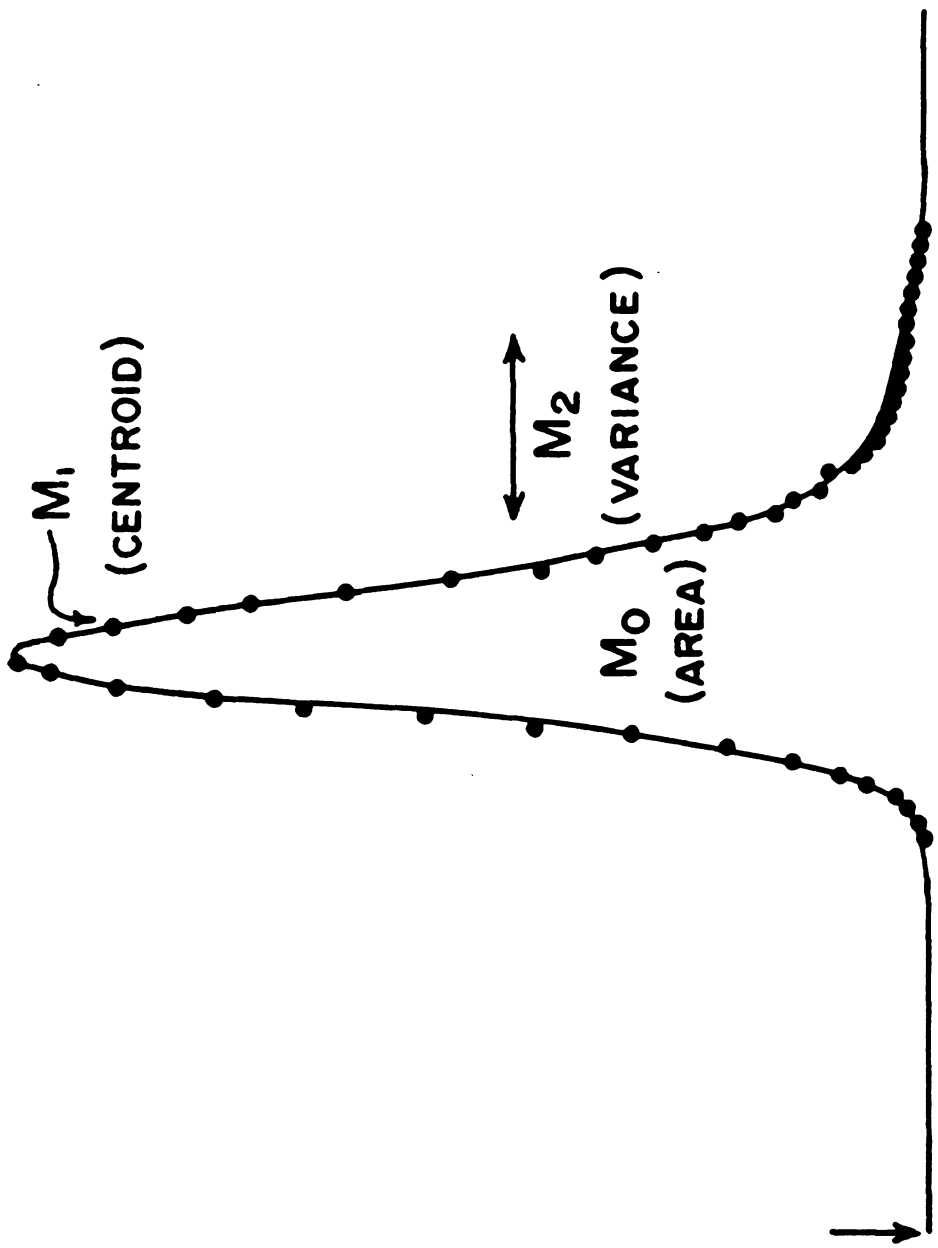

most accurate means to evaluate the fundamental processes influencing the separation.

The choice of calculational method will ultimately depend on the application of interest. If a simple and quick method for determining plate height is necessary, then a Gaussian assumption (Equation [1.23]) or the Foley-Dorsey equation (Equation [1.31]) may be appropriate. However, in the evaluation of fundamental chromatographic parameters, it is of primary importance not to introduce bias by imposing a specific model. Statistical moments appear to be the most accurate method for these fundamental determinations as no *a priori* assumptions are necessary.

Extra-column Variance. A further complication in the determination of fundamental separation parameters is that the measured zone variance may not arise solely from column processes. In practice, a number of processes external to the column may cause dispersion of the solute zone as well. Since the variance developed within the column is of interest in these measurements, extra-column effects can lead to erroneous interpretation of chromatographic processes. Moreover, extra-column sources of variance do not contribute to the separation of solutes, but may cause the overlap of neighboring solute zones. Although these detrimental contributions can be minimized, they cannot be entirely eliminated. Because of the clear importance in the design of instrumentation as well as in the determination of fundamental parameters, the sources and evaluation of extra-column variance have been the subject of numerous investigations (100,106,107).

In evaluating fundamental separation processes, the column variance is often determined directly from the measured zone profile after carefully minimizing all known extra-column sources of variance. In practice, however, it is

difficult to determine if extra-column contributions are truly negligible (108). Alternately, the extra-column variance is estimated (109-111) or measured (112-117) and then subtracted from the total measured variance. This latter method requires that all individual variance contributions are independent, so the total variance may be represented by a simple summation. Unfortunately, the present methods for evaluating the extra-column variance are prone to substantial systematic and random errors (108).

Extra-column dispersion may arise from laminar flow or mixing phenomena in the injection, detection, or connection devices. The finite rate of response of electronic circuitry in detectors, amplifiers, chart recorders, etc. may also contribute to the zone variance. The influence of these detrimental processes on chromatographic performance has been examined comprehensively by Sternberg (100) and by Guiochon and coworkers (109).

If the individual sources of variance are independent (100), the total system variance may be described as a sum of the individual contributions (Appendix 1). In a chromatographic system, the major sources of variance are due to the injection ($(\sigma^2)_{INJ}$), detection ($(\sigma^2)_{DET}$), and connection ($(\sigma^2)_{CONN}$) systems in addition to that due to the column itself ($(\sigma^2)_{COL}$). Therefore,

$$(\sigma^2)_{TOTAL} = (\sigma^2)_{INJ} + (\sigma^2)_{DET} + (\sigma^2)_{CONN} + (\sigma^2)_{COL} = (\sigma^2)_{EX} + (\sigma^2)_{COL} \qquad [1.34]$$

This additivity results in a total measured variance that is always greater than the true column variance. Thus, if the extra-column variance is a significant fraction of the column variance, the total system variance will not accurately reflect the dispersion due to column processes.

One method of expressing the extra-column contribution is as the fractional increase (θ^2) in the volumetric variance expected based on the column variance, $(\sigma_V^2)_{COL}$, and known sources of extra-column variance, $(\sigma_V^2)_{EX}$ (109).

$$\varphi = \frac{(\sigma_y$$
$$(\sigma_y$$

In this
linear
volume
to the

H_{KEAS}

Thus,
prese
heigh
prese
depe
may
dispo

acc
chro
indi
111

vol
(10
de
mi
co

$$\theta^2 = \frac{(\sigma_V^2)_{EX}}{(\sigma_V^2)_{COL}} = \frac{(\sigma_V^2)_{EX}\, u^2}{H_{COL}\,(1+k)^2\, L\, F^2} \qquad [1.35]$$

In this expression, the column plate height (H_{COL}), solute capacity factor (k), and linear velocity (u) are assumed to be constant along the column. At a constant volumetric flowrate (F), the fractional increase in the variance (θ^2) may be related to the measured plate height (H_{MEAS}) by the following expression.

$$H_{MEAS} = H_{COL}\,(1 + \theta^2) \qquad [1.36]$$

Thus, the accuracy of plate height determinations are directly affected by the presence of extra-column sources of variance. In addition, the measured plate height dependence on linear velocity and capacity factor are influenced by the presence of extra-column sources of variance. Whether arising from the actual dependence of $(\sigma_V^2)_{EX}$ on u and k or from Equation [1.35], extra-column effects may lead to misinterpretation of the fundamental processes contributing to dispersion on the chromatographic column (108,118).

As seen above, extra-column effects can play an important role in the accurate determination of the fundamental parameters influencing chromatographic separations. For this reason, it is often informative to estimate individual sources of extra-column dispersion based on ideal conditions (109-111).

The variance contributed by the injection process may arise from the volume of sample injected as well as from the shape of the injected profile (100,109). While the profile shape is primarily dependent on instrumentation design, the choice of injection volume must be a compromise between minimizing extra-column dispersion and maximizing the detection of all sample components. The maximum permissible injection volume (V_{INJ}), which will

produce a fractional (θ^2) increase in the volumetric variance of a nonretained peak, is given by the following equation (109):

$$(\sigma_V^2)_{INJ} = V^2_{INJ}/K^2 = (\theta\ \pi\ r^2\ \varepsilon_T)^2\ H_{COL}\ L \qquad [1.37]$$

The constant K^2 is characteristic of the shape injection profile, and is equal to 12 for an ideal plug or delta function, 1 for an exponential function, and intermediate values for a combination of these injection profiles (100).

The variance arising from the detection process is primarily the result of the finite volume inherent in any detection system. Because the detector responds to an average solute composition in the sensing volume, the detector acts to integrate the actual zone profile. The extra-column variance contributed by the commonly utilized cylindrical flowcell is given by (111):

$$(\sigma_V^2)_{DET} = V^2_{DET}/12 = (\pi\ r^2_{FC}\ L_{FC})^2/12 \qquad [1.38]$$

where V_{DET} is the detection volume in a flowcell of radius r_{FC} and illuminated length L_{FC}. In this expression, dispersion due to flow processes within the detection volume are assumed to be negligible, and only the detector volume itself is considered.

In addition to the detection volume, extra-column dispersion may also arise from the finite rate of response of electronic circuitry (87,100,119). Because any resistor-capacitor network responds in an exponential manner, the amplifiers, and converters necessary for solute detection may contribute to the measured dispersion of a zone profile. The volumetric variance arising from temporal extra-column sources, $(\sigma_V^2)_{RC}$, may be described by the following expression:

$$(\sigma_V^2)_{RC} = (\pi\ r^2\ \varepsilon_T\ u)^2\ \tau_{RC}^2 \qquad [1.39]$$

where τ_{RC} is the RC time constant of the detection system, or the time required for the output signal to reach 63% of the input value. The maximum permissible time constant resulting in a fractional (θ^2) increase in the volumetric variance of a nonretained peak is given by (109,111)

$$\tau_{RC}^2 = \theta^2 H_{COL} L / u^2 \qquad [1.40]$$

If each of these sources of extra-column variance is independent, the total extra-column contribution may be determined by a simple summation as described in Equation [1.34].

Through careful experimental design, these detrimental extra-column effects can be minimized but never entirely eliminated. The maximum permissible injection and detection volumes together with the maximum time constants for conventional and microcolumn applications are summarized in Table 1.2. These values, calculated from Equations [1.37], [1.38], and [1.40], represent a fractional increase (θ^2) of 0.05 which is often considered acceptable in the design of instrumentation. As can be seen in Table 1.2, the design requirements for microcolumn applications are quite stringent. Even if these requirements are successfully met ($\theta^2 = 0.05$), the variance measured is at least 15% greater than the variance of the column itself. While many techniques have been developed to minimize these extra-column sources of dispersion (120,121), none has been able to eliminate the errors inherent in the measurement of true column variance.

Several methods of measurement are commonly utilized as an alternative to the estimation of extra-column variance. In the first method, the variance of the system is measured with all instrumental components in place except the column. Because of complications in obtaining identical flow conditions without the column present, a minimum of 5% deviation from the actual extra-column

Table 1.

COLUM

conven
(4.

microb
(1.

packe
(0.

open-
(0
(0

a M
d

b C
=

Table 1.2: Maximum variance, volume, and time constant for injection and detection systems.

COLUMN TYPE	$(\sigma^2)_{COL}$[a]	$(\sigma^2)_{INJ/DET}$[b]	$V_{INJ/DET}$[b]	τ_{RC}[b]
conventional (4.6 mm x 0.25 m)	570 μL^2	29 μL^2	19 μL	0.14 s
microbore (1.0 mm x 0.50 m)	2.6 μL^2	0.13 μL^2	1.2 μL	0.19 s
packed capillary (0.20 mm x 1.0 m)	0.0082 μL^2	410 nL^2	70 nL	0.27 s
open-tubular capillary (0.040 mm x 3.0 m)	55 nL^2	2.7 nL^2	5.7 nL	3.8 s
(0.010 mm x 5.0 m)	0.089 nL^2	0.0045 nL^2	0.23 nL	0.61 s

[a] Minimum plate height and no retention ($k = 0$) assumed. Packed columns: $d_p = 5\ \mu m$, $\varepsilon_T = 0.85$. Open-tubular columns: $\varepsilon_T = 1$.

[b] Optimum velocity with $D_M = 10^{-5}\ cm^2/s$ assumed. Plug injection assumed ($K^2 = 12$) and 5% increase in variance ($\theta^2 = 0.05$) allowed.

variance
the me
calculat
the ext
depend
column
measu
determ
metho
in cor
accur
techn
and
proce

diffic
expe
the

1.5

me
ap
m
ac

variance is expected (108,112,115). In the second approach, linear regression of the measured peak variance with the square of the retention volume is calculated. The variance at zero retention volume is then used as an estimate of the extra-column variance (108,116,117). Because the column variance is dependent on solute capacity factor, this approach will underestimate the extra-column variance by ~15-20% (108). In the final method, the zone variance is measured as a function of the column length. The extra-column variance is then determined by extrapolating the measured variance to zero distance. This method requires that the variance is constant along the column and any change in connections does not influence the measured variance. Unfortunately, the accuracy and precision of this method is presently unknown. None of these techniques, however, is sufficiently well-characterized or provides the accuracy and precision necessary for the determination of the fundamental column processes (108).

Thus, the accurate measurement of column dispersion remains a major difficulty in fundamental studies of chromatographic separations. This experimental shortcoming seriously limits the verification of theoretical models of the chromatographic process.

1.5 Direct On-Column Detection Scheme

In this dissertation, a novel approach to the accurate experimental measurement of solute retention and dispersion is proposed, verified, and applied to separation problems of fundamental interest. The accurate measurement of separation processes, exclusive of extra-column effects, is accomplished by detecting solute zones as they traverse the chromatographic

column. By positioning two detectors directly on the column, the local retention and dispersion arising between detectors may be measured. This concept is illustrated graphically in Figure 1-6. If all contributions to the dispersion are independent, the zone variance measured at the first detector is simply the sum of all processes up to and including detector 1. The solute zone then migrates along the column and is detected by the second detector. The variance measured at this detector, likewise, includes all processes up to the point of detection. By calculation of the simple arithmetic difference between the variances measured at the two identical detectors, extra-column sources of dispersion can be effectively canceled. Therefore, any difference in zone characteristics between the two detectors will be primarily the result of hydrodynamic and kinetic processes within the column proper.

This detection scheme makes possible fundamental studies of column performance and separation mechanisms previously deemed impossible. Detailed investigations of the hydrodynamics and chemical interactions present during the separation will yield the understanding necessary to minimize zone dispersion, thus increasing the separation performance. With access to any point along the column, local environment effects often assumed to be uniform may be directly probed. Therefore, true optimization of factors affecting both zone dispersion and differential migration rate, necessary for difficult separations in complex matrices, can be realized.

In this dissertation, the validity of this approach is verified utilizing open-tubular capillaries. The technique is then applied to the measurement of retention and dispersion as a function of distance along packed capillary columns. Nearly ideal chromatographic and spectroscopic conditions are utilized throughout these preliminary investigations. The understanding gained in this endeavor may then be applied to the less ideal conditions commonly

Figure 1-6: Illustration of the on-column measurement of variance for a single solute zone.

Figure 1-6

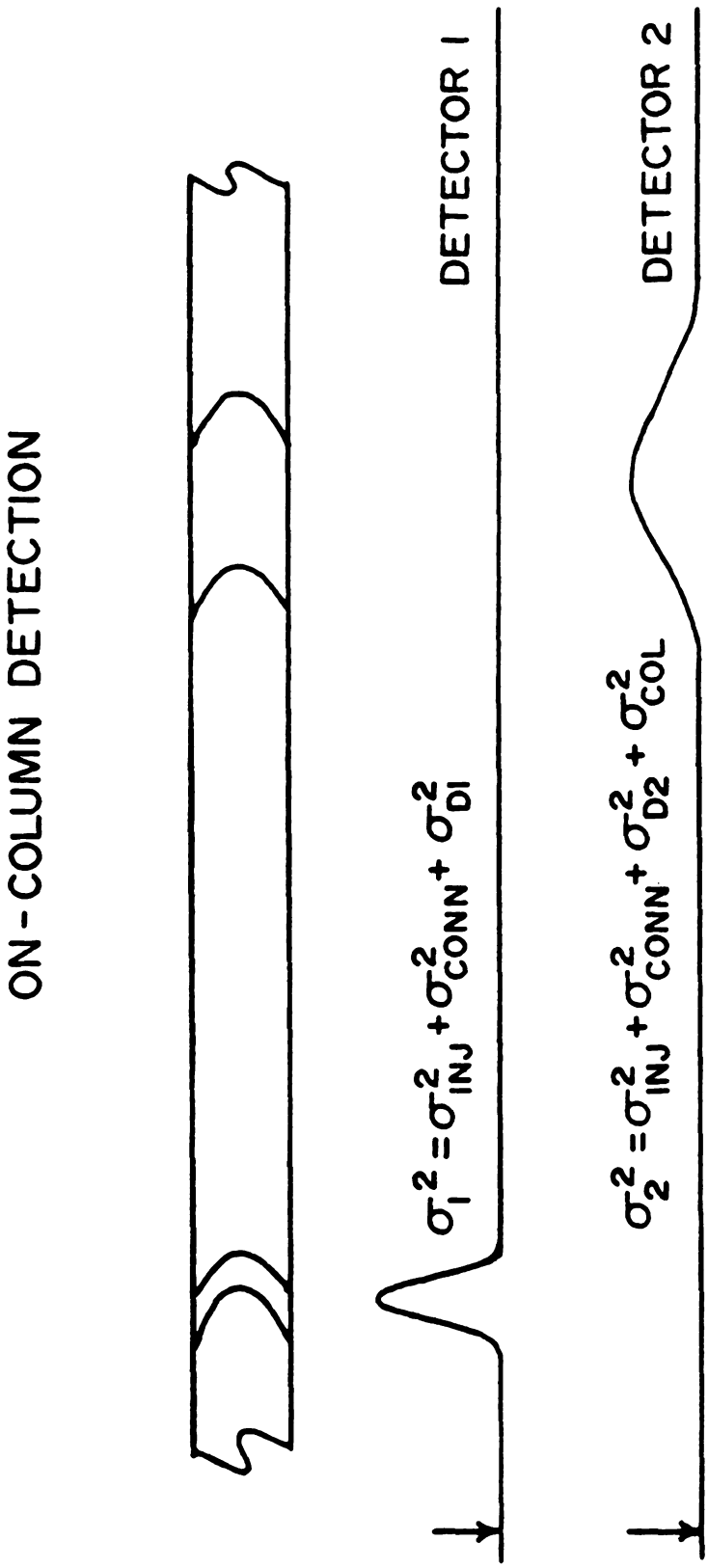
ON-COLUMN DETECTION
DETECTOR 1
DETECTOR 2
$\sigma_1^2 = \sigma_{INJ}^2 + \sigma_{CONN}^2 + \sigma_{D1}^2$
$\sigma_2^2 = \sigma_{INJ}^2 + \sigma_{CONN}^2 + \sigma_{D2}^2 + \sigma_{COL}^2$

encounte
understa
may be
systema

encountered in practical applications. It is hoped that by this increased understanding, column technology as well as chromatographic system design may be significantly advanced and the separation of complex mixtures systematically improved.

1.6 Literature Cited in Chapter 1

1. Martin, A.J.P.; Synge, R.L.M. *Biochem. J.* **1941**, *35*, 1358.
2. Davis, J.M.; Giddings, J.C. *Anal. Chem.* **1983**, *55*, 418.
3. Knox, J.H. *J. Chromatogr. Sci.* **1980**, *18*, 453.
4. Scott, R.P.W. *Small-bore Liquid Chromatography Columns*; Wiley: New York, **1984**.
5. Novotny, M.V.; Ishii, D. *Microcolumn Separations*; Elsevier: Amsterdam, **1985**.
6. de Wit, J.S.M.; Parker, C.E.; Tomer, K.B.; Jorgenson, J.W. *Anal. Chem.* **1987**, *59*, 2400.
7. Guthrie, E.J.; Jorgenson, J.W.; Dluzneski, P.R. *J. Chromatogr. Sci.* **1984**, *22*, 171.
8. Locke, D.C. *J. Chromatogr. Sci.* **1977**, *15*, 393.
9. Horvath, Cs.; Melander, W.; Molnar, I. *J. Chromatogr.* **1976**, *125*, 129.
10. Horvath, Cs.; Melander, W. *J. Chromatogr. Sci.* **1977**, *15*, 393.
11. Tijssen, R.; Billiet, H.A.H.; Schoenmakers, P.J. *J. Chromatogr.* **1976**, *122*, 185.
12. Schoenmakers, P.J.; Billiet, H.A.H.; deGalan, L. *Chromatographia* **1982**, *15*, 205.
13. Dill, K.A. *J. Phys. Chem.* **1987**, *91*, 1980.
14. Katz, E.D.; Ogan, K.; Scott, R.P.W. *J. Chromatogr.* **1986**, *352*, 67.
15. Martire, D.E. *J. Liq. Chromatogr.* **1987**, *10*, 1569.
16. Martire, D.E.; Boehm, R.E. *J. Phys. Chem.* **1987**, *91*, 2433.
17. Cheong, W.J.; Carr, P.W. *J. Chromatogr.* **1990**, *499*, 373.
18. Unger, K.K. *Packings and Stationary Phases in Chromatographic Techniques*, Marcel Dekker: New York, **1990**, pp. 235-250.
19. Smith, D.L.; Cooper, W.T. *Chromatographia* **1988**, *25*, 55.
20. Yamamoto, F.M.; Rokushika, S. *J. Chromatogr.* **1990**, *515*, 3.
21. Kuppers, J.R.; Carriker, N.E. *J. Magn. Resonance* **1971**, *5*, 73.
22. McCown, S.M.; Southern, D.; Morrison, B.E.; Gartiez, D. *J. Chromatogr.* **1986**, *352*, 465.

23. Street, K.W.; Acree, W.E. *J. Liq. Chromatogr.* **1986**, *9*, 2799.

24. Cheong, W.J.; Carr, P.W. *Anal. Chem.* **1988**, *60*, 820.

25. Martire, D.E. *J. Chromatogr.* **1988**, *452*, 17.

26. Funasaki, N.; Hada, S.; Neya, S. *J. Chromatogr.* **1986**, *561*, 33 and references cited therein.

27. Johnson, B.P.; Khaledi, M.G.; Dorsey, J.G. *J. Chromatogr.* **1987**, *384*, 221.

28. Michels, J.J.; Dorsey, J.G. *J. Chromatogr.* **1988**, *457*, 85.

29. Carr, J.W.; Harris, J.M. *Anal. Chem.* **1986**, *58*, 626.

30. Hildebrand, J.; Scott, R. *Regular Solutions*, Prentice-Hall: Englewood Cliffs, New Jersey, **1962**.

31. Hildebrand, J.; Scott, R. *Solubility of Non-Electrolytes*, Reinhold: New York, **1949**.

32. Schoenmakers, P.J.; Billiet, H.A.H.; deGalan, L. *J. Chromatogr.* **1981**, *218*, 261.

33. Giddings, J.C.; Myers, M.N.; McLaren, L.; Keller, R.A. *Science* **1968**, *162*, 67.

34. Barton, A.F.M. *Chem. Rev.* **1975**, *75*, 731.

35. McCormick, R.M.; Karger, B.L. *Anal. Chem.* **1980**, *52*, 2249.

36. Alhedai, A.; Martire, D.E.; Scott, R.P.W. *Analyst* **1989**, *114*, 869.

37. Martin, M.; Blu, G.; Eon, C; Guiochon, G. *J. Chromatogr.* **1975**, *112*, 399.

38. Bakalyar, S.R.; Henry, R.A. *J. Chromatogr.* **1976**, *126*, 327.

39. Foley, J.P.; Crow, J.A.; Thomas, B.A.; Zamora, M. *J. Chromatogr.* **1989**, *478*, 287.

40. Giddings, J.C. *J. Chromatogr.* **1987**, *395*, 19.

41. Davis, J.M.; Giddings, J.C. *Anal. Chem.* **1985**, *57*, 2168.

42. Davis, J.M.; Giddings, J.C. *Anal. Chem.* **1985**, *57*, 2178.

43. Poiseuille, J.L.M. *Mem. des Savants Estrang.* **1846**, 9.

44. Taylor, G. *Proc. Roy. Soc. (London)*, **1953**, *219A*, 186.

45. Aris, R. *Proc. Roy. Soc. (London)*, **1956**, *235A*, 67.

46. Westhaver, J.W. *J. Res. Nat. Bur. Stand.* **1947**, *38*, 169.

47. Golay, M.J.E.; Atwood, J.G. *J. Chromatogr.* **1979**, *186*, 353.

48. Atwood, J.G.; Golay, M.J.E. *J. Chromatogr.* **1981**, *218*, 97.

49. Paine, M.A.; Carbonell, R.G.; Whitaker, S. *Chem. Eng. Sci.* **1983**, *38*, 1781.

50. Golay, M.J.E. in *Gas Chromatography 1958*, D.H. Desty, Ed.; Butterworths, London, **1958**, pp. 36-55.

51. Fick, A. *Ann. Phys. Lpz.* **1855**, *170*, 59.

52. Einstein, A. *Ann. der Physik* **1905**, *17*, 549.

53. Clifford, A.A. *J. Chromatogr.* **1989**, *471*, 61.

54. Stokes, G.G. *Trans. Cambridge Phil. Soc.* **1845**, *8*, 287,

55. Darcy, H. *Les Fontaines Publiques de la ville de Dijon*, **1856**, Dalmont, Paris.

56. Kozeny, J.S.B. *Akad. Wiss. Wien., Abt., IIa* **1927**, *136*, 271.

57. Carman, P.C. *Trans. Inst. Chem. Eng. London* **1937**, *15*, 150.

58. Unger, K.K. *Porous Silica*; Elsevier: Amsterdam, **1979**, pp. 170-173.

59. McCormick, R.H. in *An Introduction to Separation Science*; Karger, B.L.; Snyder, L.R.; Horvath, C. Eds.; 1975, Wiley: New York, pp. 181-210.

60. Giddings, J.C. *Dynamics of Chromatography*; Marcel Dekker, Inc.: New York, **1965**, pp. 20-26.

61. Giddings, J.C. *J. Chem. Ed.* **1958**, *35*, 588.

62. Jones, W.L.; Kieselbach; R. *Anal. Chem.* **1958**, *30*, 1590.

63. Lapidus, L.; Amundson, N.R. *J. Phys. Chem.* **1952**, *56*, 984.

64. Kucera, E. *J. Chromatogr.* **1965**, *19*, 237.

65. Grushka, E. *J. Phys. Chem.* **1972**, *76*, 2586.

66. Horvath, C.; Lin, H.J. *J. Chromatogr.* **1976**, *126*, 401.

67. Horvath, C.; Lin, H.J. *J. Chromatogr.* **1978**, *149*, 43.

68. Giddings, J.C. *J. Chem. Phys.* **1957**, *26*, 1755.

69. Giddings, J.C. *Dynamics of Chromatography*; Marcel Dekker, Inc.: New York, **1965**, pp. 95-193.

70. van Deemter, J.J.; Zuiderweg, F.J.; Klinkenberg, A. *Chem. Eng. Sci.* **1956**, *5*, 271.

71. We
Bro

72. Gio
Yo

73. Gi

74. Gi

75. Kr

76. Th

77. G
Y

78. D

79. K

80. H

81. H

82. F

83. I

84.

85.

86.

87.

88.

89.

90.

91.

92.

93.

94.

95.

71. Weber, S.G.; Carr, P.W. in *High Performance Liquid Chromatography*; Brown, P.R. and Hartwick, R.A., Eds.; Wiley: New York, pp. 1-115.

72. Giddings, J.C. *Dynamics of Chromatography*; Marcel Dekker, Inc.: New York, **1965**, pp. 49-60.

73. Giddings, J.C. *Anal. Chem.* **1962**, *34*, 1186.

74. Giddings, J.C. *Anal. Chem.* **1963**, *35*, 1338.

75. Knox, J.; McLaren, L. *Anal. Chem.* **1964**, *36*, 1477.

76. Thumneum, P.; Hawkes, S. *Chromatographia* **1981**; *14*, 576.

77. Giddings, J.C. *Dynamics of Chromatography*; Marcel Dekker, Inc.: New York, **1965**, pp. 142-149.

78. Done, J.N.; Knox, J.H. *J. Chromatogr. Sci.* **1972**, *10*, 606.

79. Knox, J.H. *J. Chromatogr. Sci.* **1977**, *15*, 352.

80. Huber, J.F.K.; Hulsman, J.A.R.J. *Anal. Chim. Acta* **1967**, *38*, 305.

81. Knox, J.H. *J. Chromatogr. Sci.* **1980**, *18*, 453.

82. Pauls, R.E.; Rogers, L.B. *Sep. Sci.* **1977**, *12*, 395.

83. Bidlingmeyer, B.A.; Warren, F.V. Jr. *Anal. Chem.* **1984**, *56*, 1583A.

84. Schudel, J.V.H.; Guiochon, G. *J. Chromatogr.* **1988**, *457*, 1.

85. Papas, A.N. *CRC Crit. Rev. Anal. Chem.* **1989**, *20(6)*, 359.

86. Ball, D.; Harris, W.; Habgood, H. *Sep. Sci.* **1967**, *2*, 81.

87. Schmauch, L.J. *Anal. Chem.* **1959**, *31*, 225.

88. Johnson, H.W.; Stross, F.H. *Anal. Chem.* **1959**, *31*, 357.

89. Grushka, E. *Anal. Chem.* **1972**, *44*, 1733.

90. Barber, W.E.; Carr, P.W. *Anal. Chem.* **1981**, *53*, 1939.

91. Foley, J.P.; Dorsey, J.G. *Anal. Chem.* **1983**, *55*, 730.

92. Anderson, D.J.; Walters, R.R. *J. Chromatogr. Sci.* **1984**, *22*, 353.

93. Delley, R. *Anal. Chem.* **1985**, *57*, 388.

94. Hanggi, D.; Carr, P.W. *Anal. Chem.* **1985**, *57*, 2394.

95. Kucera, E. *J. Chromatogr.* **1965**, *19*, 273.

96. Anderson, A.H.; Gibb, T.C.; Littlewood, A.B. *J. Chromatogr. Sci.* **1970**, *8*, 640.

97. Chesler, S.N.; Cram, S.P. *Anal. Chem.* **1973**, *45*, 1354.

98. Mott, S.D.; Grushka, E. *J. Chromatogr.* **1979**, *186*, 117.

99. Dondi, F. *Anal. Chem.* **1982**, *54*, 473.

100. Sternberg, J.C. in *Advances in Chromatography*; Giddings, J.C.; Keller, R.A. Eds.; 1966; Vol. 2, pp. 205-270.

101. Grubner, O. *Adv. Chromatogr.* **1968**, *6*, 173.

102. Grushka, E.; Myers, M.N.; Schettler, P.D.; Giddings, J.C. *Anal. Chem.* **1969**, *41*, 889.

103. Chesler, S.N.; Cram, S.P. *Anal. Chem.* **1971**, *43*, 1922.

104. Chesler, S.N.; Cram, S.P. *Anal. Chem.* **1972**, *44*, 2240.

105. Eikens, D.I.; Carr, P.W. *Anal. Chem.* **1989**, *61*, 1058.

106. Kirkland, J.J. *J. Chromatogr. Sci.* **1969**, *7*, 7.

107. Halasz, I.; Walking, P. *J. Chromatogr. Sci.* **1969**, *7*, 129.

108. Huber, J.F.K.; Rizzi, A. *J. Chromatogr.* **1987**, *384*, 337.

109. Martin, M.; Eon, C.; Guiochon, G. *J. Chromatogr.* **1975**, *108*, 229.

110. Yang, F.J. *J. Chromatogr. Sci.* **1982**, *20*, 241.

111. McGuffin, V.L. Ph.D. Dissertation, Indiana University, Bloomington, IN, **1983**.

112. Lauer, H.H.; Rozing, G.P. *Chromatographia* **1981**, *14*, 641.

113. Freebairn, K.W.; Knox, J.H. *Chromatographia* **1984**, *19*, 37.

114. Scott, R.P.W.; Simpson, C.F. *J. Chromatogr. Sci.* **1982**, *20*, 62.

115. Hupe, K.P.; Jonker, R.J.; Rozing, G. *J. Chromatogr.* **1984**, *285*, 253.

116. Kutner, W.; Debowski, J.; Kemula, W. *J. Chromatogr.* **1981**, *218*, 45.

117. Kok, W.Th.; Brinkman, U.A.Th.; Frei, R.W.; Hanekamp, H.B.; Nooitgedacht, F.; Poppe, H. *J. Chromatogr.* **1982**, *237*, 357.

118. Gaspar, G.; Annino, R.; Vidal-Madjar, C.; Guiochon, G. *Anal. Chem.* **1978**, *50*, 1512.

119. McWilliams, G.; Bolton, H.C. *Anal. Chem.* **1969**, *41*, 1755.

120.

121.

120. Novotny, M.; McGuffin, V.L. *Anal. Chem.* **1983**, *55*, 580.

121. Jorgenson, J.W.; Guthrie, E.J. *Anal. Chem.* **1984**, *56*, 483.

APPENDIX 1: ADDITIVITY OF VARIANCES

In chromatographic separations a variety of processes contribute to the overall dispersion, making the characterization of individual processes very difficult. In an effort to simplify theoretical treatment and experimental evaluation, it is often assumed that each process is independent of all others. Under these circumstances, the dispersion or variance (σ^2) contributed by each process may be considered to be additive (1). Thus, the total variance of the chromatographic system may be described by the variance arising from each process, $(\sigma^2)_i$, summed over all processes.

$$(\sigma^2)_{TOTAL} = \Sigma\,(\sigma^2)_i \qquad [A.1]$$

In this equation, the variance may be expressed in either time (σ_T^2), length (σ_L^2), or volume (σ_V^2) units. It is often assumed that these domains represent the variance of the solute zone equivalently and, as such, may be used interchangeably without introducing error. This is not true, however, when nonuniformities within the separation system alter the rate of effluent movement (2).

Unfortunately, nonuniformities are an integral part of any separation system. Changes in linear velocity, for example, arise from variations in the tubing diameter or from the transition from the injector to the packed chromatographic column. Changes in the volumetric flowrate result directly from compressibility of the effluent with pressure, as well as from the addition or subtraction of effluent, as may occur in a post-column reaction system or a split injection system, respectively. In each of these nonuniform regions, the solute zone variance in the time domain increases solely as a result of normal band broadening processes, whereas that in the length and volume domain may

exhibit a further increase or decrease due to variations in flowrate. Although this latter broadening process does not alter the separation resolution, it does yield individual variance contributions in the length and volume domains that are no longer independent.

A mass-balance argument may be employed to understand the nature of this broadening process more clearly. It will be assumed that no material is gained or lost due to irreversible adsorption in the system. Thus, under steady-state conditions, the mass flowrate (dm/dt) of the column effluent is uniform throughout the separation system. That is,

$$dm/dt = \text{constant} \qquad [A.2]$$

The time necessary to move a given mass, in this case, is also constant. Under these constant mass flowrate conditions, the rate of effluent movement and thus, the time distribution of the solute, will be altered only by normal broadening processes.

This is not true, however, for the length distribution of the same solute zone. Because the mass flowrate with time must remain constant under steady-state conditions, the change in the mass per unit length (dm/dx) must vary inversely with the zone velocity (U).

$$dm/dt = \text{constant} = (dm/dx)\,(U) = (dm/dx)\,(dx/dt) \qquad [A.3]$$

Thus, variations in the linear velocity will result in a change in the mass of effluent per unit length. This variation in effluent movement yields a concomitant change in the solute zone profile and variance as a function of length, irrespective of any normal band broadening processes. This effect is illustrated schematically in Figure A-1 for a simple change in tubing diameter. In this case, the linear velocity (dx/dt) in the smaller outlet tube is greater than that in the inlet, while the

Figure A-1: Effect of change in linear velocity (dx/dt) on solute zone variance in the time, length, and volume domains.

Figure A-1

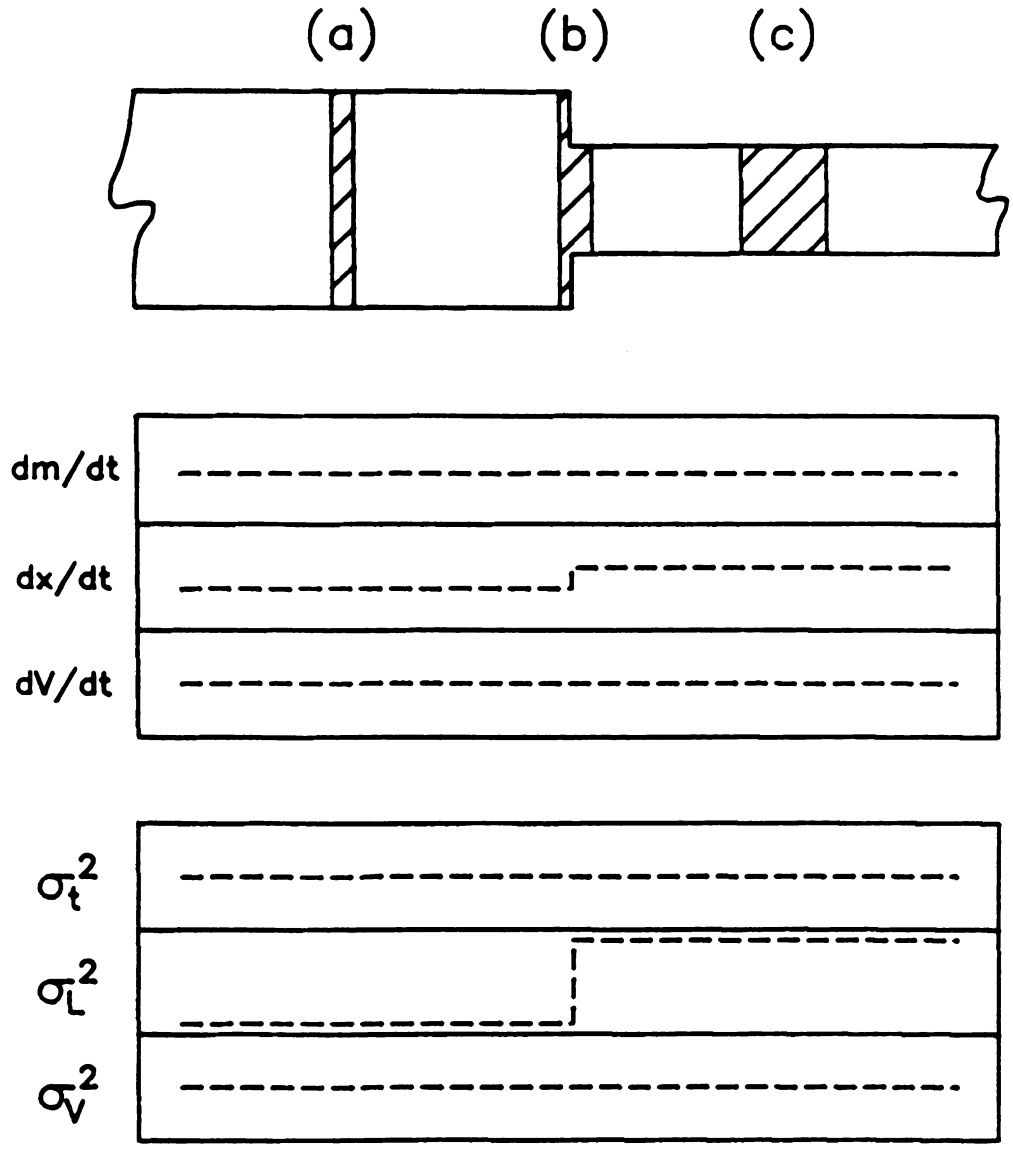

mass flowrate with time (dm/dt) and volumetric flowrate (F = dV/dt) remain constant. Thus, when the solute zone encounters the interface between the tubes (Figure A-1b), the front of the zone proceeds at the higher linear velocity, while the rear of the zone maintains the slower initial velocity. It becomes clear from the relationship between time and length variance,

$$\sigma_T^2 = \sigma_L^2 / U^2 = \sigma_V^2 / F^2 \qquad [A.4]$$

that an increase in the length variance of the zone is expected solely due to the increase in linear velocity, while the time and volume variances of the same zone will remain constant.

Likewise, variations in the volumetric flowrate (F) of the effluent along the system will affect the mass of effluent and, thus, solute per unit volume (dm/dV).

$$dm/dt = \text{constant} = (dm/dV)\,(F) = (dm/dV)\,(dV/dt) \qquad [A.5]$$

This nonuniformity in the volumetric flowrate resulting from an additional flow is shown schematically in Figure A-2. To simplify this illustration, the tubing diameters are chosen such that the mass flowrate (dm/dt) and the linear velocity (dx/dt) are constant throughout, while the volumetric flowrate (dV/dt) is greater in the outlet tube. Thus, the increased cross-section and volumetric flowrate in the outlet tube yield an increase in the volume variance (Equation [A.4]), with the time and length variances remaining constant.

It becomes clear from these examples, that any solute zone distribution and the associated variance expressed in length or volume units are influenced by nonuniformities in linear velocity and volumetric flowrate within the separation system. In contrast, the same solute distribution represented in the time domain will be unaffected by these nonuniformities, provided that the mass flowrate remains constant. As a consequence, sources of variance that are considered

Figure A-2: Effect of change in volumetric flowrate (dV/dt) on solute zone variance in the time, length, and volume domains.

Figure A-2

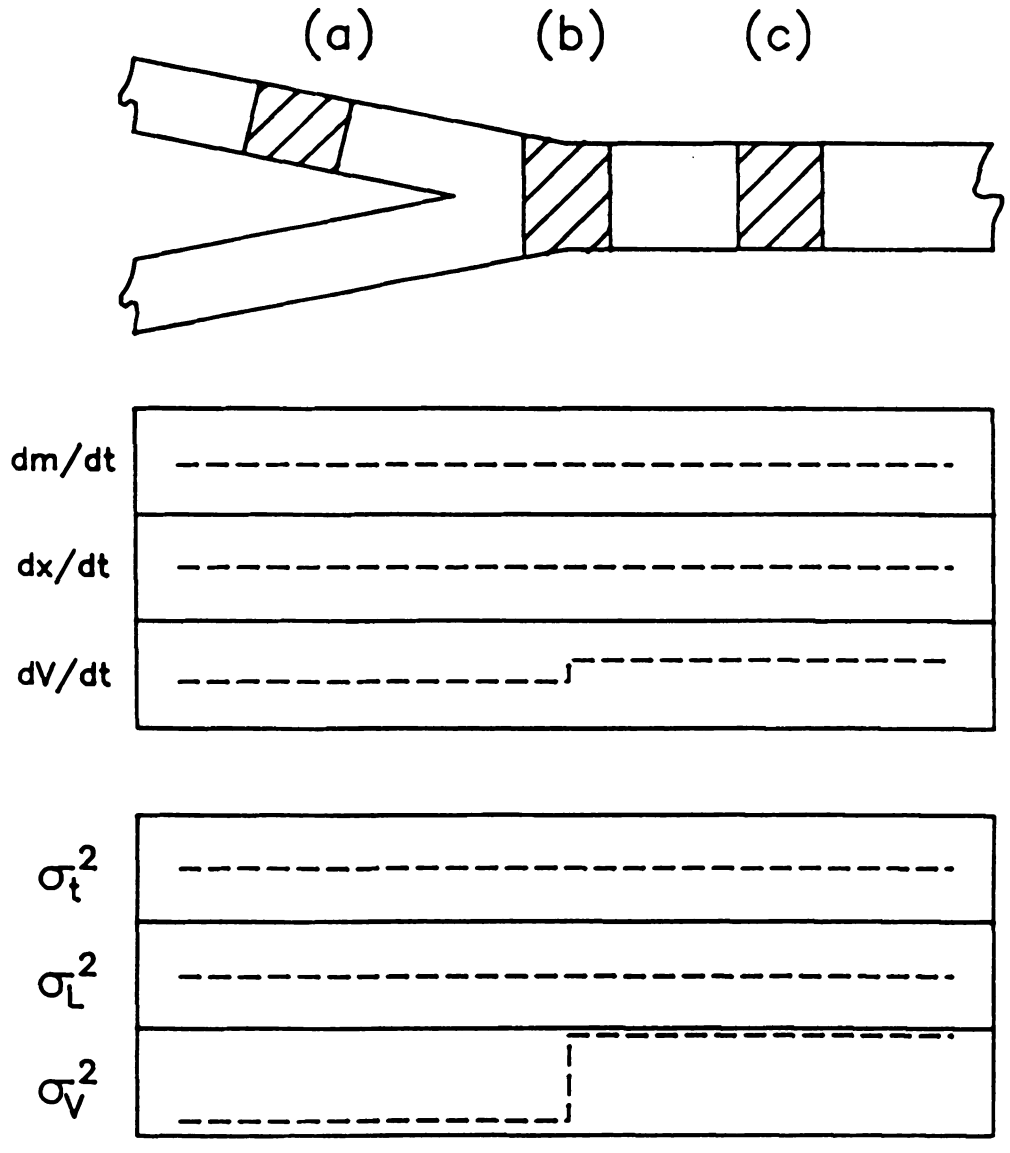

independent
domains by
Because se
be exercise
measured
considered

independent in the time domain, become dependent in the length and volume domains by virtue of these variations in velocity and volumetric flowrate. Because separation systems by their very nature are nonuniform, caution must be exercised in the determination of individual variance values from the total measured variance. **Ultimately, variance values or expressions must be considered rigorously independent and additive only in the time domain.**

Literatur

1. S
R

2. G
Y

Literature Cited in Appendix 1

1. Sternberg, J.C. in *Advances in Chromatography*; Giddings, J.C.; Keller, R.A. Eds.; Marcel Dekker, Inc.: New York, **1966**; Vol. 2, pp. 205-270.

2. Giddings, J.C. *Dynamics of Chromatography*; Marcel Dekker, Inc.: New York, **1965**; pp. 79-84.

2.1 Int

the col
with th
interfe
colum
analyt
detec
the a
the p
utility
a pac
techn
direc
rece

CHAPTER 2

FABRICATION OF ON-COLUMN FLUORESCENCE DETECTION SYSTEM

2.1 Introduction

Implementation of the dual on-column detection concept requires that both the column body and the packing material or stationary phase do not interfere with the desired detection technique. Likewise, the detection technique must not interfere with the packing structure or hydrodynamics of the chromatographic column. Unfortunately, these criteria are satisfied only by a limited number of analytical techniques. Electrochemical (1), absorption (2), and fluorescence (3-8) detection methods have met with some success for probing the column in either the axial or radial direction. Electrochemical detection may cause disruption in the packing structure, however, even when microelectrodes are employed. The utility of absorbance detection is somewhat limited by the diminished sensitivity in a packed bed system. Fluorescence detection appears to be the most promising technique, allowing sensitive as well as selective detection of solute zones directly on the packed bed. The feasibility of fluorescence detection has been recently demonstrated with both packed and open-tubular microcolumns

fabricated from optically transparent fused-silica capillaries (3-8). In addition, laser-induced fluorescence provides a very sensitive means of detection (9-11), with recent reports of subattomole detection limits (12). Thus, laser-induced fluorescence detection seems particularly well suited for the implementation of the dual on-column detection scheme.

2.2 Instrumentation

In designing and fabricating the dual on-column detection system, it is necessary for the dispersion characteristics of the two, mobile detectors to be well matched. To this end, all mechanical, optical, and electronic components used to fabricate the two detection systems are chosen to be identical. This includes carefully matched components for the individual detector blocks, emission collection systems, and current-to-voltage converters. In addition, the chromatographic system is designed for near theoretical performance, and therefore, every precaution is taken to minimize all known sources of extra-column variance.

Chromatographic System. A diagram of the chromatographic system used in this research is illustrated in Figure 2-1. Solvent delivery is accomplished through the use of a dual-syringe micropump (Applied Biosystems, MPLC Model MG) operated in the constant flow mode. The effluent is split between the microcolumn and a restricting capillary (1:20 to 1:2000). Samples are introduced by the split injection method by using a 1.0-μL valve injector (Valco, Model EC14W1.) with the aforementioned split ratios. The microcolumn is either an open-tubular capillary, used for verification studies, or a packed capillary described below.

Figure 2-1: Schematic diagram of microcolumn liquid chromatography system with dual on-column laser fluorescence detection system: I, injection valve; T, splitting tee; R, restricting capillary; L, lens; F, filter; FO, fiber optics; FOP, fiber-optic positioner; M, monochromator; PMT, photomultiplier tube; AMP, amplifier; REC, chart recorder or computer.

Figure 2-1

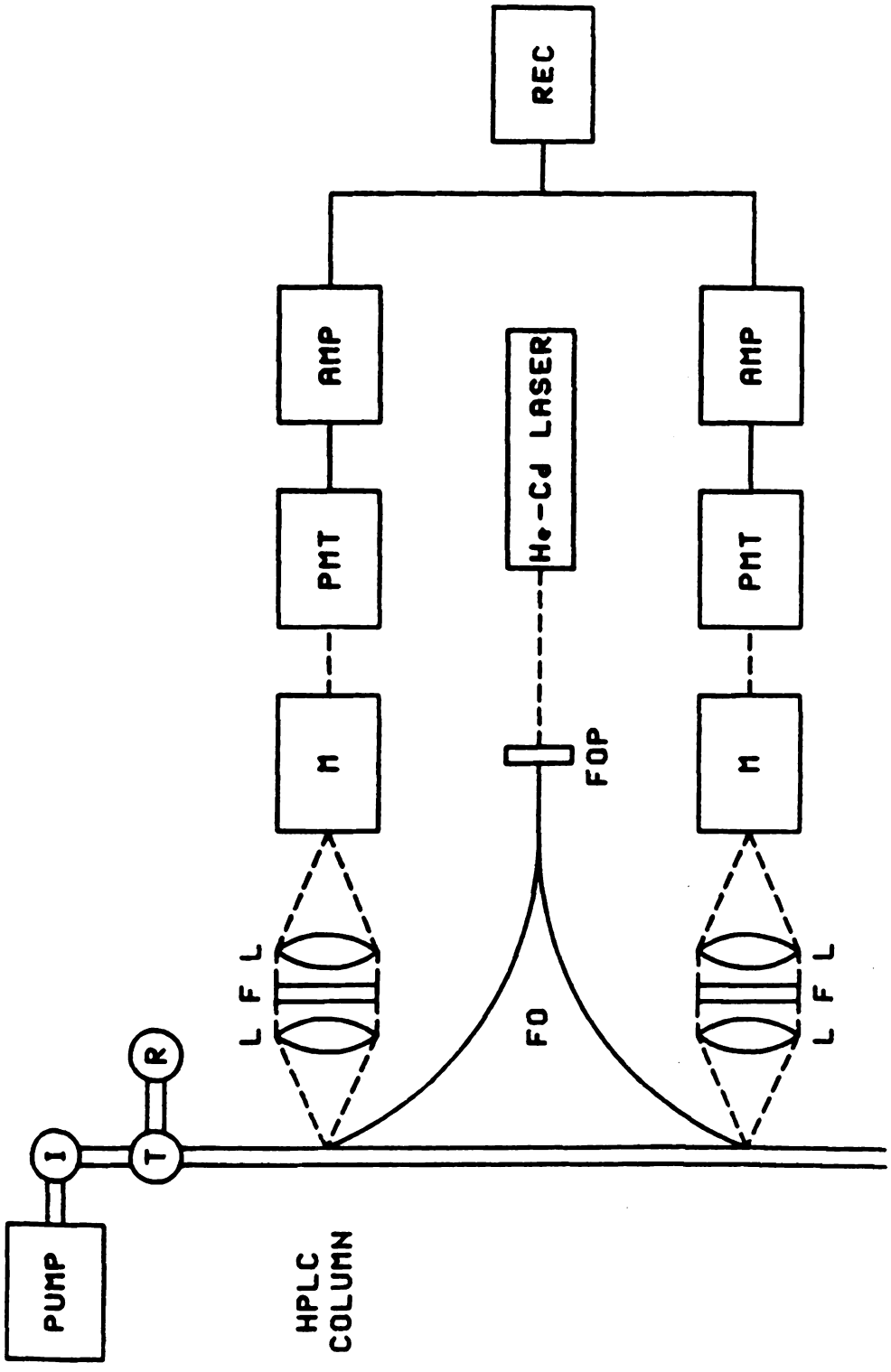
REC
AMP
PMT
M
He-Cd LASER
FOP
FO
LFL
AMP
PMT
M
LFL
R
I
T
PUMP
HPLC
COLUMN

Microc
obtaine
modifica
tubing
to pack
position
porous
packin
moder
theore
100,0

On-C
syste
allow
in Fi
311
sour
micr
Tec
emi
dia
the
foc
H1
(H
do

Microcolumn Preparation. The open-tubular capillary column of 40 μm i.d. is obtained from Polymicro Technologies and is used without further surface modification. Packed capillary columns are prepared from fused-silica capillary tubing of 0.220 mm i.d. and approximately 1 m in length (Hewlett-Packard). Prior to packing, the polyimide coating is removed from the capillary at the detection positions of interest, and the column is terminated with either a quartz wool or a porous teflon frit (13). An acetone slurry of 3 μm spherical octadecylsilica packing material (Varian, MicroPak SP) is then forced into this tube under moderate pressure (14). Microcolumns prepared in this manner approach the theoretical limits of efficiency and can readily achieve plate numbers in excess of 100,000 (14).

On-Column Laser-Induced Fluorescence Detector. The on-column detection system uses two or more parallel detectors with carefully matched components to allow direct correlation of the zone profiles calculated at each detector. As shown in Figure 2-1, a continuous-wave helium-cadmium laser (Omnichrome, Model 3112-10S), with 10 mW output power at 325 nm, is utilized as the excitation source for each fluorescence detector. Laser radiation is transmitted to the microcolumn via small diameter (100 μm), UV-grade optical fibers (Polymicro Technologies), which are positioned in two, mobile detector blocks. Fluorescent emission is collected in a right-angle geometry with an optical fiber of larger diameter (500 μm). A long-pass filter (Corion; $\lambda > 400$ nm) is utilized to reduce the scattered and second-order radiation, and the fluorescent emission is focussed on the entrance slit of a monochromator (Instruments SA, Model H1061). The resultant emission is transmitted to a photomultiplier tube (Hamamatsu, R1463), subsequently amplified and converted to the voltage domain with matching current-to-voltage converter circuits. Analog-to-digital

conversi

accomp

from ea

microco

data a

softwar

Calcul

determ

discus

been

metho

most

integr

summ

M_0 =

M_1 =

M_2 =

M_4 =

The

sum

data

sta

Eq

m

conversion (Data Translation, Model 3405/5716) of the resultant voltage is accomplished with a resolution of 16 bits over a 100 nA range. Chromatograms from each detector block may be acquired simultaneously, and stored on a microcomputer (IBM PC-XT) as well as displayed in real time. Algorithms for data acquisition and calculations are written using the Forth-based Asyst software (Macmillan).

Calculations. Statistical moments are chosen as the most accurate means to determine the retention time and dispersion of each solute zone (15). As discussed in Chapter 1, the use of statistical moments in chromatography has been well established (15-20). In contrast with many other techniques, this method requires no *a priori* assumptions about the peak profile, thus allowing the most accurate characterization possible (15). Although rigorously defined as integrals (Equation 1.19), statistical moments are often calculated based on finite summation of the fluorescence intensity as a function of time, I(t).

$$M_0 = \Sigma\, I(t)\, \Delta t \qquad \text{zeroth moment}$$

$$M_1 = \Sigma\, t\, I(t)\, \Delta t / M_0 \qquad \text{first moment} \qquad [2.1]$$

$$M_2 = \Sigma\, (t-M_1)^2\, I(t)\, \Delta t / M_0 \qquad \text{second moment}$$

$$M_n = \Sigma\, (t-M_1)^n\, I(t)\, \Delta t / M_0 \qquad n^{TH} \text{ moment}$$

The time interval, Δt, is chosen to be sufficiently small, so the use of the summation may be justified. To this end, all calculations use a minimum of 40 data points that are uniformly distributed across the zone profile.

For single-mode detection, the solute retention time is equal to the first statistical moment (M_1) calculated at each detector block. Thus, as described in Equation [1.5], the capacity factor (k) may be evaluated directly from the first moment of the solute zone and that of a nonretained zone, corresponding with

the elution

per unit le

second mo

$$H = \frac{\sigma_t^2}{L}$$

where L i

mode det

as the dif

Likewise,

moment

region m

capacity

column a

of the co

2.3 Sur

allows

column

matche

betwee

chroma

require

this de

the elution of acetone . Likewise, the plate height (H), or length variance (σ_L^2) per unit length (L), may be determined directly from the time variance (σ_T^2) or second moment (M_2) and the zone velocity (U),

$$H = \frac{\sigma_L^2}{L} = \frac{\sigma_T^2 U^2}{L} = \frac{M_2 (L/M_1)^2}{L} \qquad [2.2]$$

where L is the distance between injection and the point of detection. In dual-mode detection, the retention time in the region between detectors is calculated as the difference in the first statistical moments (M_1) evaluated at each detector. Likewise, the time variance is determined based on the difference in the second moment (M_2) between detectors. Therefore, the plate height in this isolated region may be determined for each solute zone using Equation [2.2]. Both capacity factor and plate height may be evaluated either as a composite of column and extra-column effects using a single detector, or in an isolated region of the column between the two detectors.

2.3 Summary of Detector Fabrication

A dual on-column detection system is designed and assembled, which allows the measurement of solute zones as they traverse the chromatographic column. Although all components in the two detection systems are carefully matched, the validity of the assumption of equal dispersion characteristics between detectors must be affirmed. Furthermore, the ability of the chromatographic system to achieve near theoretical separation efficiencies requires detailed evaluation. The following chapter will discuss the verification of this detection system under a variety of experimental conditions.

2.4 Lite

1. B
   2
2. F
   2
3. Y
4. I
5. (
6.
7.
8.
9.
10.
11.
12.
13.
14.
15.
16.
17.
18.
19.
20.

2.4 Literature Cited in Chapter 2

1. Baur, J.E.; Kristensen, E.W.; Wightman, R.M. *Anal. Chem.* **1988**, *60*, 2334.
2. Rowlen, K.L.; Duell, K.A.; Avery, J.P.; Birks, J.W. *Anal. Chem.* **1989**, *61*, 2624.
3. Yang, F. *J. High Resolut. Chromatogr. Chromatogr. Commun.* **1983**, *4*, 83.
4. Karlsson, K.; Novotny, M. *Anal. Chem.* **1988**, *60*, 1662.
5. Guthrie, E.J.; Jorgenson, J.W. *Anal. Chem.* **1984**, *56*, 483.
6. Guthrie, E.J.; Jorgenson, J.W.; Dluzneski, P.R. *J. Chromatogr. Sci.* **1984**, *22*, 171.
7. Gluckman, J.; Shelly, D.; Novotny, M. *J. Chromatogr.* **1984**, *317*, 443.
8. McGuffin, V.L.; Zare, R.N. *Appl. Spectrosc.* **1985**, *39*, 847.
9. Diebold, G.J.; Zare, R.N. *Science* **1977**, *196*, 1439.
10. Hershberger, L.W.; Callis, J.B.; Christian, G.D. *Anal. Chem.* **1979**, *51*, 1444.
11. Folestad, S.; Johnson, L.; Josefsson, B.; Galle, B. *Anal. Chem.* **1979**, *54*, 925.
12. Dovichi, N.J.; Martin, J.C.; Jett, J.H.; Trkula, M.; Keller, R.A. *Anal. Chem.* **1984**, *56*, 348.
13. Shelly, D.C.; Gluckman, J.C.; Novotny, M.V. *Anal. Chem.* **1984**, *56*, 2990.
14. Gluckman, J.C.; Hirose, A.; McGuffin, V.L.; Novotny, M.V. *Chromatographia* **1983**, *17*, 303.
15. Bidlingmeyer, B.A.; Warren, F.V. *Anal. Chem.* **1984**, *56*, 1583A.
16. Grubner, O. *Adv. Chromatogr.* **1968**, *6*, 173.
17. Grushka, E.; Myers, M.N.; Schettler, P.D.; Giddings, J.C. *Anal. Chem.* **1969**, *41*, 889.
18. Chesler, S.N.; Cram, S.P. *Anal. Chem.* **1971**, *43*, 1922.
19. Chesler, S.N.; Cram, S.P. *Anal. Chem.* **1972**, *44*, 2240.
20. Kucera, E. *J. Chromatogr.* **1965**, *19*, 273.

CHAPTER 3

VERIFICATION OF ON-COLUMN FLUORESCENCE DETECTION SYSTEM PERFORMANCE

3.1 Introduction

Initial characterization and verification of the performance of the dual on-column detection system is accomplished utilizing open-tubular capillaries. Because the hydrodynamic behavior of these columns is well understood and well documented (1), they are ideal in determining the accuracy of the dual on-column technique. As shown in Chapter 1, the dispersion of the solute zone in an open tube can be readily determined from known parameters (Equation [1.11]).

The goal of these preliminary studies is to determine the accuracy of the dual on-column detection system for the measurement of zone variance. This evaluation is accomplished by injecting a fluorescent dye onto an open-tubular capillary column and measuring the zone profile first near the column inlet and then again near the exit. Determination of the zone variance at each detector individually and as the difference between detectors allows the direct comparison of the measured variance values with those predicted based on the Golay

equation (Equation [1.11]). To make this direct comparison possible, all theoretical predictions utilize known experimental parameters. The linear velocity of the mobile phase (u), column radius (R) and length (L) are measured directly, while the diffusion coefficient in the mobile phase (D_M) is determined utilizing the Wilke-Chang equation (2). For preliminary investigations, no stationary phase is employed to decrease the uncertainty in the known parameters; therefore, the capacity factor (k), stationary phase diffusion coefficient (D_S), and film thickness (d_f) are all zero. Thus, for an open-tubular capillary with no stationary phase, the Golay equation reduces to Equation [1.10], the form developed by Taylor (3). In this way, the plate height measured for the open-tubular capillary using the dual on-column system can be directly compared to that predicted by Equation [1.10].

In preliminary measurements of plate height as a function of linear velocity, extra-column sources of variance have been carefully minimized for optimal chromatographic performance. In subsequent studies, extra-column contributions to variance are systematically increased to examine the ability of the dual on-column technique to eliminate these detrimental sources of dispersion.

3.2 Experimental Methods

Reagents. The fluorescent dye 7-(diethylamino)-4-methylcoumarin is obtained from Aldrich Chemical Co. and used without further purification. High-purity, distilled-in-glass grade methanol is obtained from Baxter Healthcare Products (Burdick and Jackson). The coumarin solute is dissolved in the pure methanol at a concentration of 3×10^{-4} M.

Chrom

illustrat

400-cm

15 nL

columr

surfac

Detec

emiss

Comp

respo

calcu

distri

mom

evalu

Cha

vari

Tab

3.3

is

lin

Al

(T

Chromatographic System. A diagram of the chromatographic system is illustrated in Figure 2-1. In this study, the coumarin solute is introduced onto a 400-cm length of 40–μm i.d. open-tubular capillary at volumes ranging from 1 to 15 nL (split ratios of 1:1000 to 1:65, respectively). This fused-silica capillary column is obtained from Polymicro Technologies and utilized without further surface modification.

Detection and Calculations. When this column is coupled with the 500 μm emission fiber, the viewed volume at each detector is no greater than 1.1 nL. Computer data acquisition is not employed for these studies, and the detector response is displayed directly onto a chart recorder. Statistical moments are calculated manually for each detector by finite summation of 30-50 points equally distributed across a peak. The arithmetic difference in the first and second moments are then determined and the linear velocity and length variance are evaluated as described in Chapter 2.

Extra-column contributions to the variance are calculated as described in Chapter 1 (Equations [1.37], [1.38], and [1.39]). The fractional increase in the variance (θ^2) that is expected for these studies (Equation [1.35]) is shown in Table 3.1.

3.3 Results and Discussion

Verification of the accuracy of the dual on-column measurement technique is accomplished by systematically varying the parameters of interest. Initially, the linear velocity of the mobile phase is varied under optimal detection conditions. All known sources of extra-column variance are kept well below 1% for this study (Table 3.1), and the dependence of the measured variance on the mobile-phase

Table 3

study	$(\sigma^2)_{INJ}$	$(\sigma^2)_{RC}$
H vs.		
H =		

Table 3.1: Fractional increase in column variance (θ^2) expected from extra-column sources.

study	u(cm/s)	V_{INJ}(nL)	τ(s)	$(\theta^2)_{INJ}$	$(\theta^2)_{RC}$
H *vs.* u	0.010	1.0	0.10	0.080%	0.00015%
	0.050	1.0	0.10	0.080%	0.0038%
	0.10	1.0	0.10	0.080%	0.015%
	0.20	1.0	0.10	0.080%	0.060%
$(\sigma^2)_{INJ}$	0.12	1.0	0.10	0.080%	0.022%
	0.12	5.0	0.10	2.0%	0.022%
	0.12	10	0.10	8.0%	0.022%
	0.12	15	0.10	18%	0.022%
$(\sigma^2)_{RC}$	0.12	1.0	0.01	0.080%	0.0022%
	0.12	1.0	0.10	0.080%	0.022%
	0.12	1.0	1.0	0.080%	2.2%
	0.12	1.0	10	0.080%	220%

H = 16.5 μm; L = 400 cm; R_{COL} = 0.0020 cm; V_{DET} = 1.1 nL, $(\theta_V^2)_{DET}$ = 0.096%.

linear
subse
determ
detect
variar
variet
syste
dispe
an e
optin
succ
be a

Plat
mec
zon
acc
the
det
are
tak
th
hi
ac
T
d

linear velocity is determined for single- as well as dual-mode detection. In subsequent studies, extra-column sources of variance are reintroduced to determine if the column variance can be measured accurately utilizing the dual-detection method. For this purpose, two different sources of extra-column variance are chosen to determine the utility of dual-mode detection under a variety of chromatographic conditions. First, the injection volume is systematically increased (Table 3.1), contributing a symmetrical source of dispersion. Second, the detector time constant is varied (Table 3.1), contributing an exponential and, thus, asymmetrical source of dispersion. Finally, under optimal detection conditions, the distance between the detector blocks is successively decreased to determine the minimum volumetric variance that may be accurately determined using the dual on-column detection system.

Plate Height *versus* Linear Velocity. By varying the linear velocity (u) and measuring the length variance (σ_L^2) or corresponding plate height (H) of a solute zone, agreement of experimental results with Golay theory can be examined. To accomplish this goal, a single solute is injected onto the open-tubular column and the variance is measured at a single detector and as the difference of two detectors. The results of varying linear velocity in the region near the optimum are shown in Figure 3-1 for the 40 μm i.d. capillary. Although great care was taken to minimize extra-column effects in the chromatographic system design, the single-detector measurements show substantial divergence from theory at higher zone velocities. In contrast, the dual-detector mode exhibits excellent agreement with Golay theory over the entire linear velocity region examined. Thus, the dual on-column detection scheme successfully measures the variance due only to the column proper as predicted by the Golay equation.

Figure 3-1: Plate height *versus* linear velocity: single mode (□), dual mode (▲), Golay theory (—); column, R_{COL} = 20 µm, L = 397 cm (single mode), L = 337 cm (dual mode); chromatographic conditions as described in text.

Figure 3-1

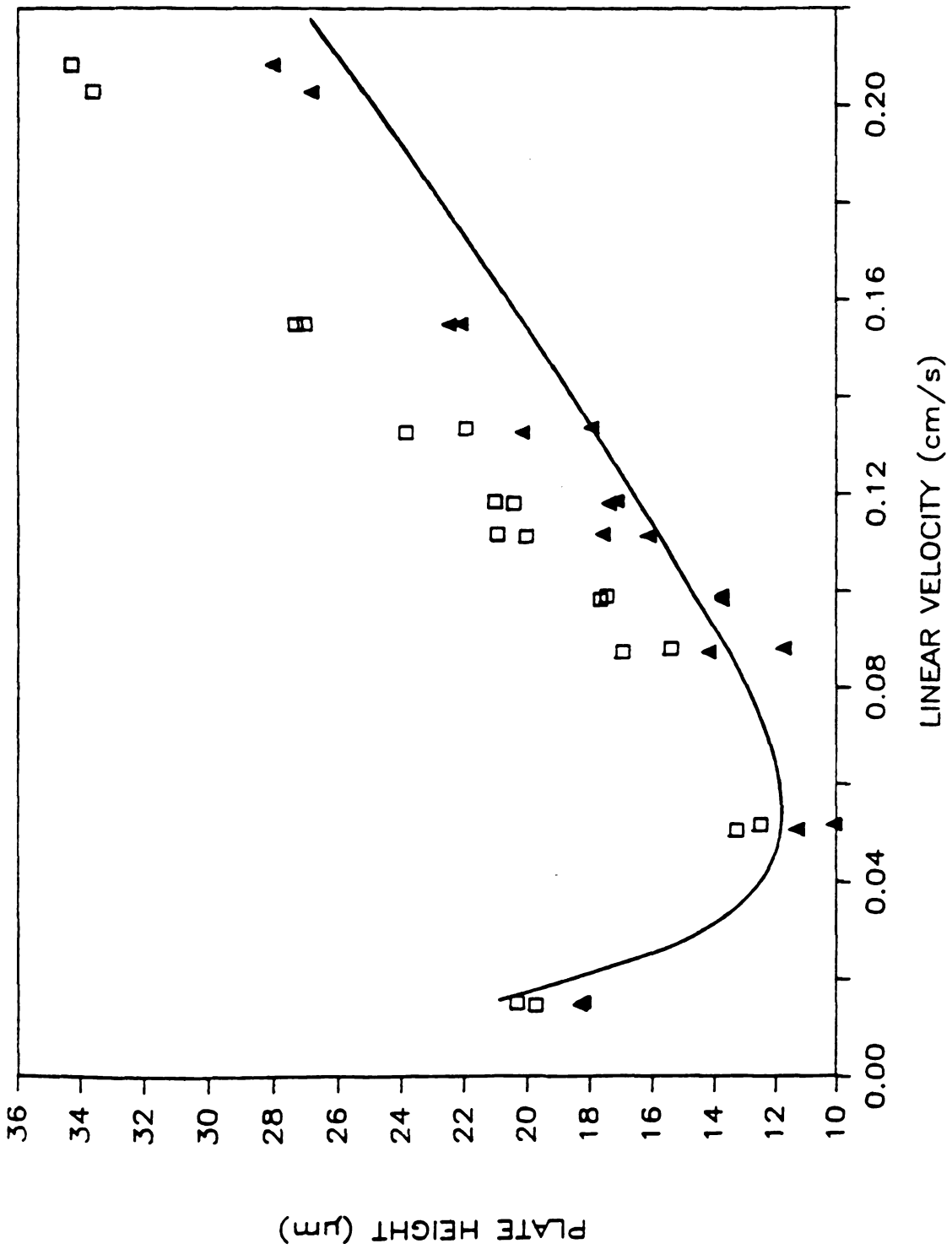
PLATE HEIGHT (μm)
36
34
32
30
28
26
24
22
20
18
16
14
12
10
0.00
0.04
0.08
0.12
0.16
0.20
LINEAR VELOCITY (cm/s)

Figure 3-1 is also a good illustration of the difficulty in evaluating the influence of experimental variables on the column variance in the presence of extra-column sources of variance. Because both the column and extra-column variance are functions of the linear velocity, the linear velocity dependence determined from a single-detector measurement is a composite of both these influences. Therefore, evaluation of the mass transfer contribution from the slope at high linear velocity results in a significantly greater C term for the single-detector measurement than is accurate for this capillary. In contrast, the mass transfer contribution measured utilizing the dual-mode approach is quite accurate. It is important to note that most commonly a single detector is employed. In this case, erroneous estimation of the mass transfer component would arise without our knowledge, even though all known sources of extra-column variance have been minimized. Thus, the dual-detection mode appears promising in the accurate determination of the various flow contributions to dispersion in chromatographic separations.

Further validation of the dual on-column detection technique is accomplished by systematically varying extra-column sources of dispersion. Both volumetric and temporal sources of extra-column variance are adjusted to examine the ability of the dual-detector mode to eliminate these variances unrelated to the actual column variance.

Injection Variance. Volumetric extra-column variance is systematically increased by varying the injection volume (Table 3.1). Sample volumes from 1 to 15 nL are injected onto the open-tubular column utilizing the split injection technique. Values for the plate height measured at a single detector and as the difference between detectors are illustrated in Figure 3-2. Substantial deviation of measured from theoretical variance values can be seen for the single-detector

Figure 3-2: Effect of injection volume on plate height: single mode (□), dual mode (▲), Golay theory (—); u = 0.12 cm/s. Conditions same as given in Figure 3-1.

Figure 3-2

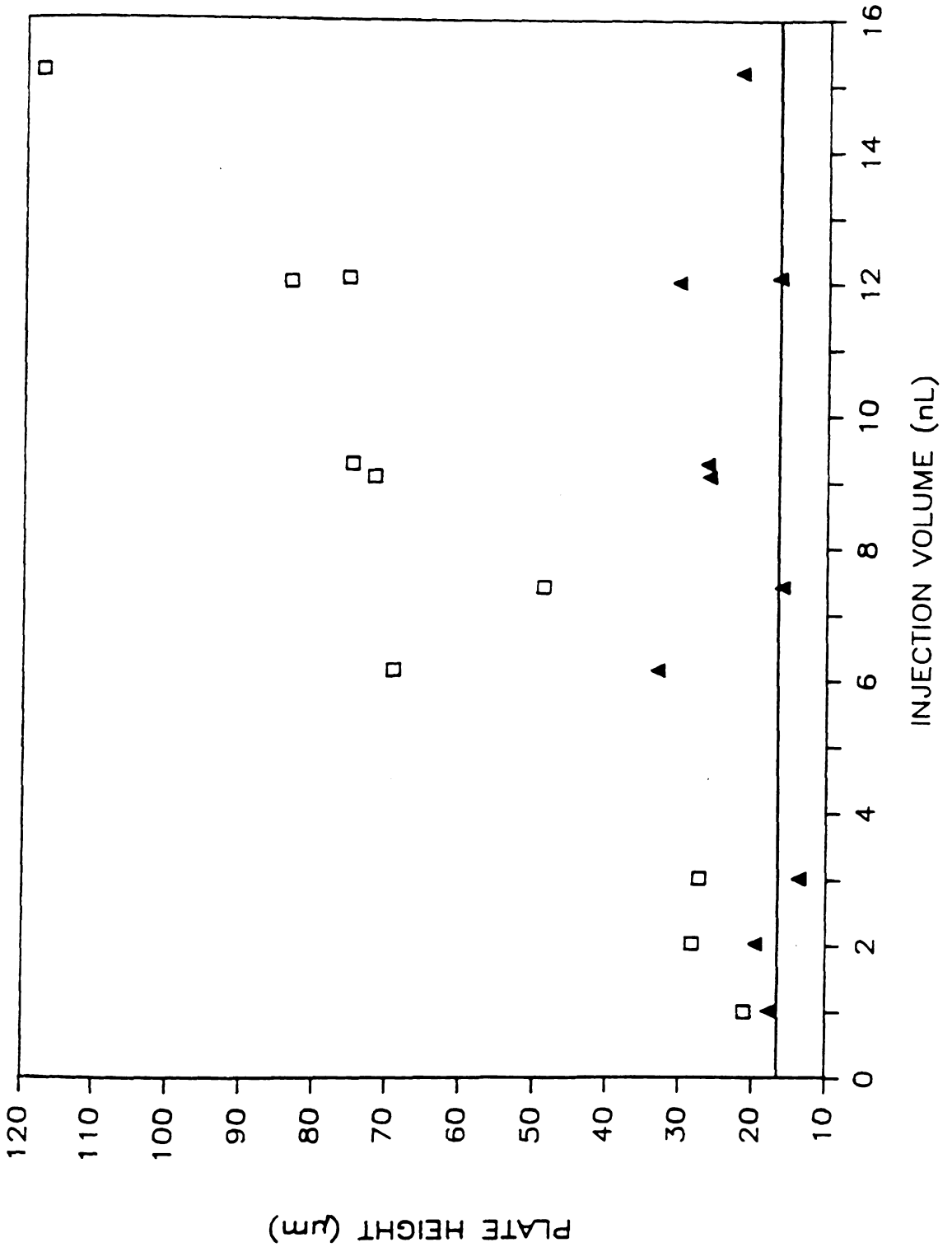
PLATE HEIGHT (μm)
120
110
100
90
80
70
60
50
40
30
20
10
0
2
4
6
8
10
12
14
16
INJECTION VOLUME (nL)

mode. T
injected t
however,
fractional
detection
allowing

Tempor
an activ
circuit, t
to 10 s.
detector
in the p
other e
from a
increas
and th
Howev
experi
of mag
the du
colum

Small
plate
detec
per u

mode. The single-detector response shows a notable dependence on volume injected for volumes greater than approximately 4 nL. Dual-mode detection, however, corresponds very closely to theory, even up to 15 nL injected volume, a fractional increase (θ^2) over the column variance of 18%. Thus, dual-mode detection successfully eliminates this volumetric form of extra-column dispersion, allowing accurate measurement of column variance.

Temporal Variance. Temporal extra-column variance is adjusted with the aid of an active lowpass filter. By varying the resistance and the capacitance of this circuit, the time constant (τ) of the amplifier for both detectors ranged from 0.01 to 10 s. These data, shown in Figure 3-3, clearly illustrate the inability of a single detector to accurately measure the column variance as predicted by Golay theory in the presence of an exponential time constant. Even for very low time constant, other extra-column sources of dispersion prevent the single-detector response from approaching the theoretically predicted value. As the time constant is increased, the disparity between the variance measured by the single detector and that predicted by theory increases drastically as expected from Table 3.1. However, when the variance is measured in the dual-detection mode, experimental variance accurately reflects theoretical predictions over three orders of magnitude in time constant. These results clearly demonstrate the ability of the dual on-column detection system to eliminate temporal sources of extra-column variance.

Small Variance. Thus far, dispersion has been discussed only in terms of the plate height or length variance per unit length. Yet, one of the advantages of this detection scheme lies in the ability to measure accurately very small variances per unit volume. Preliminary studies have been conducted to determine the

Figure 3-3: Effect of detector time constant on plate height: single mode (□), dual mode (▲), Golay theory (—); u = 0.12 cm/s. Conditions same as given in Figure 3-1.

Figure 3-3

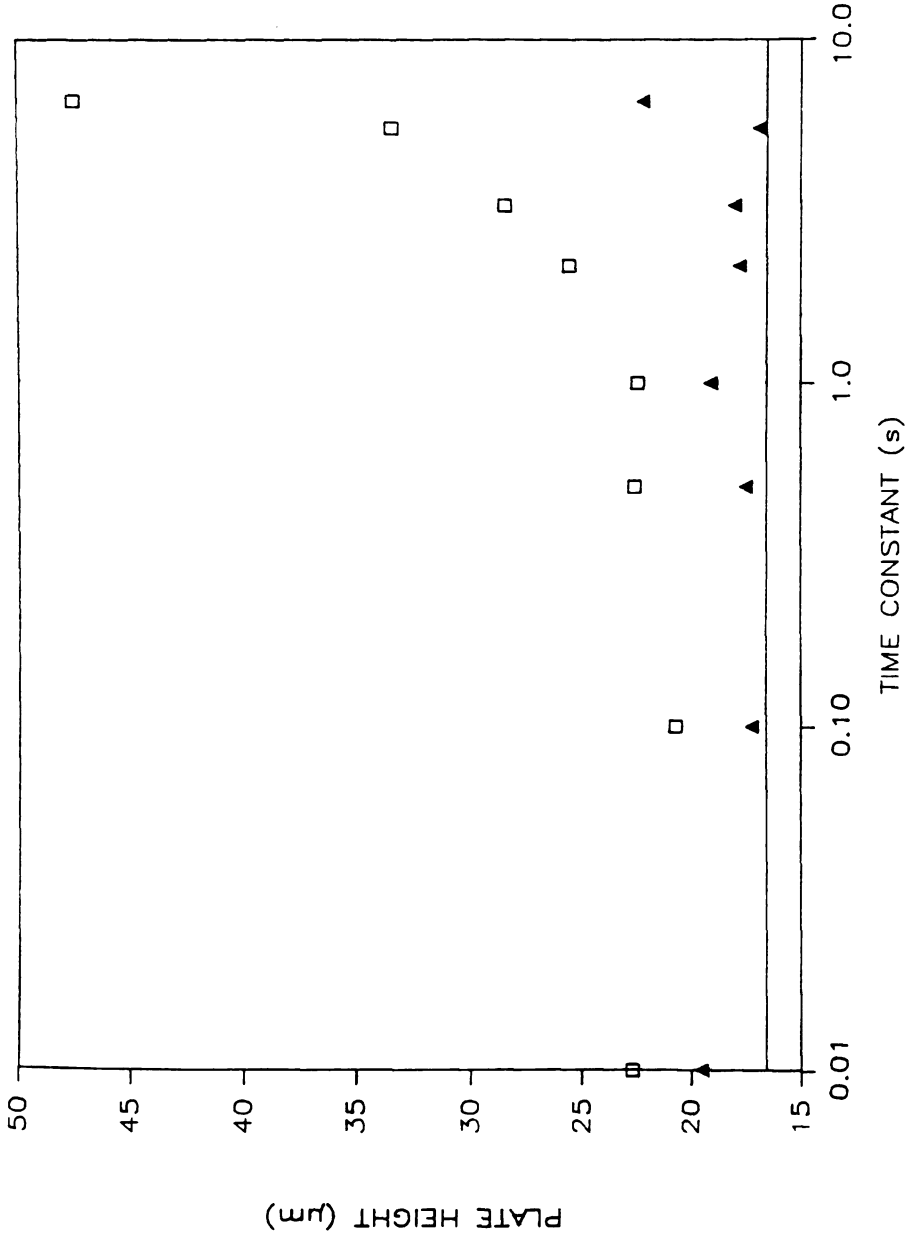

single mode (□),
Conditions same

smalles
on-colu
4, whe
predict
changi
param
measu
theory
to ine
statist
mean
scher
(4-7),

deter
meth
the
from
as
mea
vari
eva
allo
the
the

smallest volumetric variance it is possible to measure accurately using the dual on-column fluorescence detection system. This feature is illustrated in Figure 3-4, where the direct correlation of measured volumetric variance with that predicted by Golay theory can be seen. The column variance is adjusted by changing the column length between the two detectors, with all other system parameters kept constant. Substantial discrepancy is seen for single-detector measurements while the dual-detection mode shows excellent agreement with theory for variances as low as 10 nL^2. Variation in the data is thought to be due to inequality of detector characteristics as well as to difficulty in calculating statistical moments by manual methods. Thus, the values reported here by no means represent the minimum variance accurately measurable by this detection scheme. Although small variance measurements have been previously reported (4-7), none, to our knowledge, are this accurate.

Although this measurement scheme has many advantages for the *in situ* determination of separation processes, the limitations inherent in any difference method still prevail. Thus, the precision of dual-mode determinations is limited by the reproducibility of single-mode measurements. These fluctuations may arise from variations in the mobile-phase flowrate, temperature, and pressure, as well as errors in the evaluation of statistical moments. In addition, difference measurements performed in the presence of a large extra-column or column variance will inevitably lead to a decrease in precision due to the necessity for evaluating a small difference in large values. Therefore, although this technique allows the accurate determination of local retention and dispersion processes, the resulting precision in such measurements is limited by the reproducibility of the single-mode measurements.

Figure 3-4: Measured *versus* theoretical volumetric variance for small variance values: single mode (□), dual mode (▲), Golay theory (—); u = 0.12 cm/s. Conditions same as given in Figure 3-1.

Figure 3-4

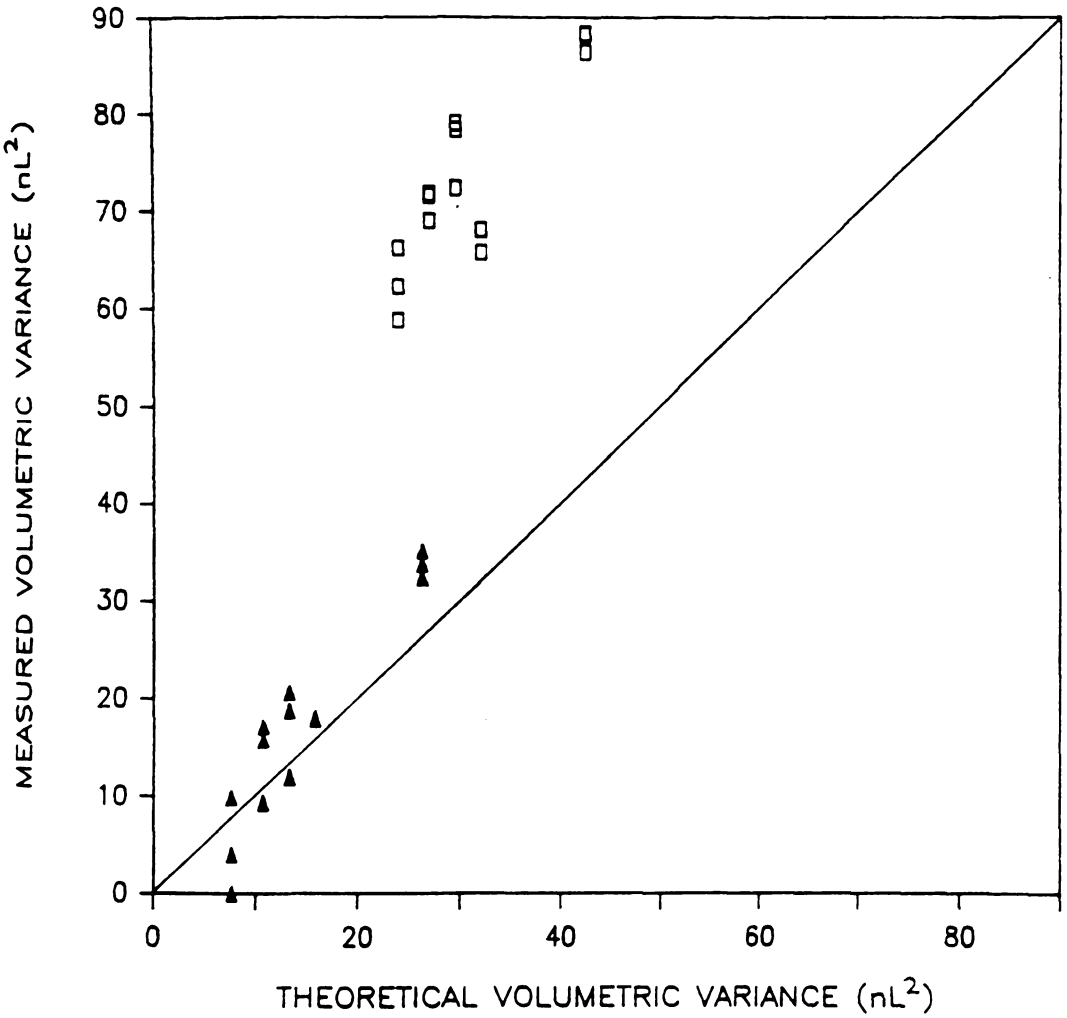
MEASURED VOLUMETRIC VARIANCE (nL²)
THEORETICAL VOLUMETRIC VARIANCE (nL²)
0
10
20
30
40
50
60
70
80
90
0
20
40
60
80

3.4 Sum

A
is capab
chromat
sources
for det
hydrody
column
optimiz
were h
possib

3.4 Summary of Performance Verification

As demonstrated here, the dual on-column fluorescence detection system is capable of accurately determining the variance of solute zones directly on the chromatographic column. Even in the presence of symmetrical and asymmetrical sources of extra-column variance, dual-mode detection provides a reliable means for determining the true column variance. Thus, fundamental studies of hydrodynamic as well as chemical processes in both open-tubular and packed columns are feasible utilizing this technique. In particular, the examination and optimization of solute retention, band broadening, and nonequilibrium, which were hindered in previous investigations by extra-column dispersion, are now possible.

3.5 Literatu

1. Golay New

2. Wilke

3. Tayl

4. Sep 198

5. van

6. Fol

7. Mc Chr

3.5 Literature Cited in Chapter 3

1. Golay, M.J.E. *Gas Chromatography 1958*; Desty, D.H., Ed.; Academic: New York, **1958**; pp. 36-55.

2. Wilke, C.R.; Chang, P. *AIChE J.* **1955**, *1*, 264.

3. Taylor, G. *Proc. Roy. Soc. (London)* **1953**, *219A*, 186.

4. Sepaniak, M.J.; Vargo, J.D.; Kettler, C.N.; Maskarinec, M.P. *Anal. Chem.* **1984**, *56*, 1252.

5. van Vliet, H.P.M.; Poppe, H. *J. Chromatogr.* **1985**, *346*, 149.

6. Folestad, S.; Galle, B.; Josefsson, B. *J. Chromatogr. Sci.* **1985**, *23*, 273.

7. McGuffin, V.L.; Higgins, J.W. International Symposium on Column Liquid Chromatography, Edinburgh, Scotland, **1985**.

4.1 Int

tubular
packe
elucid
in pa
theore
nearly
phase
simpl
chro
comp
mea

CHAPTER 4

RETENTION AND DISPERSION ALONG THE CHROMATOGRAPHIC COLUMN

4.1 Introduction

Although verification of the dual on-column detection system utilized open-tubular columns, most applications in liquid chromatography rely on the use of packed columns. The remainder of the studies, therefore, focus on the elucidation and characterization of the fundamental factors affecting separations in packed beds. In an effort to correlate experimental measurements with theoretical expectations, these preliminary studies address separations under nearly ideal conditions. Only reversed-phase separations, where the mobile phase is more polar than the stationary phase, are utilized because of the relative simplicity of their theoretical treatment. In the first of these studies, a single chromatographic column is examined in detail under constant mobile-phase composition and velocity conditions. Solute zone retention and dispersion are measured as a function of distance along the high-efficiency packed column.

Preliminary investigations of these fundamental parameters necessitates the choice of solutes which are chromatographically as well as spectroscopically well behaved. To facilitate direct comparison with theoretical predictions, a homologous series of fatty acids, labeled with 4-bromomethyl-7-methoxycoumarin, have been chosen as suitable model solutes. The separation and concomitant detection of these solutes along the packed microcolumn are shown in Figure 4-1. When separated on a reversed-phase octadecylsilica packing material, the straight-chain, saturated fatty acids exhibit a wide range of capacity factors under isocratic conditions (approximately 0.5 to 5 in pure methanol). In addition, these solutes behave ideally, displaying symmetrical peak shapes and the logarithmic dependence of capacity factor on carbon number expected from Equation [1.6] for a homologous series (Figure 4-2). Finally, the fluorescence characteristics of these derivatives indicate favorable fluorescence in the methanol mobile phase, while no fluorescence is detected when *n*-decane is used to mimic the stationary phase (Figure 4-3). This appears to be due to lack of solubility of the polar coumarin molecule in the nonpolar media. It is hypothesized that on a chromatographic column, the alkyl portion of these molecules resides in the stationary phase, whereas the coumarin moiety remains in the more polar mobile phase. This condition results in fluorescence characteristics that are not a function of solute retention. Thus, both chromatographically and spectroscopically, these model solutes seem ideally suited as systematic probes of retention and dispersion along the chromatographic column.

Figure 4-1: On-column chromatogram of derivatized fatty acid standards detected at 50 cm along the column. Solutes: *n*-$C_{10:0}$, *n*-$C_{12:0}$, *n*-$C_{14:0}$, *n*-$C_{16:0}$, *n*-$C_{18:0}$, *n*-$C_{20:0}$ fatty acids derivatized with 4-bromomethyl-7-methoxycoumarin (100 nA full scale). Chromatographic and detection conditions described in the text.

Figure 4-1

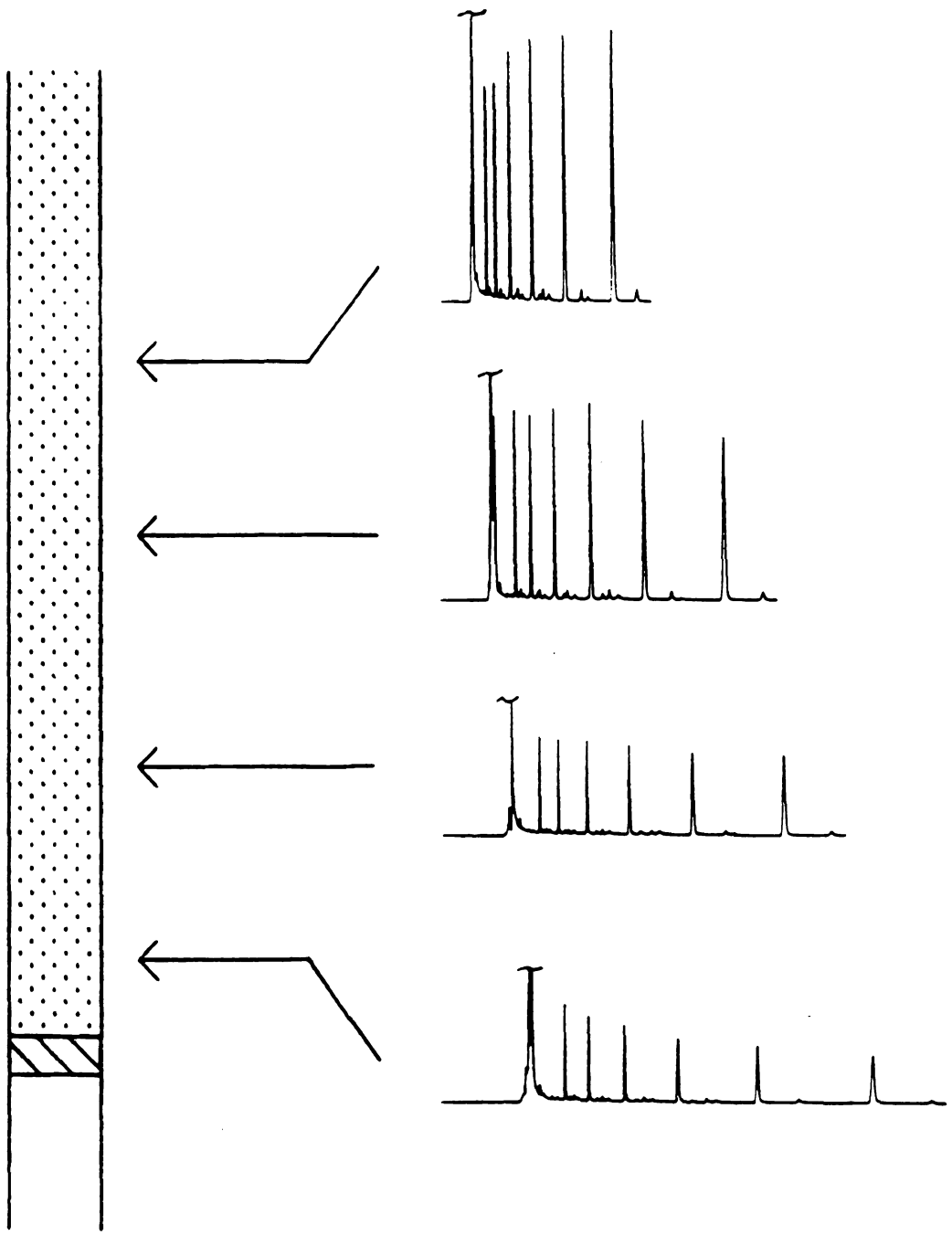

Figure 4-2: Capacity factor *versus* carbon number for fatty acid derivative *n*-$C_{20:0}$, as measured directly on-column at a distance 50 cm from the inlet. Chromatographic and detection conditions described in the text.

Figure 4-2

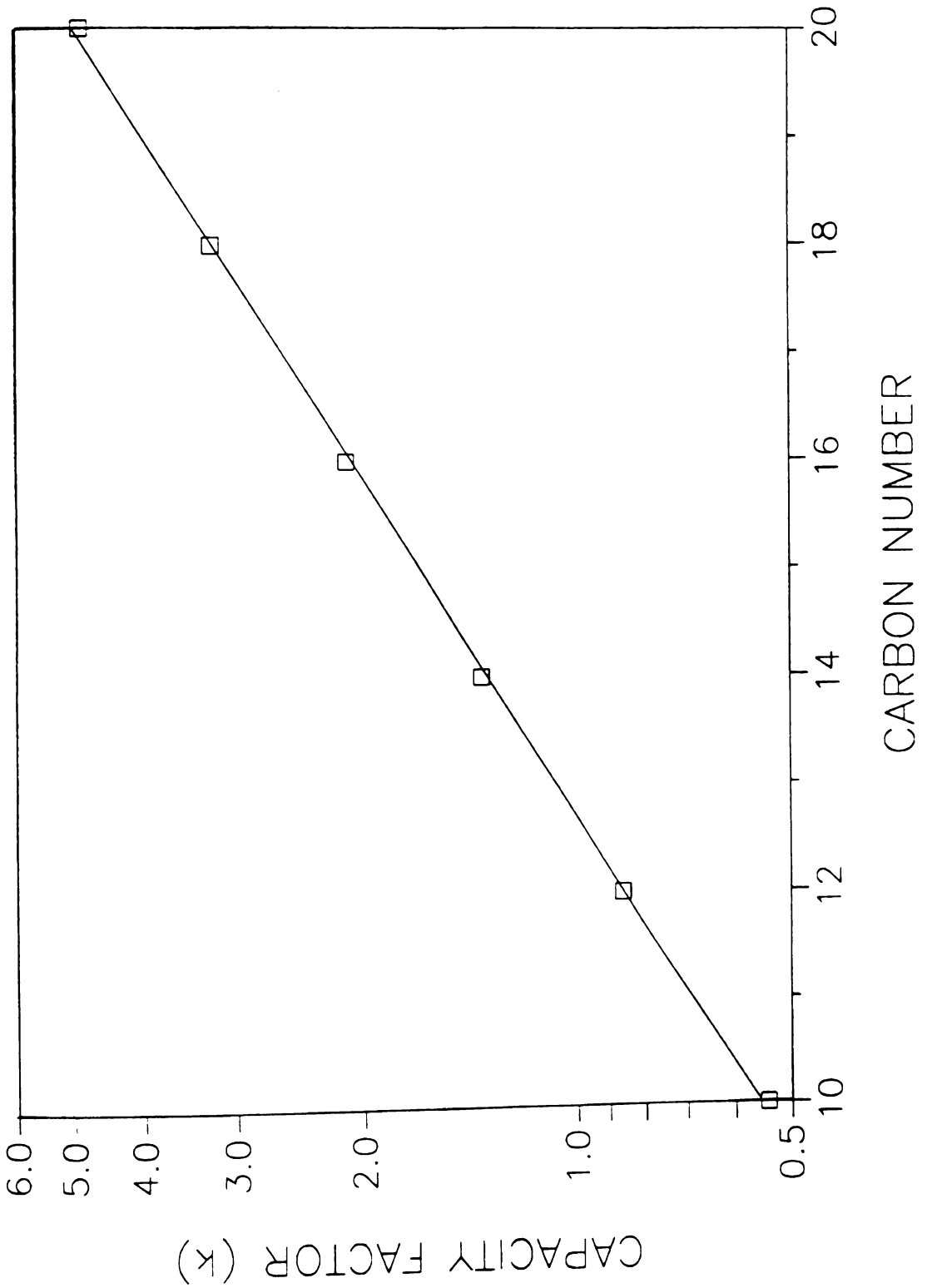
CAPACITY FACTOR (K)
6.0
5.0
4.0
3.0
2.0
1.0
0.5
10
12
14
16
18
20
CARBON NUMBER

Figure 4-3: Fluorescence excitation and emission spectra of 4-bromomethyl-7-methoxycoumarin in methanol (—) and *n*-decane (– –).

Figure 4-3

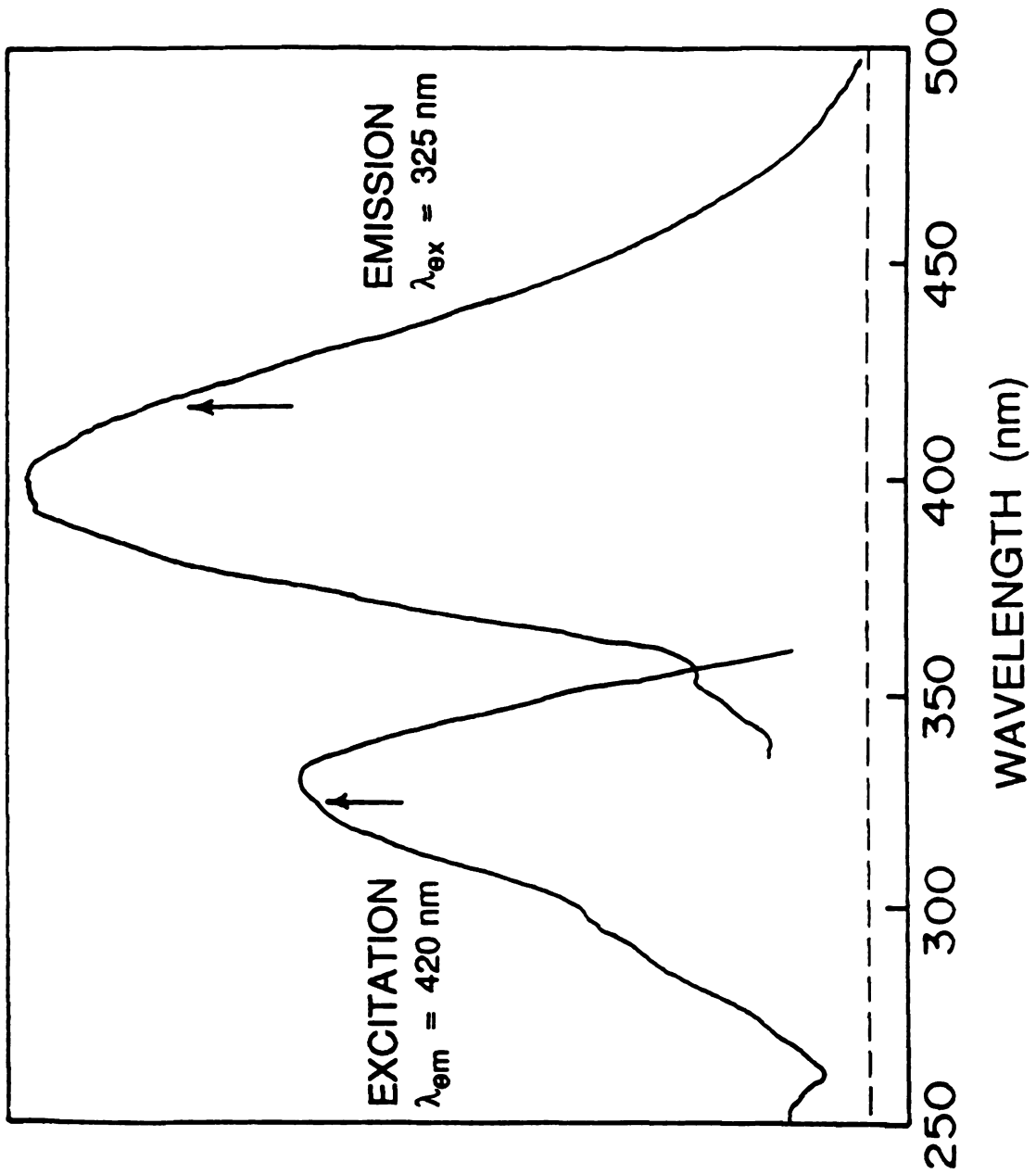
EMISSION
λ_{ex} = 325 nm
EXCITATION
λ_{em} = 420 nm
250
300
350
400
450
500
WAVELENGTH (nm)

4.2 Ex

Analy

n-C_{10}

(Sigm

sulfat

powd

mixtu

forme

After

solut

cour

proc

the

x 10

obt

Fig

em

(Ba

sh

Ch

in

pl

fo

4.2 Experimental Methods

Analytical Methodology. Saturated fatty acid standards (Sigma) ranging from *n*-$C_{10:0}$ to *n*-$C_{20:0}$ are derivatized with 4-bromomethyl-7-methoxycoumarin (Sigma), as described previously (1). An anhydrous mixture of 0.144 g sodium sulfate (J.T. Baker) and 0.100 g potassium bicarbonate (MCB Reagents) are powdered together to form a homogenous mixture. A 0.005 g portion of this base mixture is combined with 0.0036 g dibenzo-18-crown-6 (Aldrich) in a slurry formed using 0.2 mL dry acetone (Baxter Healthcare, Burdick and Jackson). After stirring this solution for 10 minutes, a 0.500 mL aliquot of 10^{-3} M stock solution containing the fatty acid standards is added along with 0.0027 g of the coumarin reagent. The mixture is quickly stirred and the reaction is allowed to proceed in the dark at 50 °C for 2.5 hours with intermittent stirring. Aliquots of the derivatized standards are then diluted in acetone to a final concentration of 3×10^{-4} M.

Fluorescence excitation and emission spectra of the coumarin reagent are obtained with a grating fluorimeter (Perkin-Elmer, Model LS5). As shown in Figure 4-3, these derivatives exhibit an excitation maximum at 330 nm with an emission maximum at 400 nm in the methanol mobile phase. The methanol (Baxter Healthcare) and *n*-decane (J.T. Baker) solvents utilized for the spectra showed no discernible background fluorescence.

Chromatographic System. The chromatographic system is described in detail in Chapter 2 and illustrated in Figure 2-1. For this study, a pure methanol mobile phase is delivered to the column under constant flow conditions. The split ratio for these studies remains constant at 1:40, yielding an injection volume of 25 nL.

All chromatographic studies are performed on a single, packed microcolumn. The microcolumn is prepared utilizing a 0.200 mm i.d. fused-silica capillary (Hewlett-Packard), terminated with a quartz wool frit at a length of approximately 100 cm. Prior to packing, the polyimide coating is removed from the capillary at four positions, creating detection windows at approximately 30, 50, 70, and 90 cm from the inlet. An acetone slurry of 3 μm spherical octadecylsilica packing material (Varian, MicroPak SP) is then introduced onto the capillary under moderate pressure (5000 psi). The resulting microcolumn contains more than 140,000 theoretical plates (H = 7 μm) under standard test conditions (2), with a flow resistance parameter (ϕ') of 530 and a total porosity (ε_T) of 0.43. All measurements of retention and dispersion are performed utilizing a methanol mobile phase operated at slightly greater than the optimum velocity (u = 0.056 cm/s), resulting in an inlet pressure of approximately 2500 psi (170 bar).

Even though the chromatographic system is carefully designed to minimize extra-column sources of variance, it is nearly impossible to eliminate these detrimental contributions entirely. As described in Chapter 1, the influence of the injection volume, as well as the detector volume and time constant, can be calculated under ideal conditions to give an indication of the magnitude of these effects (3). The fractional increase in the measured variance (θ^2) arising from extra-column sources, shown in Table 4.1, indicates the injection volume is the primary contribution, followed by the detection volume. As expected, extra-column effects decrease with increasing column variance, or distance along the column.

Detection System. The detection conditions utilized in this study are identical to those given in Chapter 3, with excitation at 325 nm and fluorescent emission

Table

DIST

3

5

7

9

Table 4.1: Calculated fractional increase in variance (θ^2) arising from extra-column sources.

DISTANCE	$(\theta^2)_{INJ}$	$(\theta^2)_{DET}$	$(\theta^2)_{RC}$
30 cm	13.5%	3.0%	0.15%
50 cm	8.1%	1.8%	0.090%
70 cm	5.8%	1.3%	0.064%
90 cm	4.5%	0.98%	0.050%

collec

detec

comp

on th

4.3

Solu

the

dist

fact

sho

t_R =

Pr

va

U

co

U

s

A

c

s

a

collected at 420 nm. The resulting photocurrent is amplified at 100 nA/V with a detector time constant of 0.1 s. Data acquisition proceeds at a rate of 1 Hz under computer control. The maximum viewed detection volume for this study, based on the total porosity and tube diameter, is approximately 13 nL.

4.3 Results and Discussion

Solute Retention. Evaluation of solute retention is accomplished by measuring the first statistical moment (centroid) of each solute zone as a function of distance travelled. If the mobile-phase linear velocity (u) and the solute capacity factor (k) are constant along the column, the retention time (t_R) of each solute should be a simple linear function of the distance travelled (L).

$$t_R = \frac{L}{U} = \frac{L\,(1+k)}{u} \qquad [4.1]$$

Previously, this measurement has been accomplished by using columns of varying length or by successively decreasing the length of a single column. Unfortunately, the packing structure and hydrodynamics may differ between columns or may be altered in the process of performing the experiment (4). Utilizing the present detection scheme, this measurement is accomplished by simply moving the two detector blocks along the length of a single microcolumn. As shown in Figure 4-4, the retention time is the expected linear function of the distance travelled in the region from approximately 30 to 90 cm. Moreover, the slope of each line increases with carbon number and, thus, with capacity factor as predicted in Equation [4.1]. However, the intercept of each line predicts a finite retention time at zero column length, which is obviously not a meaningful

Figure 4-4: Retention time *versus* distance along the microcolumn for nonretained solute (●), *n*-$C_{10:0}$ (○), *n*-$C_{12:0}$ (□), *n*-$C_{14:0}$ (△), *n*-$C_{16:0}$ (◇), *n*-$C_{18:0}$ (▽), and *n*-$C_{20:0}$ (+) derivatized fatty acids. Chromatographic and detection conditions described in the text.

Figure 4-4

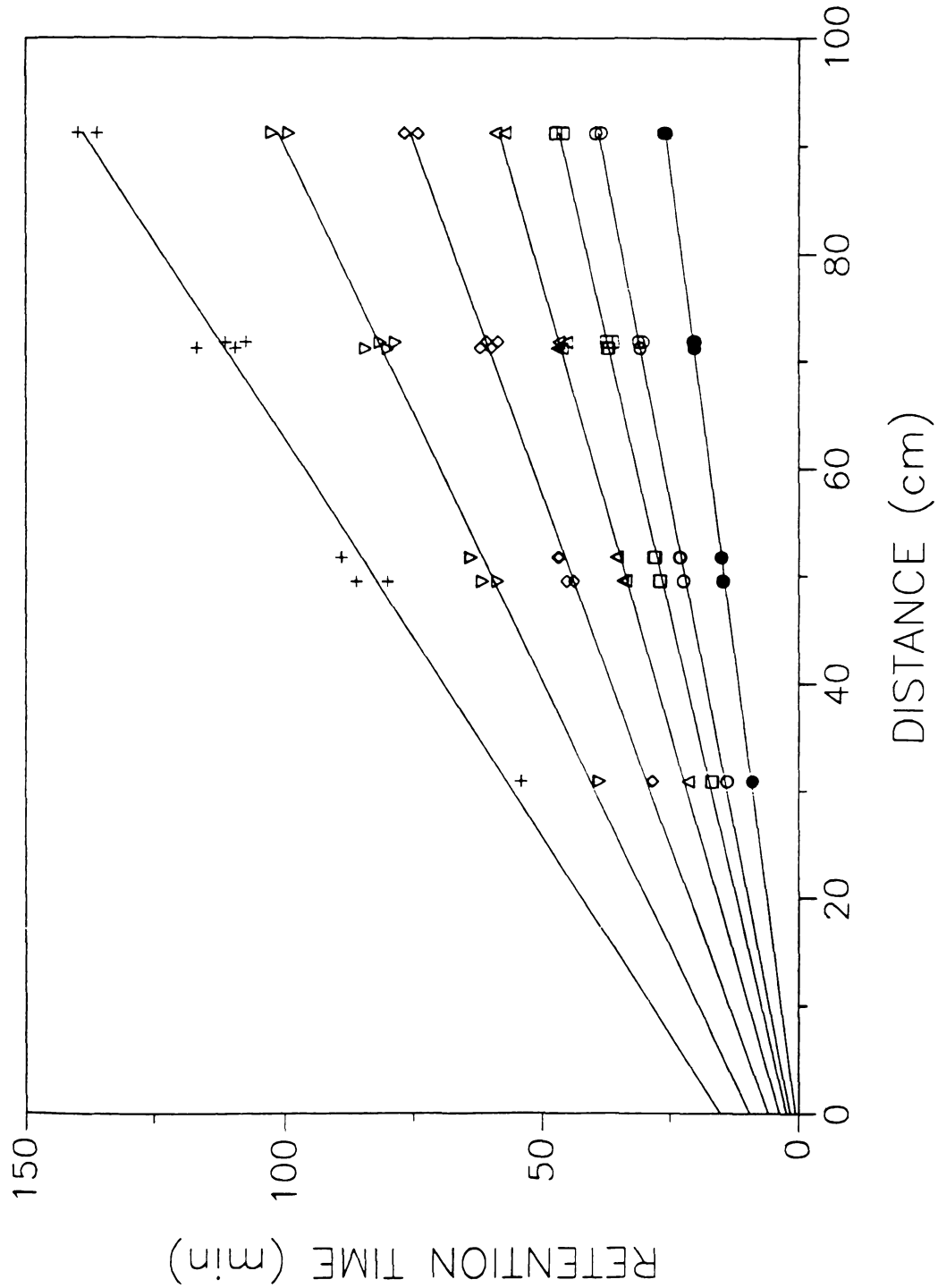

conclusion. This result clearly indicates that a gradient in zone velocity must be present in the initial portion of the column. According to Equation [4.1], this nonuniformity of movement may arise from either a decrease in the mobile-phase velocity or an increase in the capacity factor in this region. This anomaly cannot be attributed to simple perturbations in the pump flow, however, as the overall linear velocity would be affected, not just that in the initial portion of the column. Nevertheless, a decrease in linear velocity has been predicted in high-pressure regions of the column based on theoretical calculations of the variation in mobile-phase density and viscosity with pressure (5-7). Although liquids are often considered incompressible, the decrease in linear velocity expected for pure methanol under moderate pressure conditions is approximately 1-2% (5).

In an effort to distinguish this physical effect from the chemical influences on retention, the decrease in the mobile-phase linear velocity expected under pressure conditions may be evaluated. This is accomplished for the pure methanol mobile phase employed in this study using the general formalism introduced by Martire (6). Utilizing the Tait equation of state and a linear dependence of viscosity on pressure (5), the local linear velocity expected on the column (u_x) may be expressed as a function of the local pressure (P_x) and the outlet velocity (u_0),

$$u_x = \frac{u_0}{(7.527 \times 10^{-6} P_x + 1.001)} \qquad [4.2]$$

where the linear velocity is given in cm/s and pressure in psi. This expression, determined for the pure methanol mobile phase by numerical integration, has a regression coefficient of $r^2 = 0.9993$ and is valid for inlet pressures commonly encountered in liquid chromatography (500 to 5000 psi). Assuming a constant column temperature of 25 °C, the linear velocity of methanol measured on the

column may be co
Details of this deriv

The data p
expected change
Therefore, the de
column does not
appears that the r
as a function of ch
as a function of
retention clearly.
travelled using si
injection and dete
factor is evaluate
(Figure 4-5B), it b
along the length c
the assumptions
in fact, be unifor
solutes. Severa
including the inf
pressure effects
to be independe
phase induced b
this region (8) m
may thermodyn
partitioning proc
investigations of
the initial regior
studies are disc

column may be corrected for mobile-phase compression by using Equation [4.2]. Details of this derivation are given in Chapter 5.

The data presented in Figure 4-4 have already been corrected for the expected change in linear velocity with pressure described in Equation [4.2]. Therefore, the decrease in solute zone movement in the initial region of the column does not arise solely from mobile-phase velocity considerations. It appears that the retention of solutes may be greater in this portion of the column as a function of changing chemical interactions. Evaluation of the capacity factor as a function of distance, shown in Figure 4-5, illustrates this alteration in retention clearly. Figure 4-5A shows the variation in capacity factor with distance travelled using single-mode detection, where the average retention between injection and detection appears to decrease for all solutes. When the capacity factor is evaluated in specific regions of the column by dual-mode detection (Figure 4-5B), it becomes apparent that the retention is decreasing continuously along the length of the column, not merely in the initial portion. Thus, contrary to the assumptions in many theoretical derivations, chemical interactions may not, in fact, be uniform along the chromatographic column even for well-behaved solutes. Several sources of this retention gradient are under investigation, including the influence of the injection process (Chapter 8) as well as local pressure effects (Chapters 5 and 6). Although solute retention is often assumed to be independent of the injection process, the modification of the stationary phase induced by the introduction of solvent or by the abrupt nonequilibrium in this region (8) may directly affect solute retention. Alternately, the local pressure may thermodynamically influence the chemical interactions controlling the partitioning process (9-12) or the surface activity of the silica substrate. Further investigations of this apparent retention gradient have been extended to include the initial region of the chromatographic column (13) and the results of these studies are discussed in Chapters 6 and 8.

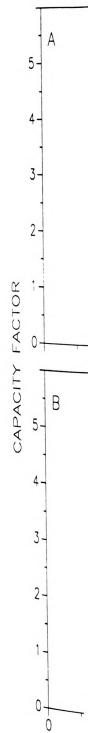

Figure 4-5: Capacity factor evaluated using single (A) and dual (B) detection as a function of distance travelled along microcolumn. Solutes are as shown in Figure 4-4.

Figure 4-5

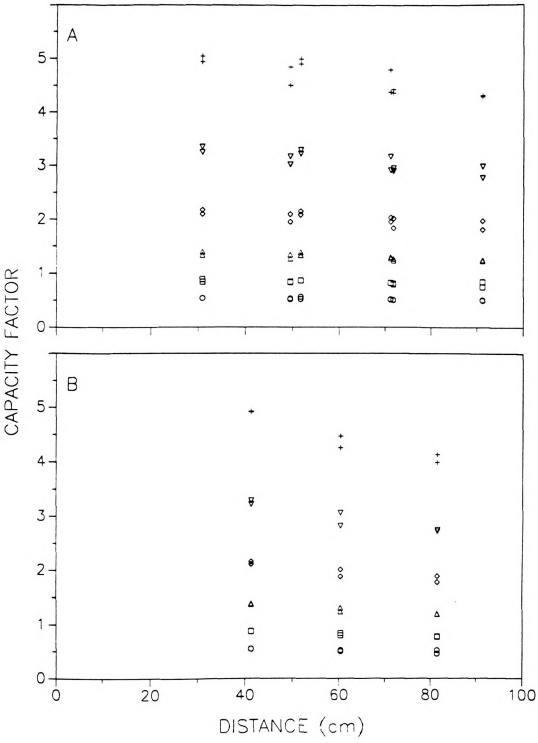

Solute Dispersi

chromatograms m

the chromatograp

substitution of the

important to not

difference in the

moment, which m

The meas

shown in Figure

mode (Figure 4-

the column. Th

n-$C_{10.0}$ (k = 0.5)

µm. In contras

remains nearly

eliminate extra-

is not due to

important contr

broadened by

Moreover, the

retained solut

Figure 4-6A.

to be seriousl

When

mode detecti

an entirely d

the magnitud

Solute Dispersion. In addition to retention information, the same chromatograms may be utilized to examine the dispersion of solute zones along the chromatographic column. The plate height on the column is calculated by substitution of the first and second statistical moments into Equation [2.2]. It is important to note that the dual-detector measurement is calculated as the difference in the time-based second moment, *not* the length-based second moment, which may not be additive (14,15) as discussed in Appendix 1.

The measured plate height as a function of distance along the column is shown in Figure 4-6, for both the single and dual detection modes. In the single mode (Figure 4-6A), the plate height changes markedly as the solutes traverse the column. This variation is most pronounced for the less retained solutes, with *n*-$C_{10:0}$ (k = 0.5) exhibiting a decrease in plate height from approximately 20 to 12 μm. In contrast, the plate height for the most retained solute (*n*-$C_{20:0}$; k = 4.8) remains nearly constant along the column. Since single-mode detection does not eliminate extra-column sources of variance, it is possible that the observed trend is not due to column processes at all. If the extra-column variance is an important contribution, it is expected that this fraction will decrease as the zone is broadened by the column, thereby decreasing the measured plate height. Moreover, the influence of extra-column effects is expected to be greater for less retained solutes, which is in agreement with the single-mode response shown in Figure 4-6A. Therefore, plate height measurements at a single detector appear to be seriously affected by extra-column sources of variance.

When the local plate height is evaluated between detectors using dual-mode detection, extra-column sources of variance are effectively eliminated and an entirely different plate height trend is observed (Figure 4-6B). Furthermore, the magnitude of the local plate height values are less than those measured at a

Figure 4-6: Plate height evaluated using single (A) and dual (B) detection as a function of distance travelled along microcolumn. Solutes are as shown in Figure 4-4.

Figure 4-6

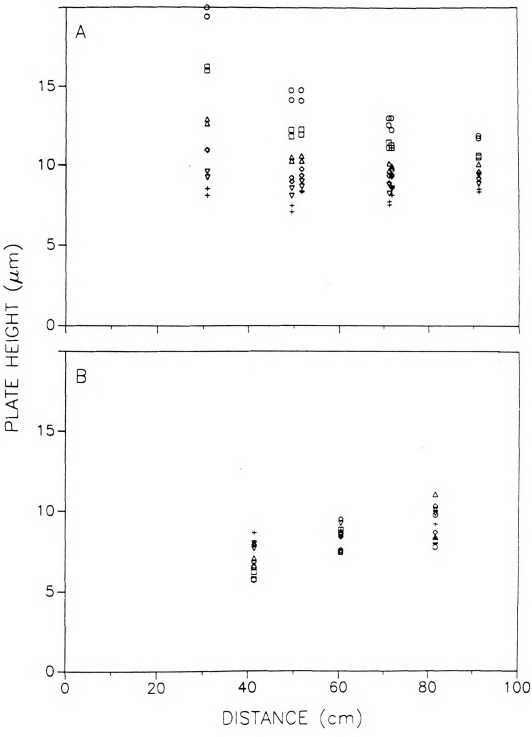

single detector, again reinforcing extra-column variance as the probable cause of the trends seen in Figure 4-6A. Although the local plate height values are more constant with distance than those evaluated at a single detector, the slight increase shown in Figure 4-6B appears to be statistically significant based on evaluation of the slope. Because many of the factors affecting dispersion are pressure dependent (Equations [1.23] to [1.26]), this increase in plate height may be a direct outcome of the pressure gradient along the column (16). In addition to the changes in local linear velocity and capacity factor described earlier, the diffusion coefficient (11,17) also varies with pressure and, thus, with position along the column. Because the influence of pressure is expected to reach an extreme in the region near the injector, studies are being extended to include this initial portion of the column. Recent results reported by Novotny *et al.* (18) do not exhibit this change in plate height with position, perhaps due to the low inlet pressure and nearly nonretained solute utilized in their study. Although the influence of the local pressure on plate height has been discussed theoretically (17), it has been previously inaccessible to direct experimental measurement.

In addition to the differing trends of plate height with column length for the single- and dual-mode detection, it is interesting to note a difference in the variation in plate height with capacity factor. In the single mode, the plate height decreases with increasing capacity factor. In contrast, the dual mode exhibits an increase in plate height with increasing capacity factor. Since the measurements are performed at linear velocities slightly greater than the optimum, the mobile- and stationary-phase mass transfer terms (C_M and C_S, respectively) are expected to have the predominant influence on plate height. If a van Deemter form of the plate height dependence on capacity factor is assumed (Equations [1.25] and [1.26]), the effect of the mobile-phase term would be an increase in plate height with capacity factor $\{f(k) = k^2/(1+k)^2\}$, while except for $k < 1$, the opposite trend is

expecte

measu

the du

is the

columi

contrit

could

[Equa

ideal

Altho

adso

simp

chen

varia

over

cont

acc

dete

sev

cha

4.4

re

expected for the stationary phase $\{f(k) = k/(1+k)^2\}$. Thus, the single-mode measurements would indicate that the stationary phase effects predominate, but the dual-detector measurements suggest that mass transfer in the mobile phase is the primary contribution. Again, this discrepancy may be caused by the extra-column influence on the single-mode measurements. That is, extra-column contributions are expected to have a larger effect on less retained solutes and could reverse the actual on-column trend of plate height with capacity factor (Equations [1.35] and [1.36]).

It is apparent from these studies that the retention and dispersion of even ideal solute zones along a chromatographic column is not yet clearly understood. Although it will be necessary in the future to extend investigations to include adsorption mechanisms and nonideal solutes, it is necessary to understand simple systems before proceeding to separations which are physically and chemically more complex. In addition, the influence of extra-column sources of variance on the accurate characterization of on-column dispersion cannot be overemphasized. The variation in the fraction of extra-column variance contributed at each detector position and to each solute profoundly affects the accurate measurement of dispersion using the single-mode technique. The dual-detection mode, which can eliminate these detrimental effects, clearly offers several distinct advantages for the more accurate measurement of solute zone characteristics.

4.4 Conclusions

Although presumed in many theoretical developments, it appears that retention and dispersion may not be truly constant along the column length. This

anomaly h

process a

physical c

phase ve

variation

will be m

anomaly has clear implications for optimization and evaluation of the separation process and merits further investigation to determined whether the origin is physical or chemical in nature. In the following chapters, the gradient in mobile-phase velocity will be examined in more detail. In addition, the systematic variation in retention behavior with distance and, apparently, with local pressure will be measured directly.

4.5 Lite

1. M
2. G
   1
3. M
4. H
5. M
6. I
7.
8.
9.
10.
11.
12.
13.
14.
15.
16.
17.
18.

4.5 Literature Cited in Chapter 4

1. McGuffin, V.L.; Zare, R.N. *Appl. Spectrosc.* **1985**, *39*, 847.
2. Gluckman, J.C.; Hirose, A.; McGuffin, V.L.; Novotny, M. *Chromatographia* **1983**, *17*, 303.
3. Martin, M.; Eon, C.; Guiochon, G. *J. Chromatogr.* **1975**, *108*, 229.
4. Huber, J.F.K.; Rizzi, A. *J. Chromatogr.* **1987**, *384*, 337.
5. Martin, M.; Blu, G.; Guiochon, G. *J. Chromatogr. Sci.* **1973**, *11*, 641.
6. Martire, D.E. *J. Chromatogr.* **1989**, *461*, 165.
7. Foley, J.P.; Crow, J.A.; Thomas, B.A.; Zamora, M. *J. Chromatogr.* **1989**, *478*, 287.
8. Jacob, L.; Guiochon, G. *J. Chromatogr. Sci.* **1975**, *13*, 18.
9. Giddings, J.C. *Sep. Sci.* **1966**, *1*, 73.
10. Bidlingmeyer, B.A.; Rogers, L.B. *Sep. Sci.* **1972**, *7*, 131.
11. Katz, E.; Ogan, K.; Scott, R.P.W. *J. Chromatogr.* **1983**, *260*, 277.
12. Tanaka, N.; Yoshimura, T.; Araki, M. *J. Chromatogr.* **1987**, *406*, 247.
13. Evans, C.E.; McGuffin, V.L. *Anal. Chem.* submitted.
14. Giddings, J.C. *Dynamics of Chromatography*; Marcel Dekker,Inc.: New York, **1965**; pp.79-84.
15. Evans, C.E.; McGuffin, V.L. *J. Microcol. Sep.* submitted.
16. Poe, D.P.; Martire, D.E. *J. Chromatogr.* **1990**, *517*, 3.
17. Martin, M.; Guiochon, G. *Anal. Chem.* **1983**, *55*, 2302.
18. Karlsson, K.; Novotny, M. *Anal. Chem.* **1988**, *60*, 1662.

CHAPTER 5

THE INFLUENCE OF PRESSURE ON MOBILE-PHASE VELOCITY

5.1 Introduction

A spatial pressure gradient is inherent in any system where pressure is the driving force for fluid flow. This gradient has long been recognized as important in gas chromatographic applications due to the high compressibility of the mobile phase (1-3). As the pressure decreases along the column length, the gas expands to occupy an increased volume, resulting in a concomitant increase in the volumetric flowrate. Under constant mass flow conditions, this decompression of the mobile phase also yields an increase in the mobile-phase linear velocity with distance. Fortunately, while gases are quite compressible, the viscosity of gases is low and, thus, the pressure drop necessary for chromatographic flowrates is minimal (1-2 bar). Nonetheless, for typical gas chromatographic conditions, mobile-phase compression may result in increases of 50% in linear velocity over the length of a packed column (3). By contrast, liquids are generally considered incompressible and the variation in linear velocity along the column is consistently ignored in liquid chromatographic applications.

However, the mobile-phase liquids commonly utilized are significantly more viscous than their gaseous counterparts and, thus, the applied pressures necessary for fluid flow are considerably higher, typically 50 to 350 bar (700-5000 psi). Because liquids are slightly compressible, the resulting increase in linear velocity along the column under typical conditions may be 1-5% (4). Although markedly less than for gas chromatographic applications, the systematic error introduced by ignoring this pressure gradient effect may give rise to significant errors in fundamental studies of the separation process.

The on-column detection technique provides a unique opportunity to examine this effect experimentally. By measuring the mobile-phase linear velocity as a function of distance along the column, the *in situ* measurement may be directly compared with theoretical predictions. In addition, the effect of this velocity gradient on the accurate determination of column porosity may be examined. While the investigations discussed in this chapter focus on the physical effects of the pressure gradient, the next chapter will explore the influences of the local pressure on the chemical aspects of the separation process as well.

5.2 Theoretical Considerations

Because pressure influences so many physical and chemical processes, evaluation of pressure effects in chromatographic separations requires careful attention to detail. Even the seemingly obvious choice of pressure as the variable of interest has been recently questioned (5). While pressure may be applicable as a variable when the fluid is an ideal gas, density is a more directly useful state variable when nonideal fluids are of interest. Thus, because reversed-phase chromatographic conditions are investigated here, the general

formalism

employed.

the densit

function o

are given

(5) for the

Th

packed c

$$u = -\frac{B}{\varepsilon_1}$$

This ge

regime

separati

assume

may va

terms o

$$dx = -$$

where

consta

to x_j n

$$\langle p \rangle_x$$

formalism based on density that was recently introduced by Martire (5) is employed. This derivation is quite general and may be applied to any fluid where the density as a function of pressure (i.e., compressibility), and the viscosity as a function of density are known. Although portions of the theoretical development are given here for clarity, the reader is referred to the excellent paper by Martire (5) for the full derivation and validation.

Theoretical evaluation of the local mobile-phase density (ρ_x) along a packed column is accomplished based on Darcy's law (6).

$$u = - \frac{B_0}{\varepsilon_T \eta} (dP/dx) \qquad [5.1]$$

This general expression, which is valid when fluid flow is in the laminar flow regime and at constant temperature, is directly applicable to chromatographic separations. The column permeability (B_0) and total porosity (ε_T) are commonly assumed to be constant, while the viscosity (η) and pressure gradient (dP/dx) may vary with distance along the column. Equation [5.1] may be rearranged in terms of the density (ρ) to yield,

$$dx = - \frac{B_0}{\varepsilon_T \eta u} (dP/d\rho)_T \, d\rho \qquad [5.2]$$

where $(dP/d\rho)_T$ is equal to the reciprocal of the compressibility coefficient (β^{-1}) at constant temperature divided by the density ρ.

The spatial average density ($\langle\rho\rangle_x$) in the region extending from distance x_i to x_j may be described as the first statistical moment with distance.

$$\langle\rho\rangle_x = \frac{\int_{x_i}^{x_j} \rho \, dx}{\int_{x_i}^{x_j} dx} \qquad [5.3]$$

This e
assum
length
flowra
linear
densi

$u_x \rho_x$

Com
dens
dete

$\langle p \rangle$

whe
and

the
de
Ta

$\left(\right.$

In
p

This expression conveniently allows the determination of the local density by assuming a small interval from x_i to x_j, or the average density over the column length when the integration interval is 0 to L. If it is assumed that the mass flowrate is constant throughout the system, the product of the mobile-phase linear velocity and density remains constant within the column regardless of local density/pressure.

$$u_x \rho_x = u_0 \rho_0 = \text{constant} \qquad [5.4]$$

Combining Equations [5.2], [5.3], and [5.4], and changing integration variables to density, the necessary expression for the spatial average density ($<\rho>_x$) may be determined.

$$<\rho>_x = \frac{\int_{\rho_i}^{\rho_j} \rho^2 \eta^{-1} (dP/d\rho)_T \, d\rho}{\int_{\rho_i}^{\rho_j} \rho \eta^{-1} (dP/d\rho)_T \, d\rho} \qquad [5.5]$$

where ρ_i and ρ_j are the local density values corresponding to distance positions x_i and x_j, respectively.

Evaluation of Equation [5.5] requires knowledge of both the density and the viscosity as a function of pressure for the fluid of interest. For liquids, the density behavior with pressure may be evaluated using a modified form of the Tait equation of state (4,7).

$$\left(\frac{P_0 + b}{P + b} \right) = \exp \left(\frac{\rho}{\rho_0} - 1 \right) \qquad [5.6]$$

In this empirical expression, a constant mass is assumed to be present at pressure P and atmospheric pressure P_0. In the pressure region of interest in

liquid

the firs

$$\left(\frac{P_0 +}{P +}\right.$$

where

press

the a

intere

funct

mobi

the f

$\eta =$

whe

exp

set

inte

reg

the

5.

th

liquid chromatography (30 to 350 bars), Equation [5.6] may be approximated by the first term in a series expansion,

$$\left(\frac{P_0 + b}{P + b}\right)^c = \left(\frac{\rho}{\rho_0}\right) \qquad [5.7]$$

where b and c are constants for a given fluid at constant temperature, and the pressure is expressed in bars. Although this expression is valid for many liquids, the accuracy of this approximation must be determined for each mobile phase of interest.

In addition to the variation of density with pressure, viscosity is also a function of the local pressure on the column. The influence of pressure on the mobile-phase viscosity (η) is often evaluated assuming a linear dependence of the form,

$$\eta = \eta_0 (1 + \alpha P) \qquad [5.8]$$

where α and η_0 are constant for a given isothermal fluid (4). As for the density expression, the validity of Equation [5.8] must also be assessed for each specific set of experimental conditions.

Evaluation of Equations [5.7] and [5.8] for the mobile-phase fluid of interest, combined with Equation [5.5] yields the average density in specific regions of the column. From this expression, the variation in linear velocity along the column may be predicted based on Equation [5.4].

5.3 Application to Experimental Conditions

For the pure methanol mobile phase utilized in this study, the behavior of the density with pressure is accurately described by Equation [5.7], resulting in

errors

[5.7], t

and c

As sh

Equat

nearly

chron

likew

only

0.53

resu

the

<p>

Alte

alo

x/

U

d

th

i

errors of less than 0.4 ppt for pressures up to 350 bar. In evaluating Equation [5.7], the density of methanol at atmospheric pressure (ρ_o) is 0.787 g/mL, while b and c are equal to 1210 and 0.148 when the pressure is expressed in bars (4). As shown in Figure 5-1, the reduced density ($\rho_R = \rho/\rho_C$), determined from Equation [5.7] and the critical density for methanol ($\rho_C = 0.321$ g/cm^3), exhibits a nearly linear dependence on pressure in the range of interest in liquid chromatography. Experimental measurements of methanol viscosity (8,9) can likewise be utilized to verify the accuracy of Equation [5.8], resulting in an error of only 0.3 ppt in the same pressure range (with $\alpha = 4.70 \times 10^{-4}$ bar^{-1} and η_o = 0.531 cP at 25 °C).

Substitution of Equations [5.7] and [5.8] for methanol into Equation [5.5] results in the following expression for the average mobile-phase density ($\langle\rho\rangle_x$) in the specific region extending from local densities ρ_i to ρ_j.

$$\langle\rho\rangle_x = \frac{\int_{\rho_i}^{\rho_j} \rho^{7.76}\, d\rho \,/\, (0.4313 + 2.8728\,\rho^{6.76})}{\int_{\rho_i}^{\rho_j} \rho^{6.76}\, d\rho \,/\, (0.4313 + 2.8728\,\rho^{6.76})} \qquad [5.9]$$

Alternatively, this expression may be written in terms of the fractional distance along the column (x/L) upon integration of Equation [5.2].

$$x/L = \frac{\int_0^x dx}{\int_0^L dx} = \frac{\int_{\rho_i}^{\rho_x} \rho^{6.76}\, d\rho \,/\, (0.4313 + 2.8728\,\rho^{6.76})}{\int_{\rho_i}^{\rho_o} \rho^{6.76}\, d\rho \,/\, (0.4313 + 2.8728\,\rho^{6.76})} \qquad [5.10]$$

Unfortunately, this expression is cannot be solved analytically and the local density (ρ_x) used as an integration variable must be calculated as a function of the fractional distance along the column by successive approximation. As shown in Figure 5-2, the relationship between the local density (ρ_x) and fractional

Figure 5-1: Calculated reduced density as a function of pressure for methanol (Equation [5.7]).

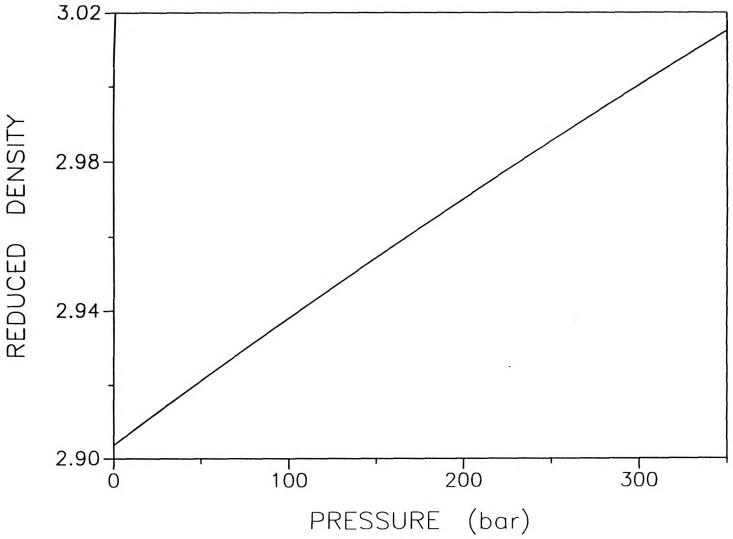

Figure 5-1

Figure 5-2: Local density (ρ_x) *versus* fractional distance along the column (x/L) calculated from Equation [5.10] (□) compared with linear interpolation (—).

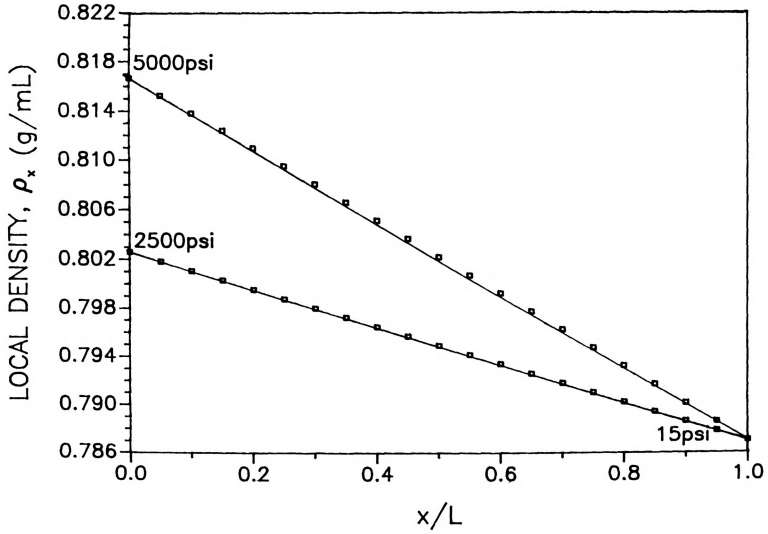
0.822
0.818
0.814
0.810
0.806
0.802
0.798
0.794
0.790
0.786
LOCAL DENSITY, ρ_x (g/mL)
5000psi
2500psi
15psi
0.0
0.2
0.4
0.6
0.8
1.0
x/L

Figure 5-2

column

pressure

170 and

$\rho_x = \rho_l -$

Thus, t

points

evaluat

$(\langle p \rangle_x)$

gradien

5.4 Es

is per

and

metha

yieldi

from

moni

cm a

linea

flow

$F =$

column distance (x/L) is linear for methanol within 0.5 ppt error for the inlet pressures commonly encountered in liquid chromatography (2500 and 5000 psi; 170 and 340 bar).

$$\rho_x = \rho_i - (\rho_i - \rho_o)\,(x/L) \qquad [5.11]$$

Thus, the spatial average density $\langle\rho\rangle_x$ can be determined between any two points along the column as a function of fractional distance. If the density is evaluated between two points in close proximity, the spatial average density ($\langle\rho\rangle_x$) and the local density (ρ_x) become equal. Finally, the effect of this density gradient on the linear velocity gradient may be predicted based on Equation [5.4].

5.4 Experimental Evaluation

Experimental measurement of the linear velocity as a function of distance is performed on the identical chromatographic column described in Chapter 4 and under similar chromatographic and spectroscopic conditions. The pure methanol mobile phase is operated in the constant flow mode (F = 0.72 μL/min), yielding an inlet pressure (P_i) of 4000 psi (270 bar). A decomposition product from the coumarin label is, again, utilized as the void marker. The void time is monitored as a function of distance using two detectors positioned at 30 and 50 cm and, subsequently, at 70 and 90 cm along the column (L = 100 cm). The linear velocity at atmospheric pressure (u_0) is calculated from the volumetric flowrate (F) measured at the column exit,

$$F = \pi R_{COL}^2 u_0 \varepsilon_T \qquad [5.12]$$

where th
the colu
P
[5.4] an
linear v
(170 an
column
column
compre
evalua
local v
may a
experi
injecti
single
alway
densi
equiv

along
5-4,
pred
How
appr
the
zon
for

where the column radius (R_{COL} = 0.0100 cm) and the total porosity (ε_T = 0.43) of the column have been determined previously.

Prediction of the linear velocity behavior is accomplished utilizing Equation [5.4] and the linear approximation of density with distance verified above. Local linear velocity ratios (u_x/u_0) expected for inlet pressures of 2500 and 5000 psi (170 and 340 bar, respectively) are shown in Figure 5-3 as a function of fractional column distance (x/L). Although the expected change in linear velocity along the column is less than for gas and supercritical fluid phases, which are highly compressible, the variation in the local velocity of 2 to 4% may be important in evaluating local retention and dispersion processes. In addition to calculating the local velocity ratio (u_x/u_0), the ratio predicted as an average from the column inlet may also be evaluated. This cumulative velocity ratio ($\langle u \rangle_x/u_0$) is that measured experimentally utilizing a single detector to determine the column void time from injection. It is clear from Figure 5-3 that the linear velocity measured using a single detector is an average of the velocity up to the point of detection and, thus, always underestimates the local linear velocity at that position. Because the local density is linear with distance, the spatial and temporal average velocities are equivalent and may be used interchangeably (5).

Experimental measurements of the cumulative velocity ratio with distance along the column are illustrated together with the theoretical predictions in Figure 5-4. Although measurements are in general agreement with theoretical predictions, the precision in replicate determinations appears to be rather poor. However, the relative standard deviation in replicate measurements of approximately 2% is quite good, considering that both the deviation in measuring the volumetric flowrate and in calculating the first moment of the nonretained zone contribute to the determination. The difficulty appears to lie in the necessity for measuring changes in the zone velocity of only a few percent. Further

Figure 5-3: Theoretically predicted ratio of the local mobile-phase linear velocity (u_x) to the linear velocity at atmospheric pressure (u_0) *versus* the fractional column distance (x/L) (—), together with the cumulative velocity ratio ($\langle u \rangle_x / u_0$) (--).

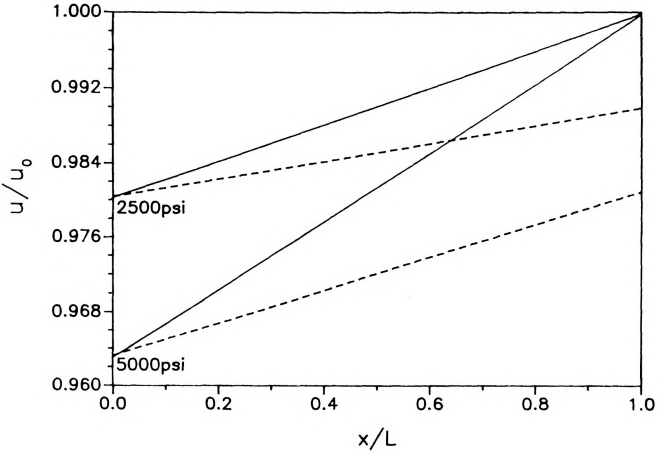
1.000
0.992
0.984
0.976
0.968
0.960
u/u0
2500psi
5000psi
0.0
0.2
0.4
0.6
0.8
1.0
x/L

Figure 5-3

Figure 5-4: Comparison of theoretically predicted local (—) and cumulative (– –) velocity ratio to experimental measurement of the cumulative velocity ratio ($\langle u \rangle_x / u_0$) using single-mode detection (O). Chromatographic conditions: Methanol F = 0.72 μL/min, P_i = 4000 psi (270 bar).

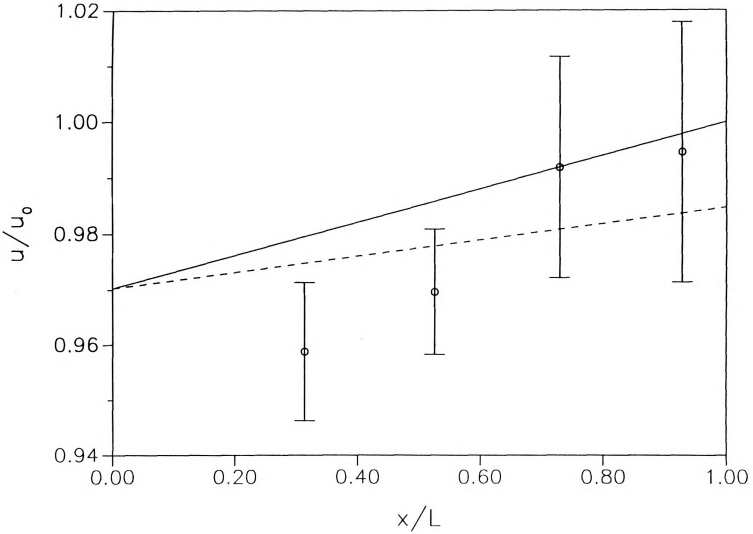

Figure 5-4

examination of this mobile-phase compression is accomplished by varying the inlet pressure and, thus, the linear velocity gradient along the column. The theoretical prediction of this effect as a function of the pressure difference (P_x - P_o) is shown in Figure 5-5 together with the measured velocity ratios. Although the measured data show considerable variation, the trend with pressure is in good agreement with that expected based on the preceding theoretical development. Thus, even though methanol is usually considered an incompressible fluid, a systematic increase in linear velocity along the length of the column is theoretically predicted and is experimentally observed.

This density/velocity gradient has important implications in the measurement of fundamental column parameters. For example, the total porosity of the column, indicative of column packing structure (10-14), is determined experimentally based on Equation [5.12] (11). However, when the fluid is compressible, the linear velocity determined from the void time is the average velocity $\langle u \rangle_x$, not the velocity at atmospheric pressure u_0. In this case, the ε_T value determined using Equation [5.12] assuming an incompressible mobile phase is in error by the factor $u_0/\langle u \rangle_x$ as shown in Equation [5.13].

$$F = \pi R_{COL}^2 \langle u \rangle_x \varepsilon_T (u_0/\langle u \rangle_x) \qquad [5.13]$$

Although this error has been addressed in the literature for gas chromatographic applications (13), it has been assumed to be unimportant in studies of liquid chromatographic columns. As shown in Figure 5-6, total porosity values calculated based on Equation [5.12] exhibit a clear increase with pressure drop. Moreover, this variation is in good agreement with the expectation that this error arises from the change in $u_0/\langle u \rangle_x$ with pressure. Thus, the often unstated assumption of incompressibility leads to a systematic overestimation of the total column porosity. From Figure 5-6, the total porosity may be determined by linear

Figure 5-5: Experimental measurement of the mobile-phase linear velocity ratio as a function of the pressure difference (P_x - P_o) on the column at 30 cm (○), 52 cm (□), and as the dual (△) measurement (u = 0.014 to 0.11 cm/s). Theoretical prediction (——) calculated based on Equations [5.7] and [5.9].

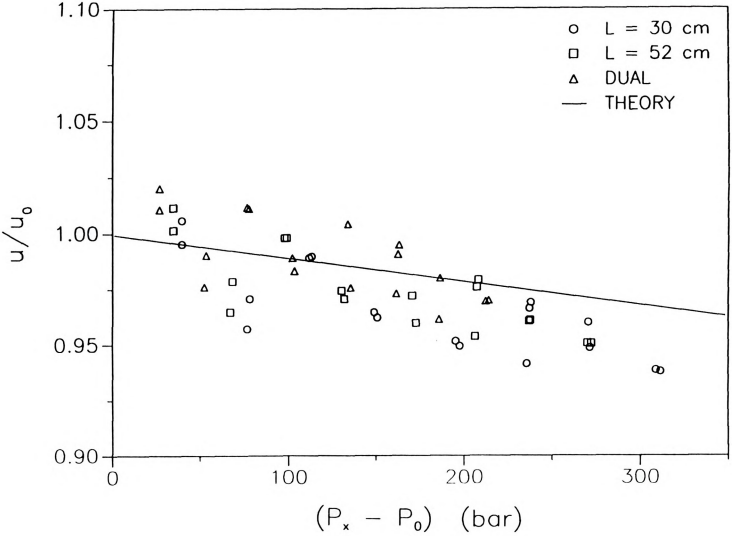
1.10
1.05
1.00
0.95
0.90
u/u0
0
100
200
300
(Px − P0) (bar)
L = 30 cm
L = 52 cm
DUAL
THEORY

Figure 5-5

Figure 5-6: Apparent increase in the total porosity with pressure difference (P_x - P_o) resulting from the compression of the mobile phase shown in Figure 5-5. Experimental conditions as described Figure 5-5.

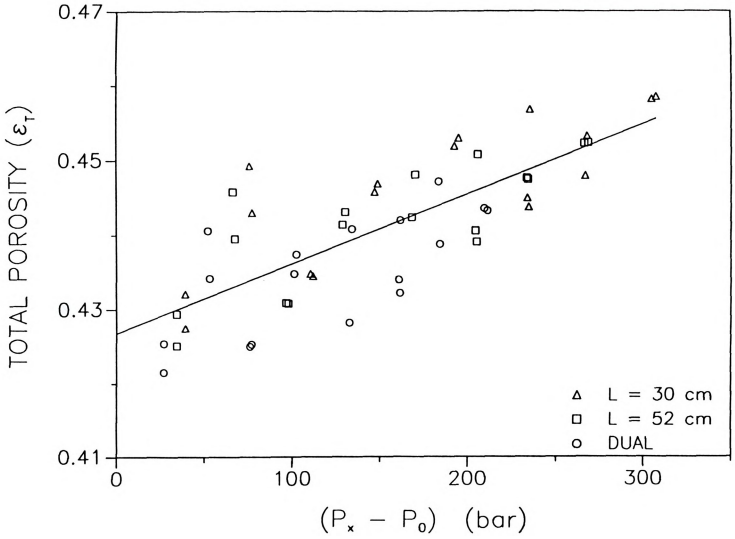
0.47
0.45
0.43
0.41
TOTAL POROSITY (ε_T)
0
100
200
300
$(P_x - P_0)$ (bar)
L = 30 cm
L = 52 cm
DUAL

Figure 5-6

extrapolation to zero pressure, resulting in an ε_T value of 0.427. Off-column measurements based on Equation [5.12] yield a total porosity of 0.446, a systematic error of +4.5% for an inlet pressure of 270 bar. Because measurements performed after the column exit yield an average of the velocity over the length of the column, total porosity determinations will always be systematically greater than the true value. Although this error is not as extreme as for gas or supercritical fluid conditions, the determination of fundamental column parameters is significantly and systematically affected. This deviation is expected to be even more pronounced in normal-phase separations, where commonly utilized mobile-phase solvents exhibit greater compressibility.

5.5 Conclusions

The pressure/density gradient along the chromatographic column has been shown to induce a linear velocity gradient under reversed-phase conditions. Thus, the linear velocity measured at the column exit is an average of that occurring over the length of the column. Under commonly encountered experimental conditions, the compressibility of even polar solvents results in an increase in mobile-phase velocity of ~3%. This result is consistent with recent reports by Foley *et al.* of errors in delivering accurate flowrates to chromatographic columns (15). This velocity gradient also has interesting implications for the dispersion of solute zones along the column (Equations [1.23] to [1.26]). In addition, the total column porosity measured at the exit will appear to be a function of the pressure drop and may be systematically overestimated by more than 4%. Thus, contrary to common misconceptions, the experimental conditions commonly encountered in liquid chromatographic separations are sufficient to induce a significant velocity gradient along the column.

5.6 L

1.

2.

3.

4.

5.

6.

7.

8.

9.

10.

11.

12

13

14

15

5.6 Literature Cited in Chapter 5

1. James, A.T.; Martin, A.J.P. *Biochem. J.* **1952**, *50*, 679.
2. Giddings, J.C. *Anal. Chem.* **1963**, *35*, 353.
3. Guiochon, G. *Chrom. Rev.* **1966**, *8*, 1.
4. Martin, M.; Blu, G.; Guiochon, G. *J. Chromatogr. Sci.* **1973** *11*, 641.
5. Martire, D.E. *J. Chromatogr.* **1989**, *461*, 165.
6. Darcy, H.P.G. *Les Fontaines Publiques de la Ville de Dijon*, Victor Dalmont, **1856**, Paris.
7. Tait, P.G. *Scientific Papers* Vol. 2, University Press: London; **1900**, pp. 343-348.
8. Bridgman, P.W. *Proc. Acad. Arts and Sci.* **1926**, *61*, 59.
9. Isakova, N.P.; Oshueva, L.A. *Russ J. Phys. Chem.* **1966** *40*, 607.
10. Unger, K.K. *Porous Silica* Elsevier: Amsterdam, **1979**.
11. Bristow, P.A.; Knox, J.H. *Chromatographia* **1977**, *10*, 279.
12. Ohmacht, R.; Halasz, J. *Chromatographia* **1981**, *14*, 155.
13. Cramers, C.A.; Rijks, J.A.; Schutjes, C.P.M. *Chromatographia* **1981**, *14*, 439.
14. Gluckman, J.C.; Hirose, A.; McGuffin, V.L.; Novotny, M. *Chromatographia* **1983**, *17*, 303.
15. Foley, J.P.; Crow, J.A.; Thomas, B.A.; Zamora, M. *J. Chromatogr.* **1989**, *478*, 287.

CHAPTER 6

THE INFLUENCE OF LOCAL PRESSURE ON SOLUTE RETENTION

6.1 Introduction

In this chapter, studies of pressure effects on separation processes are extended to include the chromatographic retention of solute zones. To understand the effect of pressure in chromatographic systems, it is important to distinguish the effect of the pressure/density gradient from the influence of the local pressure/density. As discussed in the previous chapter, the pressure gradient along the column causes decompression of the mobile phase as a function of distance, resulting in an expansion of the fluid along the column. In addition to the pressure gradient, the absolute local pressure on the column may also affect separation processes.

The influence of pressure on fundamental physical properties such as density, viscosity, diffusion coefficient, etc. is well documented (1-6). Pressure effects on equilibrium processes have been investigated as well (7,8). This fundamental understanding has made possible a number of theoretical predictions of the influence on mobile-phase velocity (9), solute retention (10),

and zone dispersion (11). The possible control and exploitation of pressure-induced equilbrium shifts for chromatographic separations was first introduced by Giddings (12,13), leading to the development of supercritical fluid chromatography. Although variations in equilibrium constants in the liquid phase may not be expected to be large when compared to those in supercritical fluids, the greater pressures commonly applied in liquid chromatographic separations may be sufficient to induce significant changes. Under high-speed conditions or with recycle systems, the increase in retention with pressure may be significant enough to limit applicability (14). Unfortunately, only a limited number of experimental investigations have been reported in the literature. Under extreme pressure conditions (20,000 psi), Rogers *et al.* (15-17) measure up to a three-fold increase in capacity factor and a significant change in selectivity with separations utilizing an adsorption/exchange mechanism. Likewise, Tanaka *et al.* (18) measure a 12% variation in capacity factor for reversed-phase separations performed under ionization control with much more modest pressure variations (3000 psi). Measurements by Katz *et al.* (19) under normal-phase conditions indicate a decrease in retention, which the authors attribute to an increase in temperature in the column interior. In all cases, variations in the absolute pressure, not the pressure gradient, lead to significant variations in solute retention.

These findings have interesting implications for the variation in retention with distance along a chromatographic column. It is clear that if a retention gradient is present, the capacity factor measured at the column exit is only an indication of the average behavior of the solute. The determination of fundamental retention parameters becomes even more complicated if the selectivity is also a function of the local pressure/distance.

The on-column detection scheme may be used to advantage in evaluating

the influence of these pressure-dependent retention processes. The direct measurement of local solute retention on the chromatographic column allows the systematic evaluation of the influence of local pressure. By varying the inlet pressure while maintaining constant pressure gradient conditions, the local retention may be directly correlated to the local pressure on the column. In addition, the use of small diameter, packed-capillary columns minimizes variations in temperature within the column that may arise from viscous flow. Finally, the model solutes chosen for these studies probe the most universal type of interactions, induced-dipole induced-dipole. Thus, systematic measurements of the dependence of local pressure on solute retention should find general applicability for liquid chromatographic separations.

6.2 Theoretical Considerations

As discussed in Chapter 1, solubility parameter theory can be utilized to predict retention behavior in liquid chromatography. Thus, insight into the possible relationship between pressure and solute retention can be gained from this theoretical approach. The cohesive energy density of interaction or solubility parameter (δ), which is utilized to estimate the species polarity, is given by (20)

$$\delta^2 = -E/V = (\partial E/\partial V)_T \qquad [6.1]$$

where E is the interaction energy and V is the molar volume. More generally, the solubility parameter is described as the partial derivative of energy with molar volume under constant temperature conditions (21). If the interaction energy is approximated from van der Waal's theory (21), δ can be expressed in terms of the van der Waal's coefficient a and the species molecular weight m.

$$\delta = (a^{1/2}/V) = (a^{1/2}/m)\,\rho \qquad [6.2]$$

Density (ρ), not pressure, is chosen as the state variable in this expression to allow more general applicability, as discussed in Chapter 5. Implicit in this relationship is the assumption that increased density/pressure acts solely to decrease the volume, without altering the nature or energy of interaction. While this assumption may be questionable for species with multiple modes of interaction, it appears to be reasonable if only dispersion interactions are present. The weak variation in the interaction energy with distance for dispersion forces ($1/r^6$) makes the presumption of little change with pressure a viable one (Equation [1.2]).

For subsequent comparison with other theories, it is convenient to write Equation [6.2] as a function of the reduced density ($\rho_R = \rho/\rho_C$).

$$\delta_i = (\rho_C\, a^{1/2}/m)\,\rho_R \qquad [6.3]$$

In this expression, the density is expressed as a fraction of the critical density (ρ_C). Based on Equation [6.3], the solubility parameter and, therefore, the species polarity is expected to increase linearly with the reduced density.

This relationship has interesting implications for the expected behavior of solute retention with pressure/density. As discussed in Chapter 1 (Equation [1.7]), the capacity factor of solute i (k_i) may be described by the following expression (22):

$$\ln k_i = \frac{V_i}{RT}\,[(\delta_i - \delta_M)^2 - (\delta_i - \delta_S)^2] - \ln \beta$$

Unfortunately, theoretical advances are presently insufficient to allow the prediction of the influence of pressure/density on all of these parameters. However, the low concentration of solute species i allows the approximation that

the solute molar volume (V_i) and solubility parameter (δ_i) are independent of the pressure/density. In addition, the stationary phase solubility parameter (δ_S) and phase ratio (β) are assumed to be less affected by the pressure/density than the mobile phase. Although not rigorously correct, this supposition is reasonable considering the stationary phase is attached to a solid support, limiting the compressibility compared to a bulk phase (10). Thus, consistent with the few experimental measurements in the literature (15-19), the primary effect of pressure/density is assumed to arise from the mobile phase. Based on this assumption, Equation [6.3] for the mobile phase may be combined with Equation [1.7] to give the solute capacity factor as a function of the mobile-phase reduced density (ρ_{RM}).

$$\ln k_i = c_1 \rho_{RM}^2 + c_2 \rho_{RM} + c_3 \qquad [6.4]$$

where

$$c_1 = \left(\frac{V_i}{RT} \right) \left(\frac{\rho_{CM} a_M^{1/2}}{m_M} \right)^2$$

$$c_2 = \left(\frac{-2V_i}{RT} \right) \left(\frac{\rho_{CM} a_M^{1/2}}{m_M} \right) \delta_i$$

$$c_3 = \left(\frac{V_i}{RT} \right) \{\delta_i^2 - (\delta_i - \delta_S)^2\} - \ln \beta$$

In this expression, c_1 represents mobile-phase/mobile-phase interactions, where ρ_{CM} is the reduced density of the mobile phase, a_M is the van der Waal's interaction coefficient, and m_M is the molecular weight. As expected, interaction of mobile-phase molecules increases with reduced density/pressure, leading to an increase in solute capacity factor. In the second constant (c_2), the solute/mobile-phase interaction is expressed in terms of the mobile-phase

interaction coefficient (a_M) and the solute solubility parameter (δ_i). As the reduced density of the mobile phase increases this parameter becomes more negative, resulting in an overall decrease in retention. Finally, solute/stationary-phase interactions are described in the third constant (c_3). As assumed in the derivation, this term is independent of the mobile-phase reduced density. An increase in these interactions results in the intuitively predicted increase in retention. This expression (Equation [6.4]) is similar to predictions based on statisitical thermodynamics developed by Martire (10). However, Martire's lattice model approach is more rigorous in describing interactions between species assumed to be independent in solubility parameter theory. Unfortunately, the estimation of these interaction parameters is quite difficult in the liquid phase.

The expected variation in the selectivity (α) or differential movement of solutes can likewise be predicted as a function of pressure/density. Combining the definition of selectivity with Equation [1.7] results in an expression for α as a function of solubility parameter values (22):

$$\ln \alpha_{ij} = \ln \frac{k_j}{k_i} = \left(\frac{V_i}{RT} \right) (\delta_i - \delta_j) (\delta_M - \delta_S) \qquad [6.5]$$

As derived above, substitution of Equation [6.3] results in an expression for the solute selectivity as a function of the mobile-phase reduced density.

$$\ln \alpha_{ij} = c_4 \rho_{RM} - c_5 \qquad [6.6]$$

$$c_4 = \left(\frac{2V_i}{RT} \right) \left(\frac{\rho_{CM} a_M^{1/2}}{m_M} \right) (\delta_i - \delta_j)$$

$$c_5 = \left(\frac{2V_i}{RT} \right) (\delta_i - \delta_j) \delta_S$$

From this expression, a simple linear variation in $\ln \alpha_{ij}$ with the mobile-phase

reduced density is predicted. The slope (c_4) in Equation [6.6] corresponds to interactions between the mobile phase and the solutes, while the intercept is indicative of solute/stationary-phase interactions.

From the above expressions, both solute retention and selectivity are predicted to be affected by the reduced density of the mobile phase and, thus, the local pressure on the column. Unfortunately, the absolute magnitude of this influence is difficult to predict *a priori*. The requirement for accurately estimating five unknown variables (δ_M, δ_S, β, δ_i, and V_i), combined with the quadratic dependence on a logarithmic term (Equation [6.4]) lead to large errors in the prediction of solute retention. However, direct comparison of theoretically predicted trends with experimental measurements should provide a good qualitative understanding of the parameters affecting retention.

6.3 Experimental Methods

Analytical Methodology. Saturated fatty acid standards from *n*-$C_{10:0}$ to *n*-$C_{20:0}$ are derivatized with 4-bromomethyl-7-methoxycoumarin as described in Chapter 4. Standards are dissolved in methanol and injected individually at a concentration of 5×10^{-4} M.

Chromatographic System. The chromatographic system is similar to that described in Chapter 2 and illustrated in Figure 2-1. In this study, however, a 25.7 cm length of open-tubular capillary (0.0050 cm i.d.) connects the injector to the column. This arrangement makes possible the placement of detectors in the high-pressure region near the column inlet.

The microcolumn utilized for these pressure studies is fabricated as

described in Chapter 4. Before packing, the polyimide coating is removed from a 43.9 cm length of fused-silica tubing at 5 cm intervals to facilitate on-column detection. The resulting column has a plate height of 9.5 μm, a total porosity of 0.43, and a flow resistance parameter of 550 under standard test conditions (23). For all measurements, a pure methanol mobile phase is delivered to the column with a single-piston, reciprocating pump (Beckman, Model 114M) under constant pressure conditions. The inlet pressure is systematically varied from 100 to 350 bar (1500 - 5000 psi) using a 20 μm i.d. restrictor at the column exit. The length of the restrictor and splitter are altered in the course of this study to allow the volumetric flowrate (F = 0.70 μL/min) and injection volume (V_{INJ} = 11 nL) to remain constant under all pressure conditions.

Detection System. The optical detection conditions are identical to those described in Chapter 2. As shown in Figure 6-1, however, six matched detector blocks are positioned along the column with optical fibers from alternate blocks connected to each detection system. Since all detectors are active continuously, solutes are injected individually, thus allowing multiple detection points for a single injection with only two monochromator/photomultiplier detection systems. The first detection block is positioned on the open tube 0.4 cm before the packed bed, while the remaining five detectors are placed on the packed bed at 4.9, 10.4, 15.5, 20.9, and 26.2 cm from the column head. The maximum viewed volumes under these conditions are 1.8 nL off-column and 12 nL on-column. Data acquisition is accomplished under computer control at 5 Hz with a 0.06 s time constant.

Figure 6-1: Schematic diagram of detection system allowing simultaneous measurement at six points along the chromatographic column with only two monochromator/photomultiplier systems. I: injection valve; T: splitting tee; R: restricting capillary; MONO: monochromator; PMT: photomultiplier; AMP: current-to-voltage converter/amplifier.

Figure 6-1

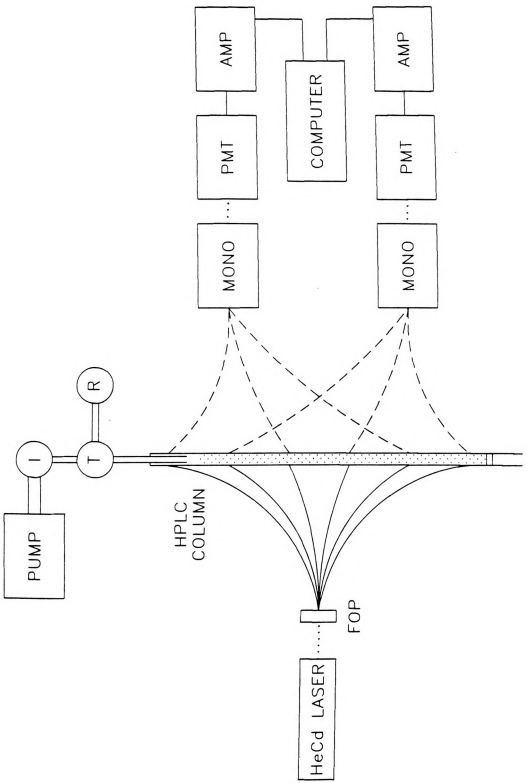
AMP
PMT
MONO
COMPUTER
AMP
PMT
MONO
R
I
T
PUMP
HPLC
COLUMN
FOP
HeCd LASER

6.4 Results and Discussion

Experimental evaluation of the pressure/density dependence of solute capacity factor is accomplished by systematically increasing the inlet pressure from 102 to 337 bar (ρ_{INLET} = 0.796 to 0.816 g/cm^3, respectively, for methanol), while maintaining a constant pressure differential of 102 bar along the column. By measuring the capacity factor using single- and dual-mode detection, the average between the injector and the point of detection as well as the local capacity factor between detectors may be determined directly on the column. In addition, measurements are performed simultaneously at five positions in the high-pressure region of the column, allowing the evaluation of the local capacity factor at several positions for a single injection. Experimental measurements performed in this manner allow the direct, *in situ* determination of solute retention as a function of local pressure under nearly ideal chromatographic conditions.

Experimental measurements of capacity factor for both single- and dual-mode detection (L = 26.2 and 23.5 cm, respectively) are shown in Figure 6-2. A significant increase in the retention of *n*-$C_{16:0}$ is observed as a function of pressure for both single and dual modes, with *n*-$C_{16:0}$ exhibiting an increase greater than 16% with a precision in duplicate determinations of 0.5%. This increase is not limited to *n*-$C_{16:0}$, and a notable increase in k is measured for all solutes under practical inlet pressure conditions. The magnitude of this increase is somewhat surprising, however, based on the common belief that reversed-phase solvents are quite incompressible. It is even more unexpected for these model solutes, where only dispersion interactions are controlling retention. However, an increase in k is theoretically predicted based on the variation in the mobile-phase solubility parameter or polarity with pressure or reduced density (Equation [6.3]). As shown in Chapter 5, the reduced density of the methanol

Figure 6-2: Single- (top) and dual- (bottom) mode measurements of solute capacity factor (L = 26.2 and 23.5 cm, respectively) for n-$C_{16:0}$ as a function of the average pressure encountered by the solute. Experimental conditions as given in the text.

Figure 6-2

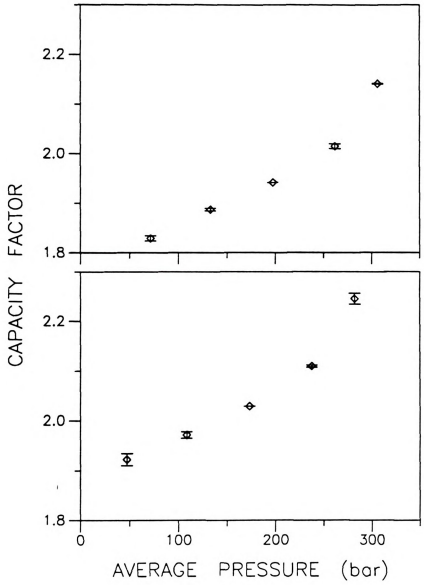
2.2
2.0
1.8
CAPACITY FACTOR
2.2
2.0
1.8
0
100
200
300
AVERAGE PRESSURE (bar)

mobile phase is approximately linearly dependent on the applied pressure (Figure 5-1). If only mobile-phase effects are considered, an increase in reduced density is predicted to yield a concomitant increase in solute retention (Equation [6.4]). As will be discussed later, determining the theoretically expected magnitude of this increase is nontrivial.

Although all solutes exhibit this increase in retention with pressure (Table 6.1), the experimentally measured percent increase ($\Delta k/k$) is systematically greater for longer chain solutes. This apparent dependence on chain length is theoretically predicted (Equation [6.4]) based on the direct dependence of ln k_i on solute molar volume (V_i) and, consequently, on carbon number. Thus, while the energy of interaction between the solute and mobile phase is assumed to remain constant, it is expected that the increase in the energy density with pressure will be greater when the solute occupies a larger volume. For this reason, the absolute pressure is expected to affect not only retention, but selectivity as well. Experimental evaluation of the solute selectivity with pressure clearly demonstrates this enhancement (Table 6.2). All adjacent solute pairs show a systematic rise in selectivity with average pressure, regardless of detection mode. Although the solutes chosen for this study are clearly separated, it is not difficult to imagine the analysis of a complex mixture where a 2% increase in selectivity would determine the success of the separation.

Thus far, solute retention and selectivity have been discussed only in terms of the predicted and observed direction of change, not the magnitude. However, as illustrated for *n*-$C_{16.0}$ (Figure 6-2), this increase is not a simple linear function of the average pressure for all solutes. This observed nonlinear increase is consistent with theoretical predictions based on the variation in capacity factor with reduced density. Although the reduced density varies nearly linearly with applied pressure (Figure 5-1), the quadratic dependence of ln k on

Table 6.1: Effect of pressure on single- and dual-mode measurements of solute capacity factor.

	CAPACITY FACTOR (k)					
	SINGLE MODE[a]			DUAL MODE[b]		
SOLUTE	P_{AVG}=72 bar	236 bar	Δk/k	48 bar	158 bar	Δk/k
n-$C_{10:0}$	0.501	0.547	+9.2%	0.520	0.571	+9.8%
n-$C_{12:0}$	0.784	0.874	+11.5%	0.818	0.921	+12.6%
n-$C_{14:0}$	1.208	1.383	+14.5%	1.261	1.441	+14.3%
n-$C_{16:0}$	1.829	2.141	+17.1%	1.923	2.245	+16.8%
n-$C_{18:0}$	2.712	3.284	+21.1%	2.827	3.419	+20.9%
n-$C_{20:0}$	3.997	4.970	+24.3%	4.197	5.205	+24.1%

[a] L = 26.2 cm
[b] L = 23.5 cm

Table 6.2: Effect of pressure on single- and dual-mode measurements of solute selectivity.

	SELECTIVITY (α)					
	SINGLE MODE[a]			DUAL MODE[b]		
SOLUTE	P_{AVG}=72 bar	236 bar	Δα/α	48 bar	158 bar	Δα/α
n-$C_{10:0/12:0}$	1.565	1.598	+2.1%	1.574	1.613	+2.5%
n-$C_{12:0/14:0}$	1.541	1.583	+2.7%	1.541	1.564	+1.5%
n-$C_{14:0/16:0}$	1.514	1.548	+2.2%	1.525	1.558	+2.2%
n-$C_{16:0/18:0}$	1.483	1.534	+3.4%	1.470	1.523	+3.6%
n-$C_{18:0/20:0}$	1.474	1.513	+2.7%	1.485	1.523	+2.6%

[a] L = 26.2 cm
[b] L = 23.5 cm

the reduced density (Equation [6.3]) leads to a predicted nonlinear increase in capacity factor with pressure. From Figure 6-2, this rise appears to be independent of detection mode, indicating that the pressure/density variation between the injector and detector induces only a small change in k. In this case, the average pressure provides a reasonable indication of the pressure experienced by the solute, regardless of the interval. Based on this hypothesis, however, the absolute magnitude of the capacity factor is expected to be greater for single-mode measurements than for the lower pressure dual-mode determinations, and the opposite trend is observed (Figure 6-2; Table 6.1). These results indicate the possibility of another source of variation in k along the column.

Based solely on the increase in solute retention and selectivity with pressure/density, it is expected that these fundamental separation parameters will not be constant along the column length, as is often assumed. In fact, capacity factor is expected to vary nonlinearly from the column inlet to exit, becoming successively less retained with distance. Thus, the capacity factor determined at the column exit is expected to be a measure of the average retention behavior of the solute along the column, and is not equal to the local retention as is often assumed. This deduction is consistent with previous measurements along the column shown in Chapter 4. As seen in Figure 6-3, however, single-mode measurements of capacity factor on this column show a clear increase with distance under different local pressure conditions. In contrast, dual-mode measurements, which are expected based on the average pressure to exhibit a capacity factor decrease of ~5%, are relatively constant with distance. These results are further evidence that the pressure/density encountered by the solute is not the only factor determining retention with distance in this system. In addition, because the average pressure encountered

Figure 6-3: Single- (top) and dual- (bottom) mode measurements of solute capacity factor as a function of distance along the column (L_{TOT} = 43.9 cm) under high and low inlet pressure conditions. Solutes: *n*-$C_{10:0}$ (○); *n*-$C_{12:0}$ (□); *n*-$C_{14:0}$ (△); *n*-$C_{16:0}$ (◇); *n*-$C_{18:0}$ (▽); and *n*-$C_{20:0}$ (+). Experimental conditions as given in the text.

Figure 6-3

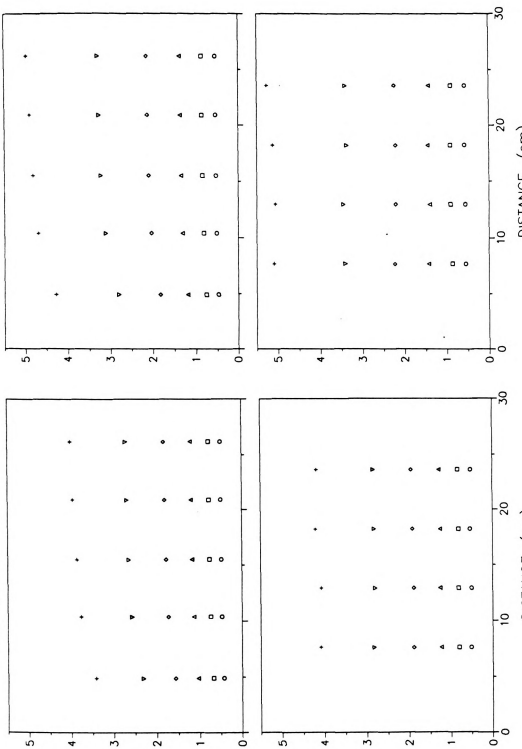
INLET PRESSURE: 1500 PSI
INLET PRESSURE: 4950 PSI
CAPACITY FACTOR
DISTANCE (cm)
DISTANCE (cm)

by the solute is always higher for single-mode determinations, it is expected that capacity factor measurements at a single detector will be greater than those evaluated in the dual mode. As seen in Table 6.1, experimental measurements show the opposite trend for all solutes. These anomalies in retention are not presently understood and may be due to nonuniformity in the stationary phase along the column caused by long-term usage, and further investigations of the column inlet region should elucidate this more clearly (Chapter 8). As shown in Figure 6-4, however, solutes continue to behave nearly ideally, exhibiting the theoretically expected logarithmic dependence of capacity factor on carbon number for both single- and dual-mode determinations.

Finally, quantitative prediction of retention is attempted for all solutes based on Equation [6.4]. As stated previously, the theoretical evaluation of capacity factor requires the accurate estimation of a number of unknown variables. Solubility parameters cited in the literature for octadecylsilica stationary phases (25,26) and methanol (20) are shown in Table 6.3. Mobile-phase solubility parameters are chosen for both bulk alkane estimates (22) as well as recent thermodynamic measurements on actual packing materials (25). Data on the coumarin-labeled fatty acids are lacking in the literature, however, requiring the approximation of molar volume based on group contributions to the van der Waal's volume (27) and the arbitrary placement of the solute solubility parameters between those of the mobile and stationary phases. Finally, the phase ratio for this column is estimated based on a 12% carbon loading on spherical particles. The resulting numerical prediction of the coefficients in Equation [6.4] is shown in Table 6.4. Comparison with experimental coefficients is accomplished by regression analysis of all dual-mode measurements. As shown in Figure 6-5, the retention behavior of all solutes is adequately described by the nonlinear regression of Equation [6.4]. While the theoretically predicted

Figure 6-4: Single- (top) and dual- (bottom) mode measurements of logarithmic dependence of capacity factor on carbon number under varying inlet pressure conditions. Experimental conditions as given in the text.

Figure 6-4

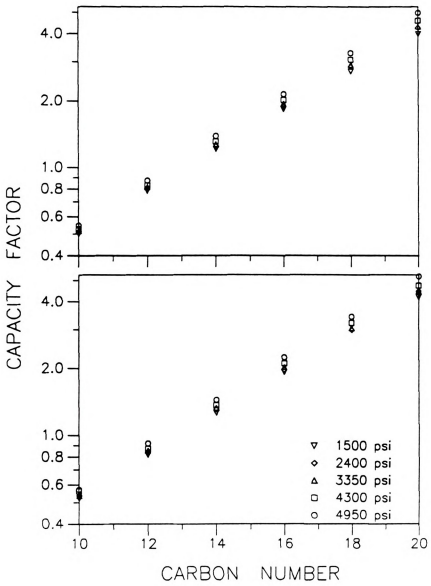
CAPACITY FACTOR
4.0
2.0
1.0
0.8
0.6
0.4
1500 psi
2400 psi
3350 psi
4300 psi
4950 psi
10
12
14
16
18
20
CARBON NUMBER

Table 6.3: Estimates of parameters for the prediction of solute capacity factor.

SOLUTE PARAMETERS (FATTY ACID DERIVATIVES)

	δ_i ($cal^{1/2}/cm^{3/2}$)	V_i [a] (cm^3/mol)
n-$C_{10:0}$	14.2	207
n-$C_{12:0}$	13.9	228
n-$C_{14:0}$	13.6	248
n-$C_{16:0}$	13.3	268
n-$C_{18:0}$	13.0	289
n-$C_{20:0}$	12.7	310

MOBILE-PHASE PARAMETERS (METHANOL)

δ_M = 14.5 $cal^{1/2}/cm^{3/2}$ [b]

ρ_C = 0.271 g/cm^3 [c]

ρ = 0.787 g/cm^3 at atmospheric pressure [c]

STATIONARY-PHASE PARAMETERS (OCTADECYL SILICA)

δ_S = 7 [d] and 12.5 $cal^{1/2}/cm^{3/2}$ [e]

β = 20

SYSTEM PARAMETERS

T = 301 K

R = 1.987 cal/K mol

---

[a] Bondi, A. *J. Phys. Chem.* **1964**, *68*, 441.

[b] Barton, A.F.M. *Chem. Rev.* **1975**, *75*, 731.

[c] Reid, R.C.; Prausnitz, J.M.; Sherwood, T.K. *The Properties of Gases and Liquids*; McGraw-Hill: New York, **1977**.

[d] Schoenmakers, P.J.; Billet, H.A.H.; de Galan, L. *Chromatographia* **1982**, *15*, 205.

[e] Yamamoto, F.M.; Rokushika, S. *J. Chromatogr.* **1990**, *515*, 3.

Table 6.4: Comparison of theoretically estimated and experimentally measured constants for Equation [6.4].

SOLUTE	C_1 EST.	C_1 MEAS.	C_2 EST.	C_2 MEAS.	C_3 EST.	C_3 MEAS.
n-$C_{10:0}$	8.63	10.6	-49.1	-61.9	49.0[a] (65.8)[b]	89.7
n-$C_{12:0}$	9.50	10.6	-52.9	-61.7	53.1 (69.9)	89.4
n-$C_{14:0}$	10.3	14.2	-56.3	-82.5	56.3 (73.2)	120
n-$C_{16:0}$	11.2	14.3	-59.5	-82.8	59.2 (76.0)	121
n-$C_{18:0}$	12.0	14.2	-62.7	-81.7	61.7 (78.5)	118
n-$C_{20:0}$	12.9	14.2	-65.7	-81.9	63.8 (80.6)	119

[a] Calculated based on $\delta_S = 7$ $cal^{1/2}/cm^{3/2}$
[b] Calculated based on $\delta_S = 12.5$ $cal^{1/2}/cm^{3/2}$

Figure 6-5: Measurements of logarithmic dependence of capacity factor on the mobile-phase reduced density for all solutes, together with nonlinear regression analysis of Equation [6.4] (—). Experimental conditions as given in the text.

Figure 6-5

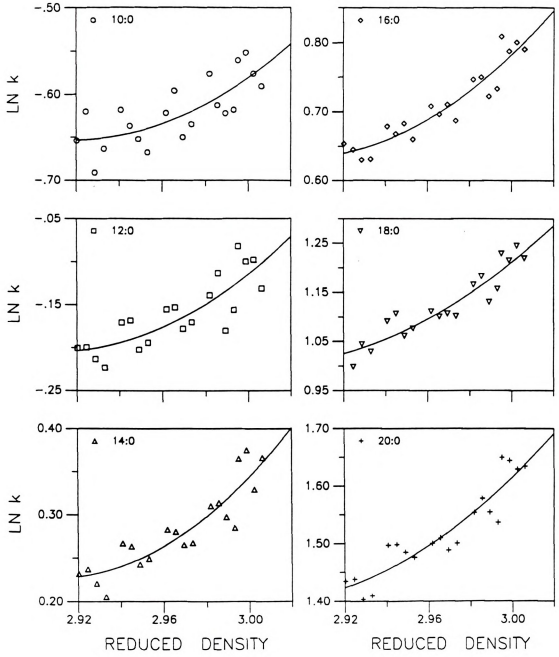
10:0
16:0
12:0
18:0
14:0
20:0
LN k
LN k
LN k
-.50
-.60
-.70
0.80
0.70
0.60
-.05
-.15
-.25
1.25
1.15
1.05
0.95
0.40
0.30
0.20
1.70
1.60
1.50
1.40
2.92
2.96
3.00
2.92
2.96
3.00
REDUCED DENSITY
REDUCED DENSITY

coefficients shown in Table 6.4 are systematically lower than those determined from experimental measurement, the overall agreement appears to be quite reasonable. The choice of stationary-phase solubility parameter value appears to influence c_3 markedly, with the more commonly used bulk alkane value of 7 $cal^{1/2}/cm^{3/2}$ resulting in a greater underestimation based on measured values. In both cases, however, actual predictions of the solute capacity factor are approximately a factor of 1000 lower than experimental measurements. This disheartening result arises from the inability to estimate the variables in Table 6.4 with sufficient accuracy, coupled with the small range of reduced density values. These difficulties have been noted in the literature and are even more pronounced for reversed-phase separations (27). Nonetheless, experimental measurements are well correlated with qualitative predictions based on Equation [6.4], providing corroborating evidence for this theoretical approach.

In like manner, the relationship between selectivity and reduced density can be explored in more detail. Unfortunately, *a priori* prediction is even more difficult for selectivity, because very accurate knowledge of the differences in solute solubility parameters is required (Equation [6.5]). However, experimental measurements can be utilized to predict differences in solubility parameters for adjacent solutes. As illustrated in Figure 6-6, although the measured change in selectivity is not large, all solutes exhibit the predicted linear dependence of ln α on the mobile-phase reduced density. Coefficients c_4 and c_5 determined from linear regression analysis are listed in Table 6.5, together with the correlation coefficient (r). Due to difficulty in measuring such small changes in α, the error in the coefficients is approximately 10%. Nonetheless, differences in the solubility parameters for these solutes are quite small, as expected for dispersion interactions within a homologous series. In addition, calculated difference in solute solubility parameters (δ_i - δ_j) exhibit a small, but systematic decrease

Figure 6-6: Measurements of logarithmic dependence of selectivity on the mobile-phase reduced density for adjacent solute pairs, together with regression analysis of Equation [6.5] (——). Experimental conditions as given in the text.

Figure 6-6

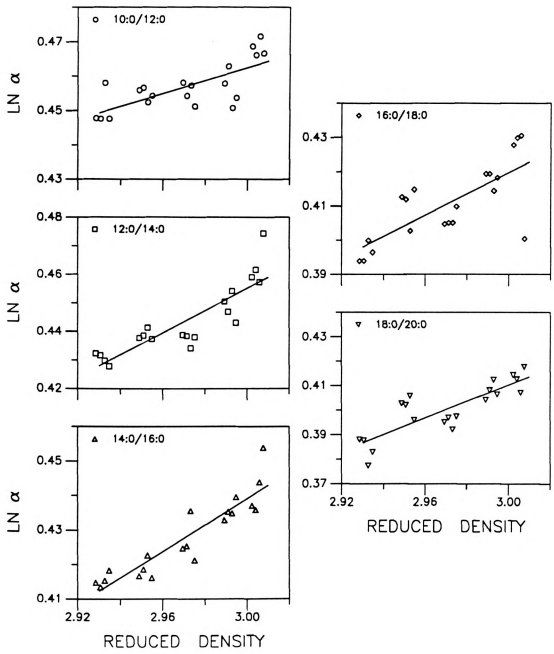
10:0/12:0
12:0/14:0
14:0/16:0
16:0/18:0
18:0/20:0
LN α
REDUCED DENSITY
0.47
0.45
0.43
0.48
0.46
0.44
0.42
0.41
0.39
0.37
2.92
2.96
3.00

Table 6.5: Difference in the solubility parameters of adjacent solutes (δ_i-δ_j) calculated from Equation [6.5]. Slope (c_4) and intercept (c_5) determined by linear regression analysis of dual-mode measurements.

SOLUTE PAIR	c_4	(δ_i-δ_j)	c_5	(δ_i-δ_j)	r
10:0/12:0	0.188	0.052	-0.0997	0.011	0.73
12:0/14:0	0.388	0.098	-0.708	0.071	0.86
14:0/16:0	0.387	0.089	-0.706	0.066	0.92
16:0/18:0	0.311	0.067	-0.514	0.044	0.75
18:0/20:0	0.338	0.068	-0.602	0.048	0.84

in magnitude with carbon number in all except the least retained pair. This result is consistent with that expected from Equation [6.1] for a homologous series. As the solute chain lengthens, the increase in volume arising from additional methylene groups becomes greater than the interaction energy added. In this case, solutes are separated based on change in molar volume more than any small change in interaction energy. As seen here, however, this is sufficient to produce an appreciable dependence of selectivity on the pressure/density.

6.5 Conclusions

Although not often considered a separation variable, the local pressure/density is shown to contribute substantially to solute retention and selectivity. Even though the separation studied here is based solely on dispersion interactions and utilizes a mobile phase which is only slightly compressible, significant increases in both retention and selectivity are measured under modest pressure conditions. Because dispersion interactions are universal in nature, the variation in retention with reduced density has important implications for all partition-based separations in liquid chromatography. These variations may become especially important for separations utilizing very small particles or high speeds, where changes in pressure and, hence, in retention and selectivity along the column length are expected to be significant. In addition, whether theoretical or experimental in approach, fundamental studies of solute retention must consider the influence of pressure under all separation conditions. Finally, with further study, these alterations may clearly be used to advantage in the design and optimization of difficult separations.

6.6 Literature Cited in Chapter 6

1. Bridgman, P.W. *Proc. Acad. Arts and Sci.* **1926**, *61*, 59.

2. Hirschfelder, J.O.; Curtiss, C.F.; Bird, R.B. *Molecular Theory of Gases and Liquids*; Wiley: New York, **1954**.

3. Reid, R.C.; Prausnitz, J.M.; Sherwood, T.K. *The Properties of Gases and Liquids*; McGraw-Hill: New York, **1977**.

4. Stephan, K.; Lucas, K. *Viscosity of Dense Fluids*; Plenum: New York, **1979**.

5. Liley, P.E.; Makita, T.; Tanaka, Y. *Properties of Inorganic and Organic Fluids*; Vol. V-1; Hemisphere Publishing: New York, **1988**.

6. Kestin, J.; Wakeham, W.A. *Transport Properties of Fluids: Thermal Conductivity, Viscosity, and Diffusion Coefficient*; Vol. I-1; Hemisphere Publishing: New York, **1988**.

7. Hamann, S.D. *J. Phys. Chem.* **1962**, *66*, 1359.

8. Macko, T.; Soltes, L.; Berek, D. *Chromatographia* **1989**, 28, 189.

9. Martin, M.; Guiochon, G. *Anal. Chem.* **1983**, *55*, 2302.

10. Martire, D.E. *J. Liq. Chromatogr.* **1987**, 10, 1569.

11. Poe, D.P.; Martire, D.E. *J. Chromatogr.* **1990**, 517, 3.

12. Giddings, J.C. *Separ. Sci.* **1966**, *1*, 73.

13. Giddings, J.C.; Myers, M.N.; McLaren, L.; Keller, R.A. *Science* **1968**, *162*, 67.

14. van der Wal, S. *Chromatographia* **1986**, *22*, 81.

15. Bidlingmeyer, B.A.; Hooker, R.P.; Lochmuller, C.H.; Rogers, L.B. *Separ. Sci.* **1969**, *4*, 439.

16. Bidlingmeyer, B.A.; Rogers, L.B. *Separ. Sci.* **1972**, *7*, 131.

17. Prukop, G.; Rogers, L.B. *Separ. Sci.* **1978**, *13*, 59.

18. Tanaka, N.; Yoshimura, T.; Araki, M. *J. Chromatogr.* **1987**, *406*, 247.

19. Katz, E.; Ogan, K.; Scott, R.P.W. *J. Chromatogr.* **1983**, *260*, 277.

20. Barton, A.F.M *Chem. Rev.* **1975**, *75*, 731.

21. Hildebrand, J.H.; Scott, R.L. *Solubility of Nonelectrolytes*; Reinhold: New York, **1950**, pp. 429-431.

22. Schoenmakers, P.J.; Billiet, H.A.H.; deGalan, L. *Chromatographia* **1982**, *15*, 205.

23. Gluckman, J.C.; Hirose, A.; McGuffin, V.L.; Novotny, M. *Chromatographia* **1983**, *17*, 303.

24. Yamamoto, F.M.; Rokushika, S. *J. Chromatogr.* **1987**, *408*, 21.

25. Yamamoto, F.M.; Rokushika, S. *J. Chromatogr.* **1990**, *515*, 3.

26. Bondi, A. *J. Phys. Chem.* **1964**, *68*, 441.

27. Schoenmakers, P.J.; Billiet, H.A.H.; Tijssen, R; deGalan, L. *J. Chromatogr.* **1978**, *149*, 519.

CHAPTER 7

THE INFLUENCE OF SOLVENT COMPOSITION ON SOLUTE RETENTION

7.1 Introduction

Studies up to now have been limited to the use of a pure methanol mobile phase. The availability of known physical constants made this choice the most viable for reversed-phase separations. In addition, more ideal experimental conditions were maintained by eliminating the possible selective partitioning of mobile-phase components into the stationary phase. However, the influence of the mobile-phase composition on solute retention is of central importance to the practical application of liquid chromatography. Because solvent composition is the primary variable utilized to control separations, a detailed understanding of the influence on solute retention is essential for the design of universally successful optimization schemes. Due the complexity of the chemical and physical environments present on a liquid chromatographic column, however, most theoretical descriptions of solute retention are empirical or semiempirical in nature (1-13). As discussed in Chapter 1, these include the solvophobic approach proposed by Horvath and coworkers (1,2), the statistical

thermodynamically model developed by Martire (7,8), and the solubility parameter theory adapted for liquid chromatography by Tijssen and coworkers (3-5). Of the models available and in use, these are the most rigorously correct and the least empirical in nature. Verification of these models requires the accurate measurement of solute retention under carefully controlled experimental conditions. Moreover, because more than one of these theories predicts a variation in retention along the column length for isocratic conditions (Chapter 6), detection after the column exit is inadequate in assessing the validity of these models. The on-column detection scheme, thus, provides a unique opportunity to measure solute retention directly on the chromatographic column. In this preliminary study of solvent composition effects, solute retention is measured at two points on the column under both constant and varying solvent composition conditions. By determining the capacity factor in this manner, solute retention can be characterized as a function of solvent composition and the resulting variation in local pressure arising from differences in viscosity with composition.

7.2 Theoretical Considerations

Similar to Chapter 6, the theoretical development based on solubility parameter theory is chosen to predict retention behavior. In the development presented here, however, the influence of solvent composition on solute retention is explored. As discussed previously, the solute capacity factor (k_i) may be described in terms of the solubility parameters for the solute, mobile phase, and stationary phase (δ_i, δ_M, and δ_S, respectively) (4):

$$\ln k_i = \frac{V_i}{RT} [(\delta_i - \delta_M)^2 - (\delta_i - \delta_S)^2] - \ln \beta \qquad [1.7]$$

where V_i and β represent the solute molar volume and phase ratio, respectively. For mixed solvent systems, the mobile-phase parameter (δ_M) can be calculated from solubility parameters for the individual components (δ_j), weighted by their respective volume fractions (ϕ_j).

$$\delta_M = \Sigma \phi_j \delta_j \qquad [7.1]$$

In this expression, the chemical interactions of the individual components are presumed to be independent and volumes must be additive. Although these conditions are rarely true for the polar solvents commonly encountered in reversed-phase separations, Equation [7.1] is often utilized as a first approximation. For a simple binary system, the solubility parameter of the mixed mobile phase is given by

$$\delta_M = \phi_A \delta_A + \phi_B \delta_B = (1 - \phi_B) \delta_A + \phi_B \delta_B \qquad [7.2]$$

where ϕ_A and δ_A are the volume fraction and solubility parameter of the weak component (A), and ϕ_B and δ_B represent the strong component (B). Substitution of Equation [7.2] into Equation [1.7] results in an expression for solute retention as a function of the volume fraction of the strong mobile-phase component (ϕ_B) (4):

$$\ln k_i = c_1 \phi_B^2 + c_2 \phi_B + c_3 \qquad [7.3]$$

where

$$c_1 = \left(\frac{V_i}{RT} \right) (\delta_B - \delta_A)^2$$

$$c_2 = \left(\frac{V_i}{RT} \right) [(\delta_i - \delta_B)^2 - (\delta_i - \delta_A)^2 - (\delta_B - \delta_A)^2]$$

$$c_3 = \left(\frac{V_i}{RT} \right) [(\delta_i - \delta_A)^2 - (\delta_i - \delta_S)^2] - \ln \beta$$

where c_1 represents the interaction of mobile-phase components, c_2 describes the solute/mobile-phase interaction, and c_3 predicts the retention of the solute in the weak mobile phase. Because the solubility parameter for the solute is always intermediate in value between that of the mobile and stationary phases ($\delta_S < \delta_i < \delta_M$), the c_2 coefficient must be negative while c_1 is expected to be slightly positive. Thus, as seen in practice, the solute capacity factor (k_i) is predicted to exhibit a marked decrease with the volume fraction of the strong solvent (ϕ_B).

In addition to the change in chemical environment with composition, mobile-phase physical properties may be altered as well. Variations in solvent composition may yield physical effects on solute retention in addition to the chemical influences described above. Prediction of this physical effect is accomplished by substitution of the relationship between the solvent solubility parameter and reduced density (Equation [6.3]) into Equation [7.2].

$$\delta_M = (1 - \phi_B) \frac{(\rho_{CA}\, a_A^{1/2})}{m_A}\, \rho_{RA} + \phi_B \frac{(\rho_{CB}\, a_B^{1/2})}{m_B}\, \rho_{RB} \qquad [7.4]$$

This expression indicates that if the interactions between individual solvents is independent, the solubility parameter of the mixed mobile phase is expected to increase with the reduced density of components A (ρ_{RA}) and B (ρ_{RB}). The effect of the density on retention is compounded by the influence of solvent composition on the mobile-phase viscosity and, thus, the reduced density. Unfortunately, the viscosity of mixed solvent systems often cannot be theoretically predicted (14) and must be measured experimentally. The effect of this change in viscosity on the pressure and reduced density can then be calculated based on Darcy's law (Equation 5.1) and the Tait equation of state (Equation 5.7) as described in Chapter 5. Thus, the solubility parameter of the binary mobile phase is expected

to vary with the volume fraction of B (ϕ_B) due to changes in the pressure/density with composition as well as the change in chemical environment.

7.3 Experimental Methods

Analytical Methodology. Saturated fatty acid standards from *n*-$C_{10:0}$ to *n*-$C_{15:0}$ are derivatized with 4-bromomethyl-7-methoxycoumarin as described in Chapter 4. Mixed standards are dissolved in acetone and injected at concentrations of 5 x 10^{-4} M. Isocratic mobile-phase solvents of 90.0%, 92.5%, 95.0%, 97.5% and 100% v/v methanol/water are prepared from stock mixtures of 90.0% methanol/water and pure methanol.

Chromatographic System. The chromatographic system is identical to that described in Chapter 4 and illustrated in Figure 2-1. The column utilized for this study is also identical to that specified in Chapter 4. The mobile-phase composition is systematically varied from 90.0 to 100% methanol/water under isocratic conditions. A dual-syringe pump (Applied Biosystems, MPLC) operated in the constant-flow mode is utilized to deliver the mobile phase at slightly greater than the optimum flowrate (F = 0.70 μL/min; 0.080 cm/s). Under isocratic conditions, this flowrate resulted in an inlet pressures of 256 bar for 100%, 272 bar for 97.5%, 340 bar for 95.0%, 360 bar for 92.5%, and 375 bar for 90.0% methanol/water mobile phases.

Detection System. The optical detection conditions are identical to those described in Chapter 2. Two detectors are positioned at approximately 30 and 90 cm along the 100 cm length of column. Data acquisition is accomplished under computer control at 1 Hz with a 0.1 s time constant.

7.4 Results and Discussion

In preliminary investigations examining the influence of solvent composition on solute retention, coumarin-derivatized fatty acids from *n*-$C_{10:0}$ to *n*-$C_{15:0}$ are evaluated under isocratic conditions. With detectors positioned at approximately 30 and 90 cm along a 100-cm packed-capillary column, capacity factors are measured for mobile-phase compositions ranging from 90.0% to 100% methanol/water. As shown in Figure 7-1, solutes appear to be well behaved under all mobile-phase conditions, exhibiting the expected logarithmic relationship between capacity factor and carbon number at both detector positions and as the local capacity factor between detectors. In addition, experimental measurements also show the decrease in k predicted with increasing methanol composition (Equation 7.3). However, the magnitude of solute capacity factors measured at 30 cm from the column inlet (Figure 7-1; top) appear to be greater than those measured at 90 cm (Figure 7-1; middle), with the dual detector measurements being the lowest (Figure 7-1; bottom). The slope of log k *versus* carbon number also exhibits a small but systematic decrease with distance along the column. This apparent decrease in k with distance is illustrated more clearly in Table 7.1 where retention in 90.0 and 100% methanol/water solvents are compared. A systematic decrease in solute capacity factor is seen from 30 to 90 cm along the column for both solvent systems. This appears to be a direct result of the difference in the average pressure/density encountered by the solutes, as described in detail in Chapter 6. As seen in Table 7.1, the difference in average pressure between detectors is substantial for 90.0% methanol/water and is appreciably less when a pure methanol mobile phase is employed. This difference in pressure between detectors results in a larger decrease in k with distance for the mobile phase with

Figure 7-1: Solute retention with carbon number measured in the single mode at 30 cm (top) and 90 cm (middle) along the column, together with the dual-mode measurement (bottom). Mobile-phase composition: 90.0% v/v (▼), 92.5% (◆), 95.0% (▲), 97.5% (■), and 100 % (●) methanol/water

Figure 7-1

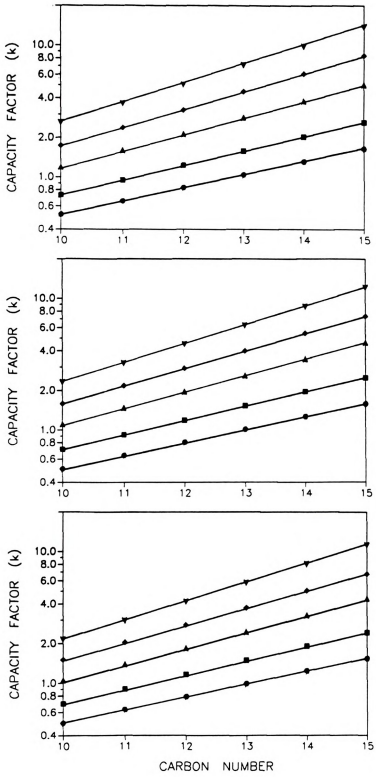
CAPACITY FACTOR (k)
10.0
8.0
6.0
4.0
2.0
1.0
0.8
0.6
0.4
10
11
12
13
14
15
CARBON NUMBER

Table 7.1: Single-mode measurements of capacity factor for 90.0% methanol/water and pure methanol mobile phases with distance.

	CAPACITY FACTOR (k)					
	90% METHANOL/WATER			METHANOL		
SOLUTE	L =30 cm P_{AVG}=313 bar	90 cm 201 bar	Δk/k	30 cm 210 bar	90cm 137 bar	Δk/k
n-$C_{10:0}$	2.60	2.31	-11.2%	0.520	0.507	-2.5%
n-$C_{11:0}$	3.64	3.22	-11.5%	0.659	0.642	-2.6%
n-$C_{12:0}$	5.06	4.49	-11.3%	0.832	0.809	-2.8%
n-$C_{13:0}$	7.05	6.24	-11.5%	1.05	1.02	-3.1%
n-$C_{14:0}$	9.80	8.66	-11.6%	1.31	1.27	-3.0%
n-$C_{15:0}$	13.6	12.1	-11.0%	1.65	1.58	-4.2%

higher water content. In addition to the pressure difference, however, the absolute magnitude of the pressure/density is greater for mixtures containing water, leading to a larger change in k for an equivalent pressure difference. Thus, under identical flowrate conditions, the capacity factor gradient along the column is expected to be greater for mobile-phase compositions containing water.

Measurements of capacity factor with mobile-phase composition are shown in Figure 7-2. Retention for all solutes follows the general trend in ln k *versus* volume fraction methanol ($\phi_{METHANOL}$) predicted using Equation 7.3, with the quadratic regression line shown for each solute. The coefficients determined as a function of position are shown in Table 7.2. Although the regression analysis appears successful based on Figure 7-2, standard errors in the measured coefficients range from approximately 400% for c_1 to 100% for c_3. In addition, negative values are determined for c_1 (Table 7.2), which are not possible based on strict solubility parameter theory (Equation 7.3). This latter result indicates that the interaction of methanol with water in the mixed mobile phase is sufficient to yield erroneous predictions of retention behavior. Unfortunately, the combination of these two factors does not allow meaningful comparison of theoretical predictions to experimental measurements. Thus, although qualitative evaluation of both theory and experiment clearly indicate that changes in solvent composition produce an additional dependence of capacity factor on the variation in local pressure/density, quantititative comparison is not possible.

Figure 7-2: Experimental measurement of the logarithm of the capacity factor (k) *versus* the volume fraction of methanol ($\phi_{METHANOL}$) evaluated at 30 cm (top) and 90 cm (middle) in the single mode, and as the dual mode (bottom). Average pressure determined from the experimental inlet pressure is listed for each mobile-phase composition at the top of each plot. Solutes: *n*-$C_{10:0}$ (○), *n*-$C_{11:0}$ (□), *n*-$C_{12:0}$ (△), *n*-$C_{13:0}$ (◇), *n*-$C_{14:0}$ (▽), and *n*-$C_{15:0}$ (+).

Figure 7-2

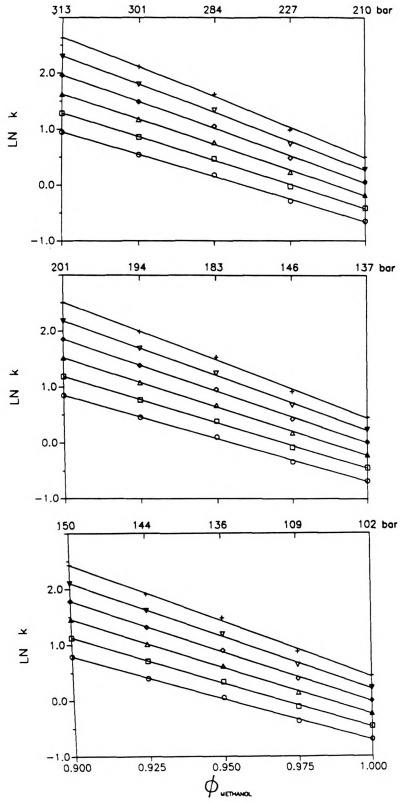
313
301
284
227
210 bar
LN k
2.0
1.0
0.0
−1.0
201
194
183
146
137 bar
LN k
2.0
1.0
0.0
−1.0
150
144
136
109
102 bar
LN k
2.0
1.0
0.0
−1.0
0.900
0.925
0.950
0.975
1.000
φ METHANOL

Table 7.2: Constants determined by nonlinear regression analysis of Equation [7.3].

SOLUTE	L(cm)	C_1 MEAS.	C_2 MEAS.	C_3 MEAS.
n-$C_{10:0}$	30	-3.0 ± 13.9	-10.4 ± 26.4	12.7 ± 12.6
	90	2.4 ± 12.3	-19.9 ± 23.4	16.8 ± 11.1
	dual	5.5 ± 11.5	-25.3 ± 21.9	19.2 ± 10.4
n-$C_{11:0}$	30	-3.5 ± 14.8	-10.4 ± 28.1	13.5 ± 13.4
	90	3.1 ± 12.7	-22.3 ± 24.1	18.7 ± 11.4
	dual	7.2 ± 11.6	-29.7 ± 22.1	22.0 ± 10.5
n-$C_{12:0}$	30	-4.5 ± 16.0	-9.7 ± 30.4	13.9 ± 14.4
	90	2.7 ± 13.5	-22.6 ± 25.6	19.6 ± 12.1
	dual	7.1 ± 12.1	-30.4 ± 23.1	23.1 ± 10.9
n-$C_{13:0}$	30	-5.3 ± 17.3	-9.2 ± 32.9	14.5 ± 15.6
	90	1.9 ± 15.0	-22.0 ± 28.4	20.1 ± 13.5
	dual	6.1 ± 13.8	-29.5 ± 26.2	23.4 ± 12.4
n-$C_{14:0}$	30	-5.9 ± 18.3	-9.2 ± 34.8	15.4 ± 16.5
	90	-0.69 ± 17.6	-18.2 ± 33.4	19.1 ± 15.8
	dual	2.2 ± 17.5	-23.1 ± 33.3	21.1 ± 15.8
n-$C_{15:0}$	30	-7.2 ± 19.5	-7.9 ± 37.1	15.6 ± 17.6
	90	-2.4 ± 20.7	-16.1 ± 39.4	18.9 ± 18.7
	dual	0.40 ± 22.3	-20.8 ± 42.5	20.8 ± 20.2

7.5 Conclusions

Experimental measurements of solute retention as a function of solvent composition are in qualitative agreement with theoretical predictions. In addition to the chemical effect of altering the mobile-phase composition, variations in the local pressure arising from differences in viscosity result in a physical influence on solute retention as well. This local pressure effect yields a capacity factor gradient along the column that is dependent on the composition of the mobile phase, even under isocratic conditions. Thus, the behavior of solute capacity factor under gradient conditions is expected to be even more complex, with the composition and local pressure varying simultaneously on the column. These preliminary results indicate that the variation in local solute retention along the chromatographic column may be more complicated than previously considered, and further investigations are clearly warranted.

7.6 Literature Cited in Chapter 7

1. Horvath, Cs.; Melander, W.; Molnar, I. *J. Chromatogr.* **1976**, *125*, 129.
2. Horvath, Cs.; Melander, W. *J. Chromatogr. Sci.* **1977**, *15*, 393.
3. Tijssen, R.; Billiet, H.A.H.; Schoenmakers, P.J. *J. Chromatogr.* **1976**, *122*, 185.
4. Schoenmakers, P.J.; Billiet, H.A.H.; de Galan, L. *Chromatographia* **1982**, *15*, 205.
5. Dill, K.A. *J. Phys. Chem.* **1987**, *91*, 1980.
6. Locke, D.C. *J. Chromatogr. Sci.* **1977**, *15*, 393.
7. Martire, D.E. *J. Liq. Chromatogr.* **1987**, *10*, 1569.
8. Martire, D.E.; Boehm, R.E. *J. Phys. Chem.* **1987**, *91*, 2433.
9. Jandera, P.; Churacek, J. *Gradient Elution in Column Liquid Chromatography: Theory and Practice; J. Chromatogr. Lib.*; Elsevier: New York, **1985**, Vol. 31.
10. Katz, E.D.; Ogan, K.; Scott, R.P.W. *J. Chromatogr.* **1986**, *352*, 67.
11. Kowalska, T. *Chromatographia* **1989**, *27*, 628.
12. Kowalska, T. *Chromatographia* **1989**, *28*, 354.
13. Cheong, W.J.; Carr, P.W. *J. Chromatogr.* **1990**, *499*, 373.
14. Janz, G.J.; Tomkins, R.P.T. *Nonaqueous Electrolytes Handbook*, Academic Press: New York, Vol. 1, **1972**, pp. 83-118.

CHAPTER 8

THE INFLUENCE OF TRANSITIONS AT THE COLUMN INLET AND EXIT ON RETENTION AND DISPERSION

8.1 Introduction

Thus far, retention and dispersion have been discussed exclusively in terms of processes occuring on the chromatographic column. In practice, however, the solute is introduced onto the column from a nonretentive injection valve and is most commonly eluted from the column before detection. These abrupt transitions may affect the measured chromatographic performance, leading to misinterpretation of the fundamental mechanisms of separation occurring on the column itself.

In simplified chromatographic theory, separations are generally modeled as an equilibrium process. In reality, however, the transfer of solute molecules between the mobile and stationary phases is rarely instantaneous. Due to the finite rate of exchange, solute molecules in the mobile phase will travel some distance along the column before transfer occurs, while molecules in the stationary phase are fixed. Consequently, the solute zone profile in the mobile

phase is slightly in advance of that in the stationary phase. This discrepancy results in broadening of the solute zone, due only to nonequilibrium processes (1).

Although this phenomenon occurs throughout the column, it is expected to reach an extreme at the entrance and exit of the chromatographic column, due to the abrupt changes in solute retention in these transition regions. In the inlet region, the effective rate of solute transfer from mobile to stationary phase, which is zero prior to the column, becomes a finite value upon entering the region containing the stationary phase. Likewise, upon elution from the column, the solute zone passes from a retentive region (on-column) into an open tube where no stationary phase is present (off-column). In these transition regions, substantial changes in solute velocity occur across the solute zone profile.

As the solute enters the column, the rate of movement of the front portion decreases due to solute interaction with the stationary phase, while the rear portion continues at the faster mobile-phase velocity. Thus, the solute zone passes from a region where it is nonretained (off-column) to a retentive region (on-column) at a rate dictated not only by the mobile-phase linear velocity but also by the solute capacity factor. This injection nonequilibrium is expected to result in a decrease in the zone length variance and a concomitant increase in solute concentration. In like manner, upon elution from the column, the front portion of the solute zone increases to the mobile-phase velocity, while the rear of the zone remains at the slower mean zone velocity. This elution nonequilibrium is predicted to result in an increase in length variance and a concomitant decrease in maximum concentration of the solute zone detected off-column.

The extent to which these discontinuities in the physical and chemical environment affect chromatographic performance has been much debated for

both gas and liquid chromatography (2-11). Although methods of theoretical treatment vary widely, it is generally agreed that the influence of these retention discontinuities is dependent on the initial peak profile and the equilibration of solutes between the mobile and stationary phases. Theoretical predictions of solute behavior in the inlet region are further complicated because the solute zone itself may affect the local environment, thus altering the local equilibrium conditions (7). This condition may arise, for example, if the increase in the solute concentration upon entering the column is sufficient to exceed the linear range of the equilibrium isotherm (12). In this case, the shape of the zone profile could be substantially altered, and the measured column efficiency adversely affected.

In this chapter, on-column detection is utilized to measure retention and dispersion in the inlet and exit regions of the column. Although the theoretical treatment of these two regions is directly analogous, experimental measurements utilizing the on-column detection approach are somewhat different. At the column inlet, five detectors are positioned along the packed bed with one detector placed immediately prior to the head of the column. With this experimental design, the solute retention and dispersion may be measured as a function of distance in the inlet region and the initial injection profile may be monitored as well (13). For the inlet region studies, a pure methanol mobile phase is chosen to eliminate the selective partitioning of individual solvents into the stationary phase which may occur with mixed solvent systems. This design also allows the influence of the injection solvent composition to be systematically evaluated. Mixtures of methanol/acetone and methanol/water are chosen as injection solvents for this study because of the wide range of solute retention possible. In the elution study, two detectors are utilized with one positioned before the frit and the other immediately after the column exit. By isolating this exit region, the broadening of solute zones upon elution from the column may be

measured directly (14). In addition, the influence of the mobile-phase linear velocity, the mobile-phase composition, and a spatial temperature gradient at the column exit are explored as well. For ease in discussion, studies of the inlet and exit regions of the column are addressed separately in this chapter.

8.2 Theoretical Considerations: Inlet Region

Some insight into the possible magnitude of these abrupt transitions can be gained by applying the nonequilibrium approach of Giddings (1). Although the theoretical development is discussed here for injection onto the column, it will be shown later that this approach is equally applicable to elution from the column. For a solute zone migrating from an open tube to a point an infinitesimal distance on-column, the time variance (σ_T^2) off- and on-column may be assumed to be equal.

$$(\sigma_T^2)_{OFF} = (\sigma_T^2)_{ON} \qquad [8.1]$$

Conversion to the length domain (σ_L^2) is accomplished utilizing Equation [8.2],

$$\sigma_L^2 = \sigma_T^2 U^2 = \sigma_T^2 [u/(1 + k)]^2 \qquad [8.2]$$

where k is the solute capacity factor, and U and u are the mean zone velocity and mobile-phase velocity, respectively. The off- and on-column length variance can then be expressed by substituting this relationship into Equation [8.1].

$$(\sigma_L^2)_{ON} = (\sigma_L^2)_{OFF} \ (u_{ON}/u_{OFF})^2 \ \frac{1}{(1 + k)^2} \qquad [8.3]$$

Because the volumetric flowrate (F) is constant off- and on-column, the mobile-phase velocities are related by

$$F = \pi R_{OFF}^2 u_{OFF} = \pi R_{ON}^2 u_{ON} \varepsilon_T \quad [8.4]$$

where R is the tube radius, and ε_T is the total porosity of the packed bed (on-column), which is unity for an open tube (off-column). Thus, the corresponding length variance on-column is given by the following expression:

$$(\sigma_L^2)_{ON} = (\sigma_L^2)_{OFF} (R_{OFF}^4/R_{ON}^4) \frac{1}{\varepsilon_T^2} \frac{1}{(1 + k_{INJ})^2} \quad [8.5]$$

According to this relationship, two distinct factors determine the change in length variance upon solute injection. Length dispersion arising from the increase or decrease in solute zone volume is reflected in the radial and porosity terms. More importantly, a substantial decrease in length variance on-column is predicted as a function of the solute capacity factor in the injection solvent (k_{INJ}) due solely to this transition in zone velocity.

8.3 Experimental Methods: Inlet Region

Analytical Methodology. Saturated fatty acid standards are derivatized with 4-bromomethyl-7-methoxycoumarin as described in Chapter 4. Standards are injected individually at a concentration of 5 x 10^{-4} M in a variety of injection solvents. The diffusion coefficient, estimated based on the Wilke-Chang equation (15), is 3 x 10^{-5} cm^2/s for the *n*-$C_{10:0}$ fatty acid derivative in methanol.

Chromatographic System. The chromatographic system is described in detail in Chapter 2 and illustrated in Figure 2-1. As in Chapter 6, this study utilizes an open-tubular capillary (0.0050 cm i.d., 25.7 cm length) extending from the injector to 0.1 cm before the packing material to transfer the injected plug to the head of the column. Connection in this manner provides the minimum band broadening, while simultaneously allowing a detector to be placed on the open tube immediately prior to the packed bed.

The microcolumn utilized for the inlet studies is fabricated using a fused-silica capillary (0.020 cm i.d., 43.9 cm length), from which the polyimide coating has been carefully removed to facilitate on-column detection. The resulting column, prepared as described in Chapter 2, has a plate height of 9.5 μm, a total porosity of 0.43, and a flow resistance parameter of 550 under standard test conditions (16,17). In all inlet region measurements, the methanol mobile phase is operated at slightly greater than the optimum velocity (F = 0.57 μL/min; u = 0.070 cm/s) resulting in an inlet pressure of approximately 1600 psi. The split ratio is 1:100 for this study resulting in an injection volume (V_{INJ}) of 9.8 nL.

Under the experimental conditions utilized in this study, most of the extra-column variance is expected to arise from the injection process, with 14% from the injection volume and 62% from the connecting tube. Only 24% of the total extra-column contribution is predicted from detector sources, with 23% from the viewed volume and less than 1% from the time constant (*vide infra*).

Detection System. The optical detection conditions are identical to those described in Chapter 2. As shown in Figure 6-1, however, six matched detector blocks are positioned along the column with optical fibers from alternate blocks connected to each detection system. If solutes are injected individually, this arrangement allows multiple detection points with only two

monochromator/photomultiplier detection systems. The first detector block is positioned on the open tube 0.4 cm before the packed bed, while the remaining five detectors are placed on the packed bed at 4.9, 10.4, 15.5, 20.9, and 26.2 cm from the column head. The maximum viewed volumes in this case are 1.8 nL off-column and 12 nL on-column. Data acquisition is accomplished under computer control at 5 Hz with a 0.06 s time constant.

8.4 Results and Discussion: Inlet Region

Retention of Solute Zones. In most theoretical approaches to chromatographic separations, equilibration of the solute zone with the stationary phase is assumed to occur instantaneously. Under chromatographic conditions when this is true, and if solute-solvent and solute-stationary phase interactions are not affected by the local pressure, retention in the inlet region of a liquid chromatographic column is predicted to be constant with distance along the column (18). With the present experimental design, it is possible to examine this theoretical prediction by measuring the retention of solutes as they traverse the chromatographic column.

Methanol Injection Solvent. Experimental measurements of capacity factor (k) with distance along the column using methanol as the injection solvent are shown in Figure 8-1 for both single- and dual-mode determinations. The solute capacity factor increases logarithmically with solute chain length, ranging from 0.54 for *n*-$C_{10:0}$ to 4.95 for *n*-$C_{20:0}$ (Table 8.1). Contrary to theoretical predictions, however, capacity factor values measured in the single mode (Figure 8-1, top) exhibit a small but systematic increase with distance travelled. This increase in k of approximately 3% in the region from 4.9 to 26.2 cm along the column appears to be independent of solute and is statistically significant at the

Figure 8-1: Capacity factor *versus* distance along the column measured in single- (top) and dual- (bottom) mode for derivatized fatty acid standards *n*-$C_{10:0}$ (○), *n*-$C_{12:0}$ (□), *n*-$C_{14:0}$ (△), *n*-$C_{16:0}$ (◇), *n*-$C_{18:0}$ (▽), and *n*-$C_{20:0}$ (+). Chromatographic and detection conditions as described in Experimental Methods.

Figure 8-1

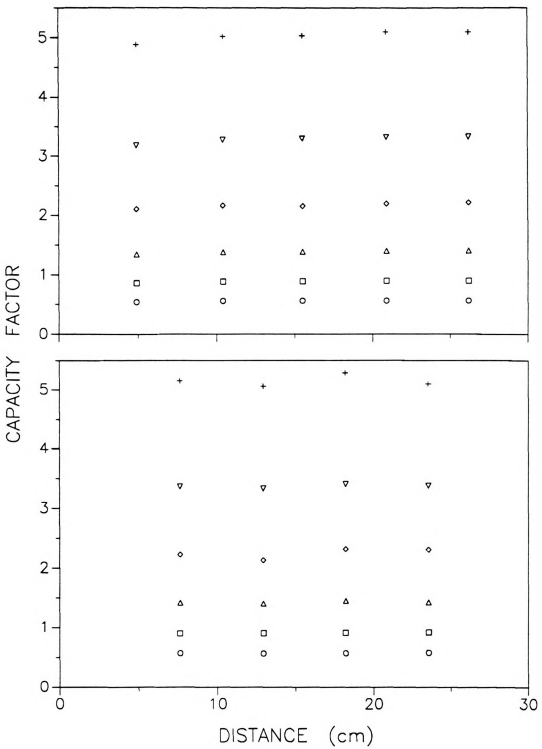

Table 8.1: Capacity factors (k_{INJ}) for derivatized fatty acid standards as a function of solvent composition.

SOLVENT	SOLUTES					
	n-$C_{10:0}$	*n*-$C_{12:0}$	*n*-$C_{14:0}$	*n*-$C_{16:0}$	*n*-$C_{18:0}$	*n*-$C_{20:0}$
90% methanol/acetone	0.44	0.68	1.06	1.62	2.48	3.66
95% methanol/acetone	0.47	0.74	1.16	1.80	2.77	4.19
methanol	0.54	0.85	1.34	2.09	3.23	4.95
95% methanol/water	1.20	2.20	3.80	6.80	12.5	21.0
90% methanol/water	2.60	5.10	9.90	19.0	37.0	72.0

95% confidence level for an average precision in replicate measurements of ±0.5% relative standard deviation (rsd). Errors in the determination of t_0 caused by slight retention of the void marker could lead to this positive trend. If so, the local capacity factor measured in the dual mode would also be expected to exhibit the same trend. However, as seen in Figure 8-1 (bottom), the local capacity factor remains constant with distance for all solutes within the average precision of ±0.6% rsd (with *n*-$C_{16:0}$ and *n*-$C_{20:0}$ exhibiting anomalously poor precision at ±4.4% and ±1.5%, respectively). Based on these measurements, it is possible that initial equilibration upon injection is not instantaneous, but does occur well before the first detector (L = 4.9 cm). Because of this decreased retention at the column inlet, all solutes exhibit single-mode capacity factor values at the last detector (L = 26.2 cm) that are systematically 0.7% less than local capacity factor values. Thus, a small systematic error may result if the capacity factor measured at the column exit is assumed to represent the local capacity factor on the column.

Variation in Injection Solvent. In this investigation, the composition of the injection solvent is systematically varied and the retention behavior is, again, evaluated as a function of distance along the column. The mixtures of methanol/acetone and methanol/water (90% and 95% v/v), chosen as the injection solvents for this study, yield a broad range of capacity factors (k_{INJ}) for the derivatized fatty acids (Table 8.1). Even though the retention behavior in the injection solvents varies markedly, no discernable variation is seen in the resulting capacity factors measured on the column. As shown in Figure 8-2, the retention measured at 26.2 cm along the column is unaffected by the composition of the injection solvent, and is in agreement with the theoretically predicted relationship between capacity factor and carbon number. Moreover, single detector measurements in all injection solvents exhibit the identical increase in

Figure 8-2: Effect of the injection solvent composition on the single-mode measurements of capacity factor at L = 26.2 cm. Injection solvent: 90% v/v methanol/acetone (▽), 95% v/v methanol/acetone (◊), methanol (△), 95% v/v methanol/water (□), 90% v/v methanol/water (○).

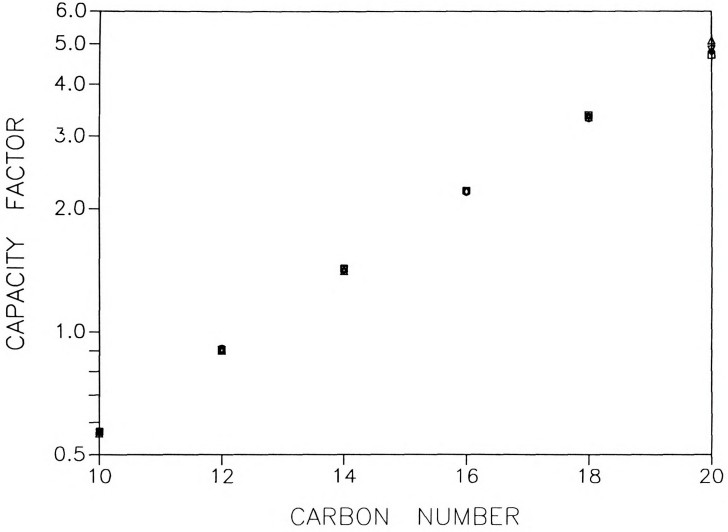
6.0
5.0
4.0
3.0
2.0
1.0
0.5
CAPACITY FACTOR
10
12
14
16
18
20
CARBON NUMBER

Figure 8-2

capacity factor with distance seen for injections in methanol (Figure 8-1). Dual-detector measurements are also similar to injections in the methanol mobile phase, and are constant with distance along the column regardless of the injection solvent composition. Thus, the injection solvent has no significant effect, either temporary or persistent, on the retention behavior of these model solutes under ideal experimental conditions.

Dispersion of Solute Zones. Systematic evaluation of the dispersion or broadening of solute zones is also essential to understanding the factors affecting chromatographic performance. Although the plate height is generally assumed to be constant along the column length, extra-column and nonequilibrium effects occurring upon injection may lead to unexpected behavior in the column inlet region. To evaluate the effect of the injection process on zone dispersion, the variance and plate height of solute zones with distance along the column are determined from data in the same set described above. Because the dispersion of solute zones in the inlet region is a complex phenomenon, it is instructive first to estimate the influence of extra-column dispersion, then to predict the effect of the transition onto the chromatographic column. Finally, single- and dual-detector measurements of the plate height with distance along the column may be evaluated. As in the study of retention, initial investigations focus on the methanol mobile phase as the injection solvent, while later studies explore the effect of the injection solvent composition.

Predicted Extra-Column Effects. Plate height measurements performed at a single detector include dispersion contributions from extra-column as well as column sources. In experimental determinations, these sources of dispersion arising outside the column may have a substantial influence on the accurate measurement of the column plate height (19). Unfortunately, plate height

measurements near the column inlet, where the solute zone has only travelled short distances on the column, may be dominated by extra-column sources of dispersion. For this reason, it is informative to predict the extra-column influence expected under the experimental conditions of this study. This detrimental influence may be estimated from the fractional increase in the column variance caused by known extra-column sources of variance (20). Under ideal conditions, the fractional increase in the variance (θ^2) is described by Equations [1.34] and [1.35]. The resulting fraction θ^2, calculated for the experimental conditions in this study, is shown in Figure 8-3A as a function of distance, for an assumed column plate height (H_{COL}) of 9.5 μm. As expected, the extra-column influence is greatest at small distances and decreases as the solute zone is further broadened by the column. A substantial decrease in θ^2 is also seen as the solute capacity factor increases, effectively increasing the volumetric variance contributed by the column. Thus, for ideal conditions, extra-column dispersion is predicted to affect not only the magnitude of the measured plate height, but the dependence of H on distance and capacity factor as well.

These estimates presuming best-case conditions (Equations [1.37] to [1.39]) are often the only indication of the expected magnitude of extra-column effects. In the present experimental design, a more realistic estimate of θ^2 may be determined from the variance of the injected profile measured immediately prior to the column (L = -0.4 cm). This *in situ* measurement allows a more accurate measure of the largest sources of extra-column variance, those contributed upon injection and flow through connecting tubing. With the methanol mobile phase as the injection solvent, this initial profile is approximately symmetric with an average time variance (σ_T^2) of 4.30 ± 0.32 s^2 (n = 12). As shown in Figure 8-3B, the θ^2 value calculated from the measured injection/connection variance indicates that the extra-column variance is

Figure 8-3: Fractional increase (θ^2) in the column variance caused by extra-column sources under (A) ideal conditions and for (B) methanol injection solvent. Chromatographic and detection conditions as described in Experimental Methods and solutes as shown in Figure 8-1.

Figure 8-3

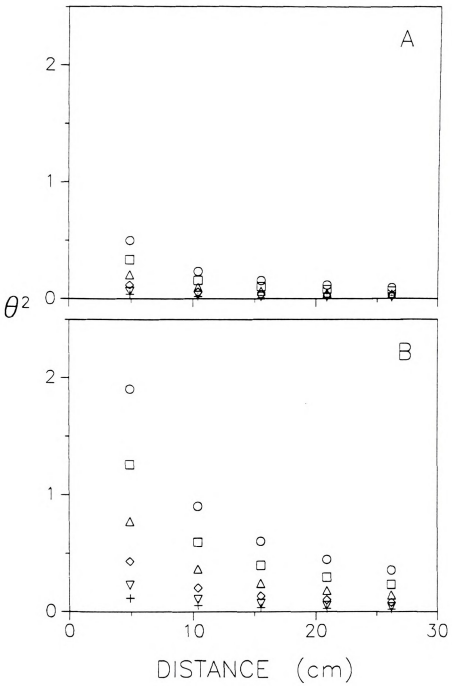

substantially greater than first estimated based on ideal injection and hydrodynamic conditions (Figure 8-3). In fact, the extra-column contributions maybe as much as twice the column variance measured at the first detector.

Variation in the injection solvent is ideally expected to have no effect on the fractional increase in the column variance (θ^2). However, measurements immediately prior to the column indicate a systematic change in the variance contributed by injection/connection sources with injection solvent. When 90% and 95% v/v methanol/acetone injection solvents are utilized, the measured time variances are statistically equivalent (4.68 ± 0.16 s^2 ($n = 25$)) and slightly greater than measured for methanol injections. In contrast, the measured time variances for 90% and 95% v/v methanol/water (2.72 ± 0.22 s^2 ($n = 9$) and 3.58 ± 0.37 s^2 ($n = 12$), respectively) are substantially less than for injections in methanol. The fractional increase in the column variance (θ^2) calculated based on these unexpected results is shown in Figure 8-4. A substantial decrease in θ^2 is seen for the injection solvents containing water, solely due to this systematic decrease in the injection/connection extra-column contributions to dispersion. The origin of this decrease in injection/connection variance remains unclear, but may be due to changes in the physical properties of the solvent (viscosity, surface tension, diffusion coefficient, etc.) that influence hydrodynamic flow. Thus, not only is the magnitude of θ^2 substantially greater than expected based on ideal conditions, but the composition of the injection solvent also has a direct influence on the extra-column variance. Since neither of these trends is predicted theoretically, evaluation of extra-column dispersion based on Figure 8-3A would have greatly underestimated these detrimental effects.

Off- to On-Column Transition. The transition of the solute zone onto the chromatographic column is often assumed to have little effect on the measured plate height. However, in traveling from a nonretentive open tube to a retentive

Figure 8-4: Effect of the injection solvent compositions on the fractional increase (θ^2) in the column variance caused by extra-column sources. Injection solvents: (A) 90% v/v methanol/acetone, (B) 95% v/v methanol/acetone, (C) 95% v/v methanol/water, (D) 90% v/v methanol/water. Chromatographic and detection conditions as described in Experimental Methods and solutes as shown in Figure 8-1.

Figure 8-4

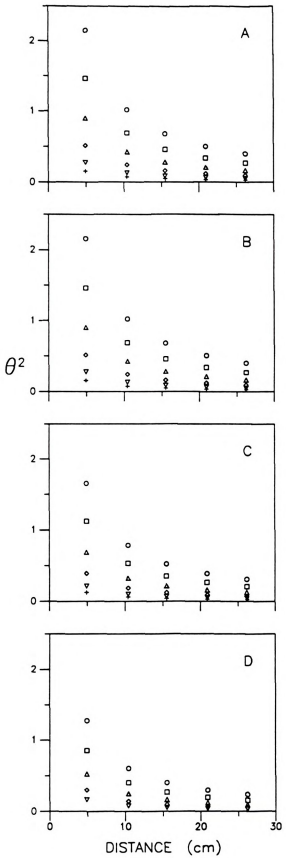

packed bed, the solute zone undergoes an abrupt change in capacity factor. As described by Equation [8.3], the length variance of the zone on the column is a function of the mobile-phase linear velocity and the solute capacity factor. In this transition, the capacity factor in the injection solvent (k_{INJ}) is identical to that in the mobile phase (k_{MP}) when samples are dissolved in the methanol mobile phase. This expression is further simplified in Equation [8.5] in terms of the column radius and porosity. Thus, based on only a few experimental parameters, the change in the zone length variance caused by this abrupt transition may be predicted.

Experimental measurement of this phenomenon is accomplished by calculating the ratio of the on-column length variance, extrapolated to zero distance, to that measured off column ($(\sigma_L^2)_{ON}/(\sigma_L^2)_{OFF}$). As shown in Figure 8-5 for the methanol injection solvent, there is excellent agreement between the measured length variance ratios and those predicted using Equation [8.5]. This decrease in the length variance of the solute zone at the column inlet effectively decreases the resulting volume injected onto the column as a function of the solute capacity factor, thus reducing the detrimental effects of extra-column dispersion.

Further studies of the decrease in extra-column variance are accomplished by altering the composition of the injection solvent. As seen in Equation [8.5] and later in Equation [8.6], the extra-column variance is expected to decrease markedly with the solute capacity factor in the injection solvent (k_{INJ}). For highly retained solutes (large k_{MP}), the influence of the injection solvent is expected to be minor. In contrast, solutes that are only slightly retained (small k_{MP}) are more affected by extra-column variance and, thus, are predicted to exhibit a substantial decrease in these detrimental effects. Experimental measurement of the length variance ratios for the least retained solute, *n*-$C_{10:0}$,

Figure 8-5: Measured ratio of the length variance on-column, $(\sigma_L^2)_{ON}$, to that immediately prior to the packed bed, $(\sigma_L^2)_{OFF}$ for methanol injection solvent: Theoretical prediction (—), Experimental measurement (○). Chromatographic and detection conditions as described in Experimental Methods.

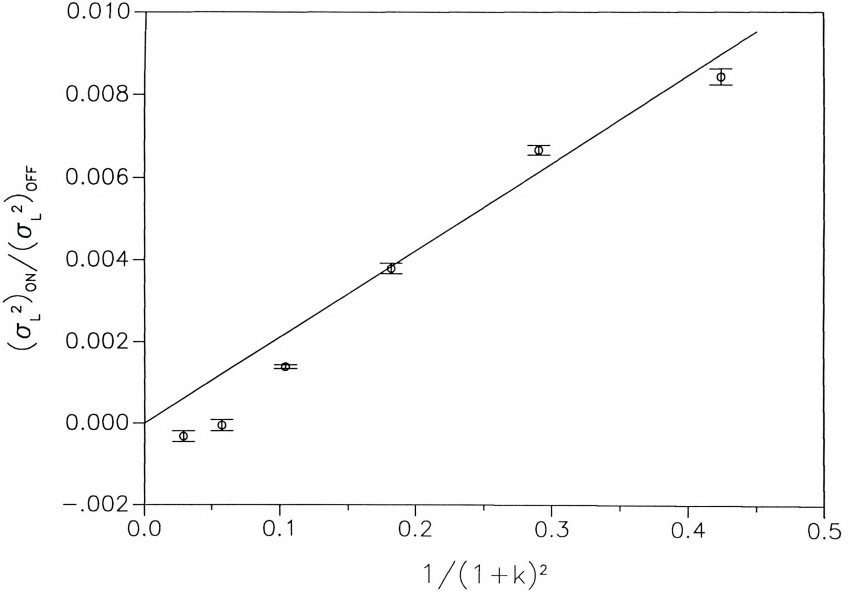
0.010
0.008
0.006
0.004
0.002
0.000
-.002
0.0
0.1
0.2
0.3
0.4
0.5
$(\sigma_L^2)_{ON}/(\sigma_L^2)_{OFF}$
$1/(1+k)^2$

Figure 8-5

as a function of injection solvent are shown in Table 8.2. As predicted, when the injection solvent is stronger than the methanol mobile phase ($k_{INJ} < k_{MP}$), the measured length variance ratio and plate height are both greater than for the pure methanol injection solvent. Under these conditions, the solute zone is expanded upon entering the column and the extra-column variance caused by the injection is actually more detrimental. Alternately, when the *n*-$C_{10:0}$ fatty acid is injected in solvents that are weaker than methanol ($k_{INJ} > k_{MP}$), a substantial decrease in the length variance ratio and measured plate height is clearly seen. Contrary to common misconceptions (21), this decrease in the extra-column variance does not require a large change in injection solvent composition to realize a notable improvement in the measured plate height, even at a distance of 26.2 cm along the column.

Plate Height Measurements. In most theoretical derivations of dispersion processes in liquid chromatography, plate height is predicted to be independent of distance along the column (22-24). As noted above, however, single-mode measurements of plate height are strongly influenced by extra-column sources of variance and, therefore, are expected to exhibit some dependence on distance. In contrast, dual-mode measurements are expected to be in agreement with theoretical predictions, because extra-column contributions to the variance have been effectively eliminated. In addition to the effect of the injection process itself, the influence of the injection solvent composition on both these measurements can be systematically evaluated.

Prediction of the extra-column influence on the measured plate height (H_{MEAS}) may be accomplished utilizing Equation [1.36]. By assuming the variance contribution from injection volume of a Gaussian band immediately prior to the column ($[6\pi R_{OFF}^2(\sigma_L)_{OFF}]^2/36$) instead of the more ideal plug injection ($V_{INJ}^2/12$), the magnitude of the extra-column influence can be more accurately

Table 8.2: Effect of injection solvent composition on the measured length variance ratio and plate height for the *n*-$C_{10:0}$ derivative.

INJECTION SOLVENT	k_{INJ}	$\frac{(\sigma_L^2)_{ON}}{(\sigma_L^2)_{OFF}}$	PLATE HEIGHT (μm) single mode (L=26.2 cm)
90% methanol/acetone	0.44	0.010	14.6
95% methanol/acetone	0.47	0.0099	13.9
methanol	0.54	0.0086	13.5
95% methanol/water	1.20	0.0045	11.9
90% methanol/water	2.60	0.0022	9.0

estimated. If this injection volume resulting from injection/connection dispersion processes is the primary source of extra-column variance, combining Equation [1.36] with Equations [1.35] and [1.37] results in the following expression for the plate height measured at a single detector (H_{MEAS}).

$$H_{MEAS} = H_{COL} \left[1 + \frac{(6\pi R_{OFF}^2 (\sigma_L)_{OFF})^2 u_{ON}^2}{36 (1+k_{INJ})^2 (1+k_{MP})^2 L F^2 H_{COL}} \right] \qquad [8.6]$$

Based on Equation [8.6], it is clearly expected that the solute capacity factors in the mobile phase (k_{MP}) and in the injection solvent (k_{INJ}) have a substantial influence on the measured plate height. When methanol is employed as the injection solvent, the extra-column contribution is predicted to be inversely proportional to $(1+k_{MP})^4$. Moreover, when extra-column effects are predominant, the measured plate height is expected to depend inversely on the distance travelled (L).

Experimental results of initial studies utilizing methanol as the injection solvent are shown in Figure 8-6. As expected, extra-column effects dominate the single-mode measurements (Figure 8-6, top) and lead to the inverse relationship between measured plate height and distance predicted in Equation [8.8]. However, the detrimental effects of extra-column variance decrease markedly with capacity factor, as predicted from the $1/(1+k_{MP})^4$ dependence (Equation [8.6]). Unfortunately, even at a distance of 26.2 cm along the column, the capacity factor dependence is reversed from that expected if resistance to mass transfer in the mobile phase is limiting solute dispersion. In contrast to the single-mode measurements, however, the local plate height (dual mode) is in good agreement with chromatographic theory (Figure 8-6, bottom), exhibiting no discernable variation with distance along the column (25). In addition, the local plate height measurements exhibit the general capacity factor trend predicted for

Figure 8-6: Plate height *versus* distance along the column for single- (top) and dual- (bottom) mode determinations. Injection solvent: methanol. Chromatographic and detection conditions as described in Experimental Methods and solutes as shown in Figure 8-1.

Figure 8-6

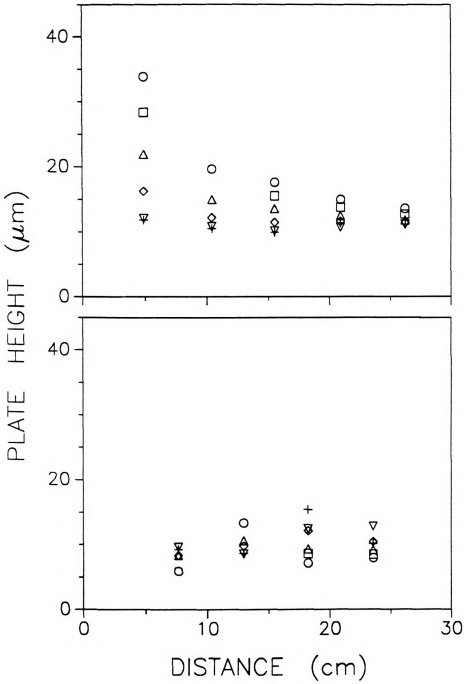

conditions where mass transfer processes in the mobile phase are limiting the column plate height.

In further studies, plate height is measured under conditions of varying injection solvent composition. Experimental measurements of plate height *versus* distance, shown in Figure 8-7, clearly demonstrate a decrease in the single-mode measurements with injection solvent. As expected based on Equation [8.6], the effect is most profound for the least retained solutes, resulting in a measured plate height for n-$C_{10.0}$ at 4.9 cm along the column of 40.59 ± 0.12 μm using 90% v/v methanol/acetone and 12.71 ± 1.37 μm using 90% v/v methanol/water. The influence of this decrease in the extra-column variance on the determination of the true column dispersion becomes apparent for injection in 90% v/v methanol/water (Figure 8-7D). At short distances, the measured plate height is dominated by the extra-column variance and decreases with increasing capacity factor. As the distance increases, the column variance becomes most prevalent, and the trend with capacity factor is reversed. Thus, injection solvent appears to play an important but routinely neglected role in the evaluation of fundamental parameters controlling solute zone dispersion.

In contrast to single-mode measurements of plate height (Figure 8-7), dual-mode determinations shown in Figure 8-8 exhibit little change with distance along the column. Moreover, these local plate height measurements show no discernable variation with the injection solvent composition. These results indicate that if the decrease in the length variance does not occur entirely within the transition region, it is certainly completed by a distance of 4.9 cm along the column and is independent of the relatively small changes in solvent composition studied here. In addition, the trend in the local plate height with capacity factor is no longer dominated by extra-column effects and exhibits the general trend predicted for mobile-phase mass transfer processes. These preliminary studies

Figure 8-7: Effect of injection solvent on single-mode measurements of plate height. Injection solvents: (A) 90% v/v methanol/acetone, (B) 95% v/v methanol/acetone, (C) 95% v/v methanol/water, (D) 90% v/v methanol/water. Chromatographic and detection conditions as described in Experimental Methods and solutes as shown in Figure 8-1.

Figure 8-7

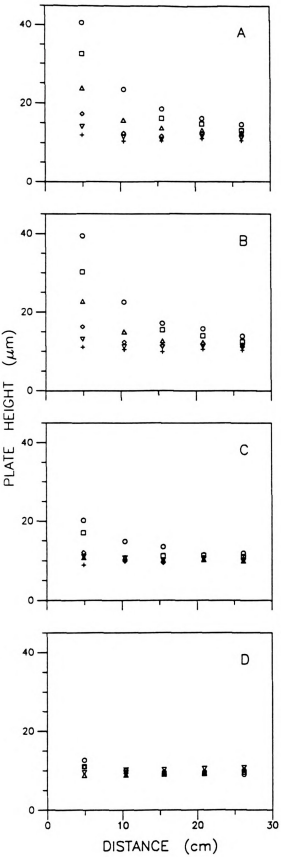

Figure 8-8: Effect of injection solvent on dual-mode measurements of plate height. Injection solvents: (A) 90% v/v methanol/acetone, (B) 95% v/v methanol/acetone, (C) 95% v/v methanol/water, (D) 90% v/v methanol/water. Chromatographic and detection conditions as described in Experimental Methods and solutes as shown in Figure 8-1.

Figure 8-8

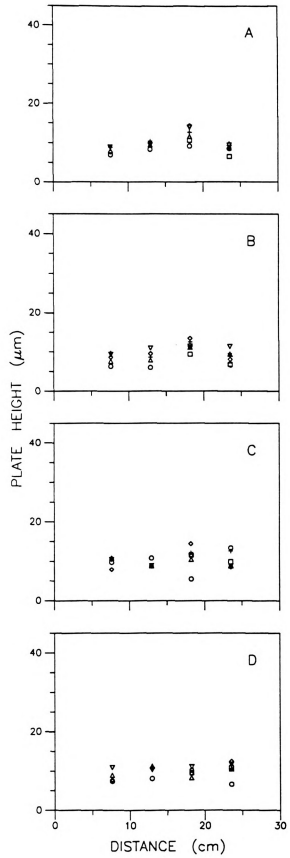

indicate that the nonequilibrium condition created by the injection process does not extend a substantial distance onto the column. Surprisingly, this result is also true when small variations in the injection solvent composition are utilized to produce large variations in the injection solvent capacity factor.

Both the accuracy and precision are important in evaluating the measured (H_{MEAS}) and column (H_{COL}) plate height. While single-mode measurements are reasonably precise with a standard deviation in the plate height pooled over distance (s_{POOLED}) of ±0.50 μm, extra-column processes directly affect the measurement accuracy by systematically increasing the measured plate height. In contrast, the dual-mode technique effectively eliminates extra-column effects and is quite accurate (26), but the precision (s_{POOLED} = ±1.1 μm) suffers from the difficulties inherent in any difference measurement. Although these standard deviation values appear to be quite similar, the relative precision of these two techniques differs markedly. The precision of single-mode measurements ranges from approximately 1.5 to 4.5% rsd, with a dual-mode precision of approximately 12% rsd. The relative precision of plate height appears to be independent of injection solvent composition. Although these values are well within the expected precision for statistical moment calculations (27), further studies will be necessary to determine the exact origin of the variability.

Injection in Pure Solvents. Until now, this discussion has focused on relatively small changes in the composition of the injection solvent. In practice, however, pure solvents other than the mobile phase are often utilized to dissolve the solutes of interest. The perturbation upon injection, in this case, is expected to be extreme and the behavior of the solute zone under these conditions is difficult to predict (28,29). In these preliminary investigations, the retention and

dispersion of a single solute injected in several common organic solvents (acetonitrile, acetone, 2-propanol, and tetrahydrofuran) is evaluated.

The unexpected effect of these pure solvents on chromatographic behavior is clearly illustrated in the chromatograms in Figure 8-9. In this figure, the response of detectors positioned 0.4 cm prior to the column is shown along with detectors at 10.4 cm and 20.9 cm along the column. A single solute (n-$C_{10:0}$) is utilized throughout this study to insure solubility in all injection solvents. The detector response shown is well within the linear dynamic range of the system, and changes with injection solvent can be directly compared at a given detector position. However, the measured photocurrent between detectors is not directly comparable due to the difficulties in matching excitation intensities.

Illustration of the detector response in this manner allows direct observation of the chromatographic development as the solute traverses the column. Although only n-$C_{10:0}$ and a small amount of nonretained solute are injected, it is clear that the development of the zone profile differs greatly with the composition of the injection solvent. Injection in methanol and acetonitrile results in well-behaved and symmetric profiles, while zone profiles in the stronger injection solvents exhibit varying degrees of asymmetry. Although exaggeration of any asymmetry in the zone profile present at the first detector is predicted for the strong solvents, the unusual peak shapes seen for injection in 2-propanol and in tetrahydrofuran are not expected. In addition, the zone profile for n-$C_{10:0}$ in acetone and 2-propanol is clearly broadened as expected, while the nonretained zone is sharpened considerably. As in the previous studies, further characterization of these anomalies is accomplished by quantitatively evaluating the retention and dispersion of the zone profiles with distance along the column.

Solute Zone Retention. In contrast to the small changes in solvent composition shown earlier, under these extreme conditions, single-mode

Figure 8-9: Development of chromatogram of derivatized fatty acid standard, *n*-$C_{10:0}$, injected in pure organic injection solvents. Detector positions at 0.4 cm before the column (L = -0.4 cm) as well as 10.4 cm and 20.9 cm along the column. Other chromatographic and detection conditions as described in Experimental Methods.

Figure 8-9

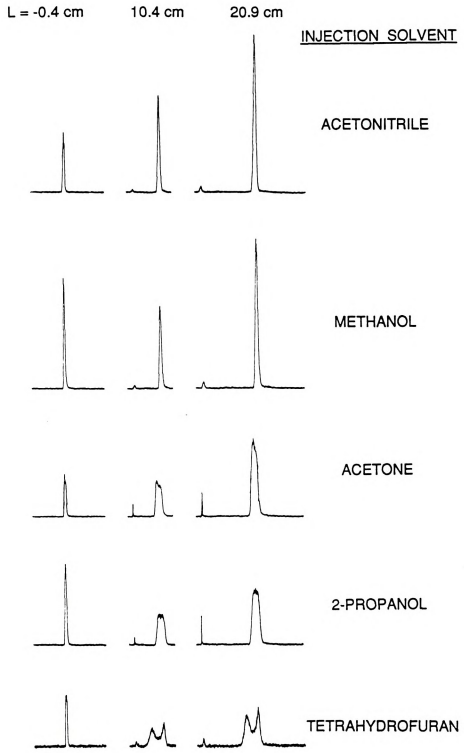
L = -0.4 cm
10.4 cm
20.9 cm
INJECTION SOLVENT
ACETONITRILE
METHANOL
ACETONE
2-PROPANOL
TETRAHYDROFURAN

measurements of retention are influenced substantially by the injection solvent. Not only are the retention times affected, as might be expected, but the void time of the nonretained solute as well. Injections in acetone exhibit the largest deviation in retention time (M_1) at -1.1% compared with injections in methanol, with injections in acetonitrile and in 2-propanol showing a deviation of only -0.3%. Negative deviations in the void time (t_o) are also measured, with injections in acetone and 2-propanol resulting in larger variations (-1.5%) than acetonitrile injections (-1.0%). These factors combine to yield substantial deviations in capacity factor with distance along the column, as shown in Figure 8-10. While injection in methanol exhibits approximately a +3% increase in capacity factor from 4.9 to 26.2 cm along the column, all other solvents produce variations of +8.5% to +9.5%. This apparent increase in nonequilibrium at the entrance to the column is unsurprising based on these large changes in solvent strength. Injections in tetrahydrofuran have not been included in the above discussion due to the anomalous peak splitting shown in Figure 8-9.

Solute Zone Dispersion. Initial comparison of detector response pre-column (Figure 8-9; L = -0.4 cm) reveals a systematic variation in both the intensity and width of solute zones with injection solvent composition. Changes in peak height at this first detector position are difficult to compare directly due to alterations in the variance of the solute zone, coupled with differences in the fluorescence quantum yield with injection solvent. As seen previously, the magnitude of the time variance of the injection profile measured immediately prior to the packed bed is quite solvent specific, with all solvents except tetrahydrofuran exhibiting variance values greater than for methanol injections. Injection in acetonitrile yields a zone variance of 5.58 ± 0.14 s^2, while variance values for injections in both acetone and 2-propanol are the greatest at 6.55 ± 0.15 s^2. This latter result is surprising if hydrodynamic flow upon split injection is

Figure 8-10: Measured capacity factor *versus* distance along the column for injection of *n*-$C_{10:0}$ in pure organic solvents: 2-propanol (◊); acetone (□); methanol (○); acetonitrile (△). Chromatographic and detection conditions as described in Experimental Methods.

Figure 8-10

the major cause of extra-column variance, because the viscosity for acetone and 2-propanol vary substantially (η = 0.36 and 2.4 cP, respectively). These changes in the variance of the injected zone are not presently predictable and are under investigation. Nevertheless, as seen previously, injection solvent composition does indeed have a large effect on the profile of the injected zone and, thus, the plate height measured on the column.

The transition onto the column is also affected by these extreme changes in solvent composition. On- to off-column length variance ratios shown in Table 8.3 appear to be in qualitative agreement with Equation [8.5], exhibiting the expected increase with solvent strength. However, the maximum value for the length variance ratio predicted from Equation [8.5] is 0.021 for a nonretained solute (k_{INJ} = 0), which is exceeded when acetone, 2-propanol, tetrahydrofuran are utilized as injection solvents. Clearly a discrete change in zone velocity in the transition region does not account for the magnitude of the variance ratios under these extreme conditions.

Rigorous evaluation of this effect will require systematic monitoring of the injection solvent zone as well as the solute profile. It is possible that the profile of the injection solvent is altered markedly upon injection onto the packed bed. Furthermore, these pure injection solvents may modify not only the strength of the mobile phase, but that of the stationary phase as well. Injection in a solvent with a substantially different composition from the mobile phase may create both mobile- and stationary-phase gradients in the inlet region of the column. In addition, temperature gradients induced by mixing of these pure solvents with the mobile phase may cause large variations in physical properties (e.g., solubility, viscosity, surface tension, diffusion coefficient) across the solute zone. Further investigations will be necessary to understand the complex interactions present upon such drastic changes in the injection solvent composition.

Table 8.3: Effect of pure injection solvents on the measured length variance ratio and plate height for the *n*-$C_{10:0}$ derivative.

INJECTION SOLVENT	$\frac{(\sigma_L^2)_{ON}}{(\sigma_L^2)_{OFF}}$	PLATE HEIGHT (μm) single mode (L=26.2 cm)
tetrahydrofuran	0.255	255
2-propanol	0.065	59.0
acetone	0.045	44.6
methanol	0.0086	13.5
acetonitrile	0.0068	12.8

8.5 Theoretical Considerations: Exit Region

A further discontinuity in physical and chemical properties is encountered by the solute zone at the column exit. Although the transition in this region is exactly opposite to that upon injection, the theoretical description of the length dispersion of solute zones upon elution is directly analogous (Section 8.2). Because the zone is passing from a retentive packed bed to a nonretentive open tube, the length variance expression may also be derived from Equations [8.2], [8.3], and [8.4] and is similar to Equation [8.5] for the injection process. The resulting length variance upon elution, $(\sigma_L^2)_{OFF}$ is given by

$$(\sigma_L^2)_{OFF} = (\sigma_L^2)_{ON} (R_{ON}^4/R_{OFF}^4) \varepsilon_T^2 (1 + k)^2 \qquad [8.7]$$

Again, the solute zone is affected by the change in structural parameters (R and ε_T) as well as the solute retention (k). From this relationship, elution from the chromatographic column is expected to broaden the solute zone in length as a function of the solute capacity factor.

The increase in length variance upon elution will result in a concomitant decrease in concentration, directly influencing the minimum detectable concentration off-column. The effect of this increase in length variance on solute concentration (C) can be derived assuming a Gaussian zone profile, where

$$C = \frac{1}{\sigma_L (2\pi)^{1/2}} \exp - \frac{1}{2} \left(\frac{(x - \mu)}{\sigma_L} \right)^2 \qquad [8.8]$$

In this normalized form, x represents the length displacement along the column with a zone center at μ. At the concentration maximum of the zone ($x = \mu$), the ratio of concentrations off- and on-column is given by

$$\frac{C_{OFF}}{C_{ON}} = \frac{(\sigma_L)_{ON}}{(\sigma_L)_{OFF}} \qquad [8.9]$$

Direct substitution of Equation [8.7] yields an expression for maximum concentrations present on and off the chromatographic column.

$$\frac{C_{OFF}}{C_{ON}} = \frac{R_{OFF}^2}{R_{ON}^2} \frac{1}{\varepsilon_T} \frac{1}{(1 + k)} \qquad [8.10]$$

Thus, an increase in off-column variance yields a concomitant decrease in concentration due solely to this transition region.

These theoretical predictions are shown schematically in Figure 8-11, which illustrates the movement and dispersion of solute zones along an open-tubular column of length L. In this pictorial representation, the zone variance on-column was calculated to increase with capacity factor according to Golay theory (30),

$$H_{COL} = \frac{\sigma_L^2}{L} = \frac{2 D_M}{u} + \frac{(1 + 6k + 11k^2) R^2 u}{24 (1+k)^2 \quad D_M} \qquad [8.11]$$

normalized to a nonretained solute. The off-column variance was subsequently determined utilizing Equation [8.9] for an open-tubular column with no change in radius. During the transition from on- to off-column, the nonretained solute exhibits no change in velocity or zone characteristics, whereas the retained solutes are substantially affected. For a solute with a capacity factor of ten, the length variance is predicted to increase more than one hundred-fold while the concentration at the zone maximum is decreased more than ten-fold. This diagram clearly indicates the detrimental influence of this transition region on solute detectability. Furthermore, this effect appears to be a substantial contribution to the commonly termed "general elution problem" in chromatographic separations.

Figure 8-11: Illustration of the predicted influence of elution nonequilibrium on solute length variance (σ_L^2) and concentration (C) as a function of capacity factor (k).

Figure 8-11

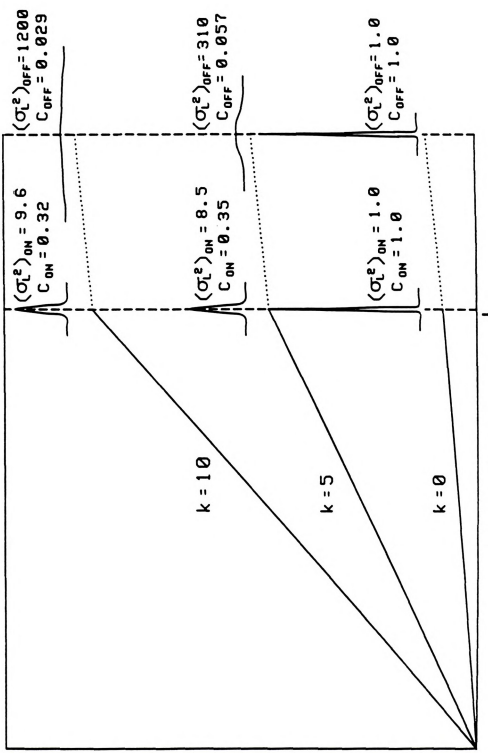
$(\sigma_L^2)_{OFF}$=1200
C_{OFF} = 0.029
$(\sigma_L^2)_{ON}$ = 9.6
C_{ON} =0.32
$(\sigma_L^2)_{OFF}$=310
C_{OFF} = 0.057
$(\sigma_L^2)_{ON}$ = 8.5
C_{ON} =0.35
$(\sigma_L^2)_{OFF}$=1.0
C_{OFF} = 1.0
$(\sigma_L^2)_{ON}$ = 1.0
C_{ON} = 1.0
k = 10
k = 5
k = 0
L
DISTANCE
TIME

8.6 Experimental Methods: Exit Region

Analytical Methodology. A mixed standard of n-$C_{10:0}$ to n-$C_{20:0}$ fatty acids derivatized with 4-bromomethyl-7-methoxycoumarin is injected at a concentration of 1 x 10^{-3} M in acetone.

Chromatographic System. Similar to the inlet study, a single microcolumn is utilized to examine the exit region. The column is prepared as described in Chapter 2, with a porous teflon frit (31) and 30 cm length of 0.0050 cm i.d. capillary used to terminate this 86 cm length of 0.0200 cm i.d. column. Packed with a methanol slurry under moderate pressure (305 bar; 4500 psi), the resulting microcolumn has a plate height of 10.5 μm, a total porosity of 0.43, and a separation impedance of 380. Throughout this study the mobile phase is operated under flow control (F = 0.60 μL/min) at a linear velocity of 0.070 cm/s, and concomitant inlet pressure of 180 bar. The split ratio remains constant at 1:110, yielding an injection volume of 9.1 nL.

Detection System. As shown in Figure 8-12, the detection configuration for the elution study is quite similar to that described in Chapter 2. In this study, however, one detector is positioned on-column, 2.9 cm before the frit, while the second detector resides off-column, 2.3 cm after the column exit. The maximum viewed volumes for the elution study are 12 nL and 1.8 nL, on- and off-column respectively. Data acquisition is accomplished under computer control at 2 Hz with a 0.1 s time constant.

Temperature Controller. For the final portion of this study, the temperature in the exit region of the column is systematically varied. A schematic diagram of the

Figure 8-12: Schematic diagram of on-column detection in exit region. I = injection valve, T = splitting tee, R = restricting capillary, FOP = fiber optic positioner, L = lens, F = filter, M = monochromator, PMT = photomultiplier tube, AMP = current-to-voltage converter and amplifier, REC = recorder/computer.

Figure 8-12

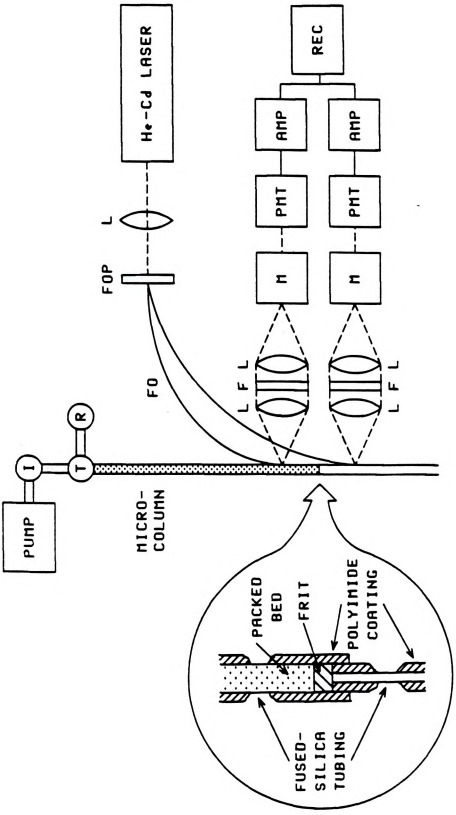
PUMP
I
T
R
MICRO-
COLUMN
FO
FOP
L
He-Cd LASER
L F L
M
PMT
AMP
REC
PACKED
BED
FRIT
POLYIMIDE
COATING
FUSED-
SILICA
TUBING

heater system in the column exit region is shown in Figure 8-13. Temperature is maintained by coupling a 40 W temperature controller (Omega, Model CN9000) and a 100-Ω potentiometer, with a 4 cm length of ceramic tubing (0.0635 cm i.d., 0.236 o.d.; Scientific Instruments Services). The capillary column is inserted into the ceramic tubing and silver conductive paint (GC Electronics) is utilized to ensure contact between the ceramic tube and the microcolumn. The temperature is monitored inside the ceramic tube with three chromel-alumel thermocouples (0.0254 cm o.d.) positioned along the tubing length. When the ceramic tube is insulated with ceramic tape (Scientific Instruments Services), the stability of this heater assembly is ± 1 °C.

8.7 Results and Discussion: Exit Region

Detection of solute zones in chromatography is commonly performed after the exit of the chromatographic column. It is presumed that post-column detection accurately reflects zone characteristics occurring on the column. Although widely accepted, this assumption appears to be incorrect due, at least in part, to nonequilibrium effects within the solute zone when eluting from the column (32). Theoretically, this nonequilibrium effect can result in a substantial increase in length variance (Equation [8.7]) and decrease in concentration (Equation [8.10]) of the solute zone as it elutes from the column.

In previous studies, this effect has been described as an apparent enhancement of the fluorescence signal when detection is performed on the chromatographic column (32-35). Using a simple steady-state model, Guthrie and Jorgenson (32) derived an expression, whereby on-column detection should have better sensitivity than post-column detection by a factor of (1+k). Takeuchi

Figure 8-13: Schematic diagram of temperature controller at column exit.

Figure 8-13

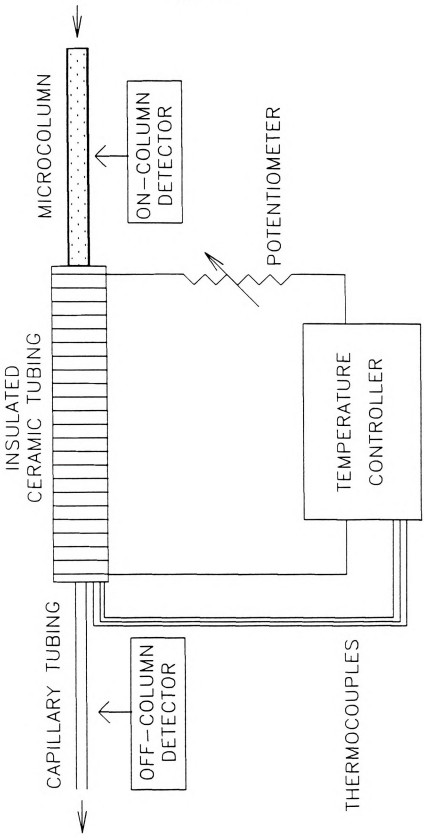
MICROCOLUMN
ON-COLUMN DETECTOR
POTENTIOMETER
INSULATED CERAMIC TUBING
TEMPERATURE CONTROLLER
CAPILLARY TUBING
OFF-COLUMN DETECTOR
THERMOCOUPLES

and Yeung (33) described the influence of mobile- and stationary-phase environment on fluorescence intensity for the on- and off-column cases. Although these factors have been discussed previously, the influence of nonequilibrium at the exit of the chromatographic column has been largely ignored. With the present experimental design, it is possible to detect solute zones as they elute from the column. In addition, the fluorescent label in the model solutes resides in the mobile phase (Chapter 4), allowing the elution nonequilibrium to be isolated from any change in fluorescence intensity due to environmental factors.

On/Off-Column Detection. Chromatograms of the model solutes detected on- and off-column are illustrated in Figure 8-14. When detected on-column, solutes with identical concentration exhibit a detector response that appears to be independent of retention. In contrast, when detection is performed after the column exit, the same injection shows a marked decrease in the detector response with increasing solute retention.

Representative determinations of time and length variance for both on- and off-column detection of the model solutes are summarized in Table 8.4. The fatty acid derivatives, listed here by carbon number, are separated using a pure methanol mobile phase at a linear velocity of 0.07 cm/s. The time variance (σ_T^2) of each solute zone profile is evaluated both on- and off-column directly from the second statistical moment (M_2). Length variance values are subsequently determined using Equation [8.2]. For this calculation, the on-column zone velocity (U) is determined using the first moment (M_1) for each solute zone together with the distance between the injector and on-column detector. The off-column zone velocity (u) is constant for all solutes, and is derived from the volumetric flowrate using Equation [8.4].

Figure 8-14: Chromatograms of *n*-$C_{10:0}$ to *n*-$C_{20:0}$ fatty acid derivatives on and off the chromatographic column at 25 °C. Conditions given in Experimental Methods.

Figure 8-14

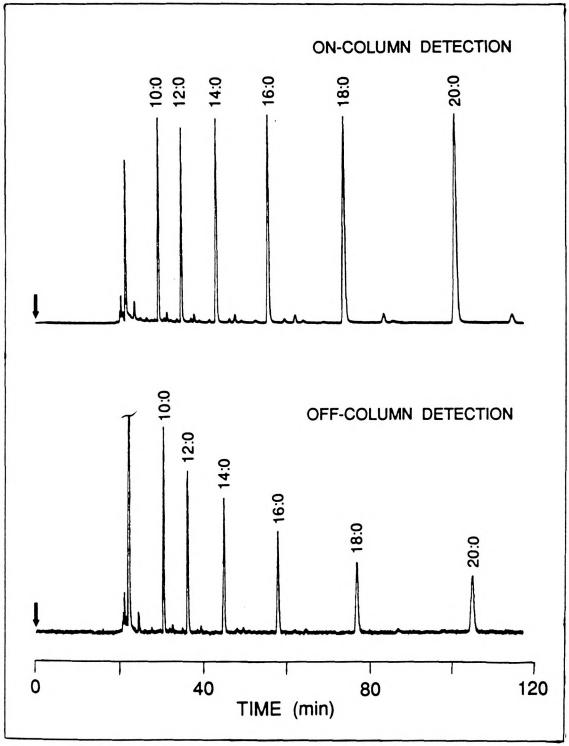
ON-COLUMN DETECTION
10:0
12:0
14:0
16:0
18:0
20:0
OFF-COLUMN DETECTION
10:0
12:0
14:0
16:0
18:0
20:0
0
40
80
120
TIME (min)

As can be seen in Table 8.4, time variance values for a single solute zone measured on- and off-column are approximately equal. Consequently, dispersion contributions to the variance between the two detectors appear to be negligible. The observed equality of time variance values confirms the basic assumption (Equation [8.1]) used to derive theoretical expressions relating on- and off-column length variance and concentration (Equations [8.7] and [8.10]).

In contrast to the time variance, the length variance values determined for each solute zone are not constant on- and off-column. Moreover, the length variance evaluated on-column decreases slightly with increasing capacity factor, while those measured off-column increase markedly. These results imply that elution nonequilibrium is a substantial contribution to retention-dependent sources of length dispersion at the column exit. Thus, the solute zone broadening and concomitant decrease in concentration commonly ascribed to the general elution problem may not arise from the column proper, as previously thought, but may occur as the solute elutes from the chromatographic column.

To investigate the magnitude of this elution nonequilibrium effect, the ratio of the off- to on-column length variance is calculated as a function of capacity factor for the data in Table 8.4. These experimentally determined length variance ratios at 25 °C are compared with theoretical predictions in Figure 8-15. A linear relationship is observed between the length variance ratio and the function of capacity factor $(1+k)^2$, as predicted by Equation [8.7]. Excellent agreement is seen between experimentally determined and theoretically predicted length variance ratios over a wide range of capacity factors. In a related study (14), this length variance ratio was shown to be independent of the mobile-phase linear velocity in the range from 0.06 to 0.13 cm/s, as expected from Equation [8.7]. These results indicate that elution nonequilibrium contributes significantly to length dispersion in a manner which is consistent with theoretical considerations.

Table 8.4: Retention and Variance of Fatty Acid Derivatives at 25 °C by Simultaneous On- and Off-Column Detection.

		σ_T^2 (s^2)		σ_L^2 (cm^2)	
C#	k	ON	OFF	ON	OFF
10	0.49	44.9	45.1	0.1107	11.8
12	0.79	54.9	58.9	0.0947	15.4
14	1.2	78.8	78.4	0.0872	20.5
16	1.9	124.2	144.7	0.0814	37.8
18	2.9	206.5	227.1	0.0750	59.3
20	4.4	375.1	388.7	0.0719	101.5

Figure 8-15: Ratio of the length variance measured on- and off-column *versus* $(1+k)^2$ in the exit region (25 °C). Theoretical prediction (—).

Figure 8-15

In concurrent studies, the influence of elution nonequilibrium on solute zone concentration has been examined with the same experimental data. The concentration is measured directly from the maximum photocurrent of the fluorescence signal both on- and off-column. The experimental concentration ratios, normalized to the least retained solute, appear to correlate well with theoretical predictions (Figure 8-16). These concentration ratios are linearly dependent on the function 1/(1+k), as predicted by Equation [8.10]. No apparent dependence of the concentration ratio on mobile-phase velocity is theoretically predicted or experimentally observed (14). Thus, the solute zone concentration off-column decreases markedly with capacity factor, solely due to the increase in length variance upon elution from the column.

Although nonequilibrium at the column exit directly influences the length variance off-column, the chromatographic resolution remains unaffected. Because the velocity of all molecules increase upon elution from the column, the difference in time between them remains constant. However, the decrease in concentration with increasing retention, which is often attributed to on-column processes, appears to actually arise from elution processes at the exit of the chromatographic column.

Variation in Solvent Composition and Temperature. In practice, this general elution problem is often overcome either by programming the solvent composition or the entire column temperature with time. Although these techniques influence the solute differently, the zone becomes successively less retained in both cases and is moving at approximately the mobile-phase velocity upon elution from the column. Thus, the discontinuity in solute retention, and the associated decrease in concentration at the column exit, is effectively reduced using either technique. Unfortunately, under these changing conditions, it is difficult to determine

Figure 8-16: Normalized ratio of maximum concentration measured on- and off-column *versus* (1+k) in the exit region (25 °C). Theoretical prediction (—).

Figure 8-16

experimentally the instantaneous capacity factor upon elution from the column. However, the effect of solvent composition operated isocratically and the influence of a spatial temperature gradient may be examined individually as a relatively simple means to reduce this elution broadening effect. By decreasing the discontinuity in retention upon elution from the column, it is hoped to increase the solute detectability off-column.

The influence of solvent composition on the retention behavior of the model solutes is shown in Table 8.1. For this investigation, the mobile phase is operated under isocratic conditions and is systematically varied from 90% v/v to 100% v/v methanol in water. The resulting length variance ratios, illustrated in Figure 8-17, show excellent agreement with theoretical predictions based on Equation [8.7]. Thus, the steady-state model appears to be valid in describing elution from the column for a wide variety of capacity factor values ($k = 0.44$ to 72.0) (Table 8.1). In addition, the length variance ratio is affected only by the magnitude of the capacity factor, regardless of whether retention arises from different solutes or from different mobile phase conditions.

Solute capacity factor is further altered utilizing a spatial temperature gradient at the column exit. The retention behavior of the model solutes with temperature is shown in Figures 8-18 and 8-19. In Figure 8-18, the derivatized fatty acid standards utilized for this study exhibit the logarithmic relationship of capacity factor (k) with carbon number expected for a homologous series. Furthermore, Figure 8-19 shows the logarithmic dependence of the capacity factor on the inverse of the temperature. This relationship, predicted from partition interactions, is described by the interaction energy ($\Delta G°$) and the phase ratio (β) (Equation [1.6]). In the temperature range from 20 to 60 °C these model solutes are well behaved, with capacity factors decreasing by a factor of approximately three. By heating the column exit region, solutes will become less

Figure 8-17: Effect of solvent composition on the off- to on-column length variance ratio. Mobile-phase composition, methanol/water: 90.0% v/v (✳), 92.5% v/v (◆), 95.0% v/v (△), 97.5% v/v (■), 100% v/v (○), Theory (—).

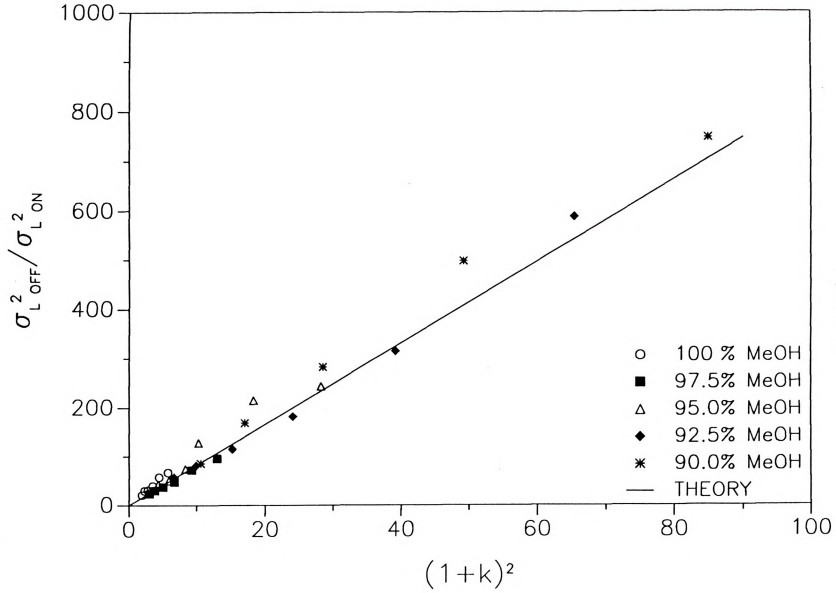
1000
800
600
400
200
0
0
20
40
60
80
100
$\sigma^2_{L\,OFF}/\sigma^2_{L\,ON}$
$(1+k)^2$
100 % MeOH
97.5% MeOH
95.0% MeOH
92.5% MeOH
90.0% MeOH
THEORY

Figure 8-17

Figure 8-18: Effect of temperature on the retention behavior of fatty acid derivatives: logarithm of capacity factor *versus* carbon number. Conditions given in Experimental Methods.

Figure 8-18

CAPACITY FACTOR (k)
6.0
4.0
2.0
1.0
0.8
0.6
0.4
0.2
10
12
14
16
18
20
CARBON NUMBER
20 C
25 C
30 C
40 C
50 C
60 C

Figure 8-19: Effect of temperature on the retention behavior of fatty acid derivatives: logarithm of capacity factor *versus* 1/T. Conditions given in Experimental Methods.

Figure 8-19

CAPACITY FACTOR (k)
6.0
4.0
2.0
1.0
0.8
0.6
0.4
0.2
2.9
3.0
3.1
3.2
3.3
3.4
3.5
1/T (x1000)
o 10:0
* 12:0
Δ 14:0
◇ 16:0
▽ 18:0
+ 20:0

retained prior to the column exit. It is hoped that the detrimental effect of elution nonequilibrium on zone variance and concentration will be minimized by effectively decreasing the abruptness of this transition in retention.

This hypothesis is experimentally evaluated by heating the column exit region between the two detectors (Figure 8-13). The temperature behavior of this apparatus, shown in Figure 8-20, is constant in the heated region and decreases to room temperature less than 1 cm from the ceramic temperature controller. With this system, the length variance and maximum concentration of each solute zone may be determined sequentially on- and off-column, as a function of temperature in this heated zone. The influence of temperature on the ratio of the length variance measured off-column to that measured on-column ($\sigma_L{}^2{}_{OFF}/\sigma_L{}^2{}_{ON}$) *versus* $(1+k)^2$ is shown in Figure 8-21. Measured length variance ratios show excellent agreement with theoretical predictions described by Equation [8.7]. Unfortunately, this relationship appears to be independent of temperature in the exit region of the column. This result is consistent with the prediction by Giddings (36) that the total change in the zone velocity determines the change in length variance, not the spatial location of such a change. The concomitant decrease in the maximum concentration predicted based on a Gaussian zone profile, described by Equation [8.10], is shown in Figure 8-22. The concentration ratio has been normalized to the least retained solute due to difficulty in matching the excitation intensity for the two detectors. The measured ratios show good agreement with those predicted by Equation [8.10], independent of the temperature in the heated zone. Based on these measurements, a spatial temperature gradient is not successful in minimizing the detrimental effects of elution at the column exit.

Apparently, the temperature gradient only acts to displace the retention discontinuity, and whenever the change in solute retention is spatially specific,

Figure 8-20: Temperature variation with distance in the column exit region.

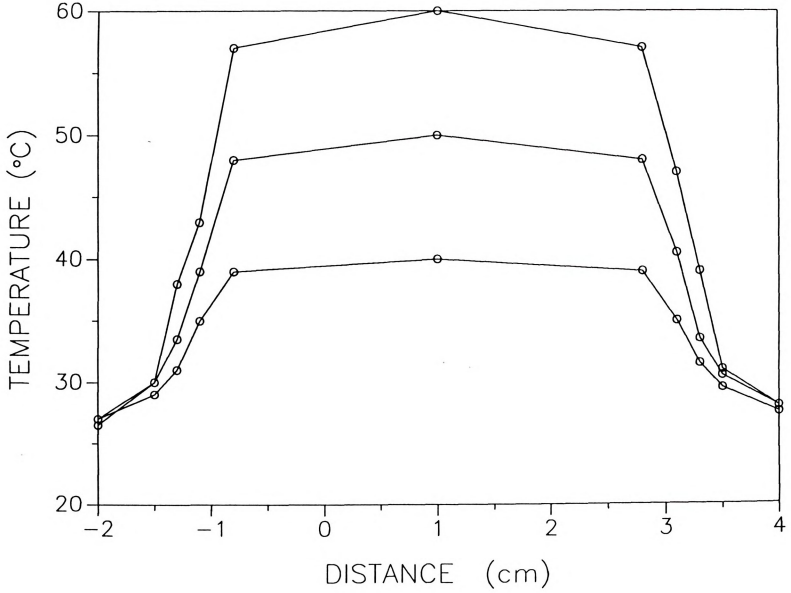

254
Figure 8-20

Figure 8-21: Effect of temperature on the ratio of the length variance measured on- and off-column *versus* $(1+k)^2$. Theoretical prediction (—) based on Equation [8.9]; T = 40 °C (○), 50 °C (□), 60 °C (△), 90 °C (▼).

Figure 8-21

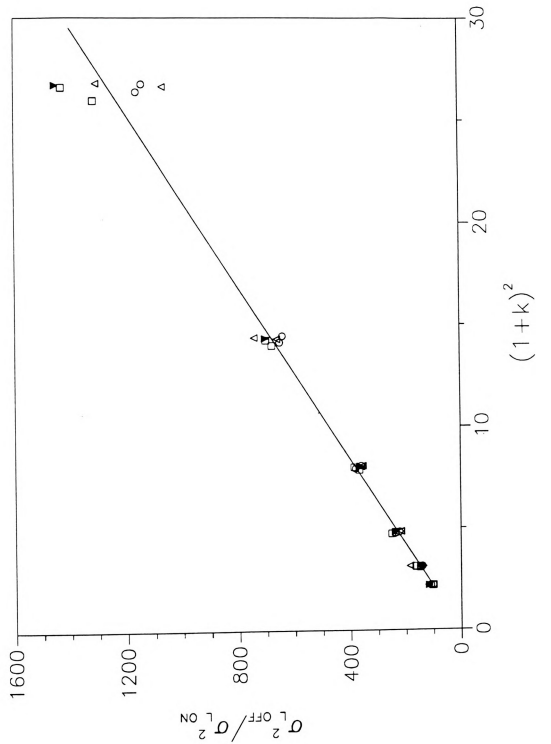

Figure 8-22: Effect of temperature on the normalized ratio of the concentration measured on- and off-column *versus* 1/(1+k). Theoretical prediction (—) based on Equation [8.12]; T = 40 °C (○), 50 °C (□), 60 °C (△), 90 °C (▼).

Figure 8-22

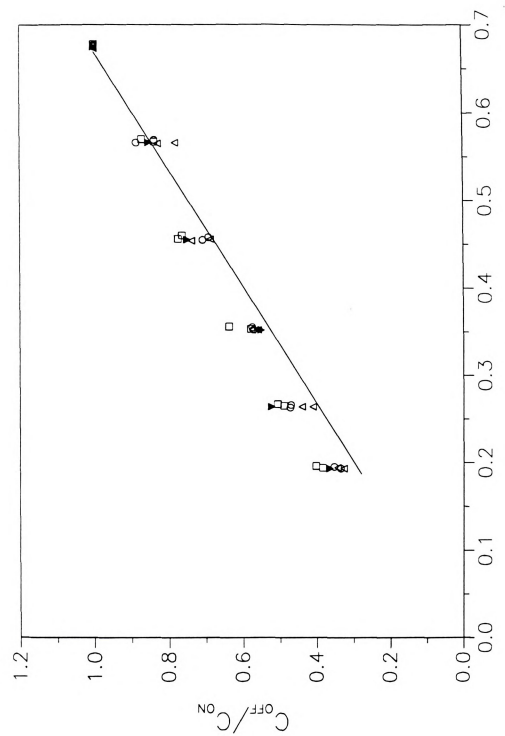

the velocity of the front of the solute zone increases before the rear portion. In order to move the zone off the column without altering the length variance, it would be necessary to transfer the entire zone into the mobile phase simultaneously. Although this would be technically possible if the entire zone encounters a temperature jump immediately before the zone elutes from the column, this solution is not very feasible for complex separations of a large number of components.

8.8 Conclusions

The extent of broadening that occurs at the column inlet and exit due to abrupt changes in the zone velocity can be described theoretically. Sequential measurements of length variance in these transition regions show excellent agreement with theoretical predictions for the model solutes utilized in these studies. Concentration ratios, measured from the maximum photocurrent on- and off-column, are also in good agreement with predictions based on a Gaussian zone profile. Thus, the change in the zone profile in these transition regions arises primarily from the abrupt change in the zone velocity.

As the solute zone enters the column, the length variance changes inversely with $(1+k)^2$ and the solute concentration increases by a factor of $(1+k)$. Measurements in the inlet region indicate that the nonequilibrium condition does not persist long after the transition onto the column. Under the ideal chromatographic conditions examined here, equilibration of the model solutes between the mobile and stationary phases occurs well before 4.9 cm along the column. However, drastic changes in the zone profile develop when the injection

solvent differs markedly from the mobile phase, and these results warrant further investigation.

In like manner to the inlet region, as solute zones elute from the column, an increase in length variance proportional to $(1+k)^2$ and a concomitant decrease in concentration proportional to $(1/1+k)$ is predicted theoretically and measured experimentally. Although this transition does not affect chromatographic resolution, a decrease in solute concentration with increasing retention is a direct outcome. Thus, elution from the chromatographic column appears to be the primary source of the decrease in solute detectability with increased retention, known as the general elution problem in separations. Attempts to minimize this detrimental effect with a spatial temperature gradient were unsuccessful.

8.9 Literature Cited in Chapter 8

1. Giddings, J.C. *Dynamics of Chromatography*; Marcel Dekker, Inc.: New York, 1965; pp. 95-118.
2. Ettre, L.S. *Sample Introduction in Capillary Gas Chromatography, Vol. 1*; Sandra, P., Ed.; Verlag: Heidelberg, 1985; and references cited therein.
3. deVault, D. *J. Amer. Chem. Soc.* **1943**, *65*, 532.
4. Reilley, C.N.; Hildebrand, G.P.; Ashley, J.W. Jr. *Anal. Chem.* **1962**, *34*, 1198.
5. Scott, R.P.W *J. Chromatogr. Sci.* **1971**, *9*, 449.
6. Snyder, L.R. *J. Chromatogr. Sci.* **1972**, *10*, 187.
7. Karger, B.L.; Martin, M.; Guiochon, G. *Anal. Chem.* **1974**, *46*, 1640.
8. Jacob, L.; Guiochon, G. *J. Chromatogr. Sci.* **1975**, *13*, 18.
9. Conder, J.R. *J. High Resolut. Chromatogr. Chromatogr. Commun.* **1984**, *7*, 615.
10. Lovkvist, P.; Jonsson, J.A. *J. Chromatogr.* **1986**, *356*, 1.
11. Hoffman, N.E.; Rahman, A. *J. Liq. Chromatogr.* **1988**, *11*, 2685.
12. Dose, E.V.; Guiochon, G. *Anal. Chem.* **1990**, *62*, 1723.
13. Evans, C.E.; McGuffin, V.L. *Anal. Chem.* submitted.
14. Evans, C.E.; McGuffin, V.L. *J. Liq. Chromatogr.* **1988**, *11*, 1907.
15. Wilke, C.R.; Chang, P. *AIChE J.* **1955**, *1*, 264.
16. Bristow, P.; Knox, J. *Chromatographia* **1977**, *10*, 279.
17. Gluckman, J.C.; Hirose, A.; McGuffin, V.L.; Novotny, M.V. *Chromatographia* **1983**, *17*, 303.
18. Martire, D.E. *J. Chromatogr.* **1989**, *461*, 165.
19. Huber, J.F.K.; Rizzi, A. *J. Chromatogr.* **1987**, *384*, 337.
20. Martin, M.; Eon, C.; Guiochon, G. *J. Chromatogr.* **1975**, *108*, 229.
21. Yang, F.J. *J. Chromatogr.* **1982**, *236*, 265.
22. van Deemter, J.J.; Zuiderweg, F.J.; Klinkenberg, A. *Chem. Eng. Sci.* **1956**, *5*, 271.
23. Giddings, J.C. *Dynamics of Chromatography*; Marcel Dekker, Inc.: New York, 1965; pp. 310-312.

24. Knox, J.H. *J. Chromatogr. Sci.* **1977**, *15*, 352.

25. Poe, D.P.; Martire, D.E. *J. Chromatogr.* **1990**, *517*, 3.

26. Evans, C.E.; McGuffin, V.L. *Anal. Chem.* **1988**, *60*, 573.

27. Chesler, S.N.; Cram, S.P. *Anal. Chem.* **1971**, *43*, 1922.

28. Tsimidou, M.; Macrae, R. *J. Chromatogr. Sci.* **1985**, *23*, 155.

29. Khachik, F.; Beecher, G.R.; Vanderslice, J.T.; Furrow, G. *Anal. Chem.* **1988**, *60*, 807.

30. Golay, M.J.E. *Gas Chromatography 1958*; D.H. Desty, Ed.; Academic Press Inc.: New York, **1958**; pp. 36-55.

31. Shelly, D.C.; Gluckman, J.C.; Novotny, M.V. *Anal. Chem.* **1984**, *56*, 2990.

32. Guthrie, E.J.; Jorgenson, J.W. *Anal. Chem.* **1984**, *56*, 483.

33. Takeuchi, T.; Yeung, E.S. *J. Chromatogr.* **1987**, *389*, 3.

34. Verzele, M.; Dewaele, C. *J. High Resolut. Chromatogr. Chromatogr. Commun.* **1987**, *10*, 280.

35. Takeuchi, T.; Ishii, D. *J. Chromatogr.* **1988**, *435*, 319.

36. Giddings, J.C. *Dynamics of Chromatography*; Marcel Dekker, Inc.: New York, 1965; pp. 79-84.

CHAPTER 9

FUTURE STUDIES

The studies presented in this thesis offer new insight into separation processes by monitoring the movement and dispersion of solute zones directly on the chromatographic column. This *in situ* approach allows the fundamental parameters influencing separations to be measured during the actual chromatographic process. Moreover, the progression of the separation along the column can be determined directly under the variety of experimental conditions commonly encountered in modern practice. Thus, the advances in fundamental understanding gained with this on-column measurement technique may be applied to the practical aspects of separations as well.

In many ways, the investigations described here serve as an introduction to this experimental approach, and the possibilities for further study appear to be quite lucrative and wide ranging. Using nearly ideal experimental conditions, it has been possible to examine such diverse phenomena as the unexpected variation in retention with local pressure, and the change in zone variance upon injection and elution. Thus, future investigations using this technique could evolve in a variety of directions including the extension to less ideal adsorption

interactions, to increased dimensionality in the spectral or time domains, or to the examination of other separation techniques (gas or supercritical chromatography, or capillary electrophoresis). In addition to these general directions, several specific areas of research call for special attention.

The resolution of conflicting results concerning solute retention with position along the column is one such area. Based on local pressure considerations (Chapter 6), solute retention is expected to decrease with pressure as a function of distance along the column. Measurements reported in Chapters 4 and 7 affirm this decrease in capacity factor along the column length. However, similar measurements on another column (Chapters 6 and 8) indicate an increase in k with distance. This discrepancy may arise due to variability in surface coverage of the stationary phase with distance caused by the injection of pure solvents. Although reported earlier in the thesis, pressure studies (Chapter 6) were performed on the same column, after experiments with injection solvent (Chapter 8). Both these results indicate the opposite trend in solute capacity factor with distance predicted based on the local pressure, with the increase in k for the pressure study ($\Delta k/k$ = 17%) being significantly greater for that for the solvent study ($\Delta k/k$ = 3%). Thus, repeated injections of a variety of mixed and pure solvents may have caused permanent alteration of the stationary phase, leading to these conflicting results. This supposition needs to be examined in more detail by systematic monitoring of retention as a function of periodic injection of pure solvents. Understanding gained in this study would provide more detailed knowledge of the effect of repeated injection on column efficacy.

In addition, the effect of solvent composition on solute retention and dispersion requires further investigation in order to be understood fully. These studies include solute injection in pure solvents, as well as isocratic and gradient mobile-phase conditions. By monitoring the local solvent composition and solute

zone profile concurrently, direct and systematic investigations of the influence of these changing environmental conditions on retention and dispersion are possible. This might be experimentally accomplished using infrared or refractive index detection to measure the mobile-phase composition, while simultaneously measuring the solute profile with fluorescence detection. In this manner, the influence of both the absolute solvent composition and the composition gradient on the resulting zone profile can be assessed. Likewise, this study could be extended to include the continuously alternating mobile-phase conditions present when the solvent modulation technique is applied (1,2). In solvent modulation, retention is controlled by introducing two or more solvents onto the column in a repeating or random sequence. Several assumptions regarding the retention and dispersion of both solute and solvent zones have been necessary in the theoretical development of this technique, which could be easily verified by direct measurement. Finally, on-column detection could be used to advantage in the experimental validation of recent theoretical developments concerning separations that incorporate nonlinear isotherms (3). Under these experimental conditions, the retention of the solute is a function of the local solute concentration. In addition, extra-column dispersion in this regime is thought to be dependent on column processes and, therefore, not additive (4). Thus, systematic experimental measurements of solute injection, as well as the movement and broadening along the column would be very beneficial.

Although the studies outlined above allow the measurement of local separation processes, they are still indicative of only the bulk retention and dispersion of solute zones. Recent technological advances in microscale measurements should provide the opportunity to explore separations on the particle scale (5). Fluorescence microscopes are presently available with the resolution of 0.5 μm, making feasible the experimental measurement of

separation processes in the region near the stationary phase surface as well as the flow dynamics between particles. Thus, it is possible to move even closer to the direct measurement of the fundamental processes controlling separations.

For these reasons, the studies described in this thesis are only a beginning to the possibilities for the direct examination of separation processes. Indeed, every experiment described in this thesis has brought new and unexpected insight into separation processes where too many believe that "everything is already understood." There is every reason to imagine that further studies utilizing this direct approach will afford even more insight into this fundamentally interesting and practically applicable field.

Literature Cited in Chapter 9

1. Wahl, J.H.; Enke, C.G.; McGuffin, V.L. *Anal. Chem.* **1990**, *62*, 1416.
2. Wahl, J.H.; Enke, C.G.; McGuffin, V.L. *Anal. Chem.* submitted for publication.
3. Golshan-Shirazi, S.; Guiochon, G. *Anal. Chem.* **1990**, *62*, 217.
4. Dose, E.V.; Guiochon, G. *Anal. Chem.* **1990**, *62*, 1723.
5. Kanistanaux, D.; Burrill, P.H. *Biomed. Prod.* **1989**, *54*, 72.